THE JOURNAL OF BIOLOGICAL CHEMISTRY VOL. 289, NO. 32, pp. 22284–22305, August 8, 2014

Human T-lymphotropic Virus Type 1-infected Cells Secrete Exosomes That Contain Tax Protein*[S]

Received for publication, January 15, 2014, and in revised form, June 16, 2014 Published, JBC Papers in Press, June 17, 2014, DOI 10.1074/jbc.M114.549659

Elizabeth Jaworski[‡1], Aarthi Narayanan[‡1], Rachel Van Duyne[‡§], Shabana Shabbeer-Meyering[‡], Sergey Iordanskiy[‡§], Mohammed Saifuddin[‡], Ravi Das[‡], Philippe V. Afonso[¶‖], Gavin C. Sampey[‡], Myung Chung[‡], Anastas Popratiloff[**], Bindesh Shrestha[‡‡], Mohit Sehgal[§§], Pooja Jain[§§], Akos Vertes[‡‡], Renaud Mahieux[¶¶], and Fatah Kashanchi[‡2]

*From the [‡]School of Systems Biology, National Center for Biodefense and Infectious Diseases, George Mason University, Manassas, Virginia 20110, the [§]Department of Microbiology, Immunology, and Tropical Medicine and [‡‡]Center for Microscopy and Image Analysis, George Washington University Medical Center, Washington, D. C. 20037, the **Department of Chemistry, George Washington University, Washington, D. C. 20037, the [¶¶]Equipe Oncogenèse Rétrovirale, Equipe labelisée "Ligue Nationale Contre le Cancer," International Center for Research in Infectiology, INSERM U1111-CNRS UMR5308, Ecole Normale Supérieure de Lyon, Université Lyon 1, Lyon 69364 Cedex 07, France, the [¶]Unité d'Epidémiologie et Physiopathologie des Virus Oncogènes, Département de Virologie, Institut Pasteur, F-75015 Paris, France, [‖]CNRS, UMR3569, F-75015 Paris, France, and the [§§]Department of Microbiology and Immunology, Drexel Institute for Biotechnology and Virology Research, Drexel University College of Medicine, Doylestown, Pennsylvania 18902*

Background: Extracellular exosomes contain various functional elements.
Results: Exosomal Tax protein causes phenotypic changes in uninfected cells.
Conclusion: Exosomes may play critical roles in extracellular delivery of oncogenic material derived from HTLV-1-infected cells.
Significance: Exosomal delivery of Tax and other putative oncogenic components produced during HTLV-1 infection potentially contributes to pathogenesis of adult T-cell leukemia, myelopathy, or tropical spastic paraparesis.

Human T-lymphotropic virus type 1 (HTLV-1) is the causative agent of adult T-cell leukemia and HTLV-1-associated myelopathy/tropical spastic paraparesis. The HTLV-1 transactivator protein Tax controls many critical cellular pathways, including host cell DNA damage response mechanisms, cell cycle progression, and apoptosis. Extracellular vesicles called exosomes play critical roles during pathogenic viral infections as delivery vehicles for host and viral components, including proteins, mRNA, and microRNA. We hypothesized that exosomes derived from HTLV-1-infected cells contain unique host and viral proteins that may contribute to HTLV-1-induced pathogenesis. We found exosomes derived from infected cells to contain Tax protein and proinflammatory mediators as well as viral mRNA transcripts, including Tax, HBZ, and Env. Furthermore, we observed that exosomes released from HTLV-1-infected Tax-expressing cells contributed to enhanced survival of exosome-recipient cells when treated with Fas antibody. This survival was cFLIP-dependent, with Tax showing induction of NF-κB in exosome-recipient cells. Finally, IL-2-dependent CTLL-2 cells that received Tax-containing exosomes were protected from apoptosis through activation of AKT. Similar experiments with primary cultures showed protection and survival of peripheral blood mononuclear cells even in the absence of phytohemagglutinin/IL-2. Surviving cells contained more phosphorylated Rb, consistent with the role of Tax in regulation of the cell cycle. Collectively, these results suggest that exosomes may play an important role in extracellular delivery of functional HTLV-1 proteins and mRNA to recipient cells.

Discovered in the early 1980s, human T-lymphotropic virus type 1 (HTLV-1)[3] is the first identified human oncogenic retrovirus (1, 2). In addition to causing adult T-cell leukemia, HTLV-1 is associated with inflammatory disease states, including HTLV-1-associated myelopathy (HAM)/tropical spastic paraparesis (TSP), HTLV-1-associated uveitis, and infective dermatitis (3–5). HTLV-1 infects ~5–10 million people worldwide and geographically impacts populations in Japan, Africa, the Caribbean, and Central and South America (1, 3, 6–8). In terms of HTLV-1 pathogenesis, the HTLV-1 transactivator protein Tax has been identified as a critical component in the proliferation and transformation of human primary T-cells (1, 9–12). This 40-kDa phosphoprotein not only controls cellular general gene expression, including chromatin remodeling

* This work was supported, in whole or in part, by National Institutes of Health (NIH), NCI, Grant R01 CA054559 and NIH, NIAID, Grant R01 AI077414 (supporting P. J. and M. S.) and NIH Grants AI078859, AI074410, and AI043894 (to F. K.). This work was also supported by United States Department of Energy Grant DE-SC0001599 (to F. K.), an indirect account at George Mason University, and equipe labelisée Ligue Contre le Cancer (to R. M.). This work was also supported by the United States Department of Energy through Grant DE-FG02-01ER15129 (to A. V.) for conducting the LAESI-MS measurements.
[S] This article contains supplemental Table 1.
[1] Both authors contributed equally to this work.
[2] To whom correspondence should be addressed: George Mason University, Discovery Hall, Rm. 182, 10900 University Blvd. MS 1H8, Manassas, VA 20110. Tel.: 703-993-9160; Fax: 703-993-7022; E-mail: fkashanc@gmu.edu.

[3] The abbreviations used are: HTLV-1, human T-lymphotropic virus type 1; HAM, HTLV-1-associated myelopathy; TSP, tropical spastic paraparesis; ILV, intraluminal vesicle; TEM, transmission electron microscopy; miRNA, microRNA; PHA, phytohemagglutinin; C81, C8166-45; ED(−), Tax-negative ED40515(−); PBMC, peripheral blood mononuclear cell; D-PBS, Dulbecco's PBS; LAESI, laser ablation electrospray ionization; CAT, chloramphenicol acetyltransferase; WCE, whole-cell extract; ABC, ATP-binding cassette.

within the host, but also subverts host cell DNA damage response mechanisms, cell cycle progression, and the apoptotic pathway (13–24).

Nanovesicles called exosomes play important roles in intercellular communication, cellular inflammation, antigen presentation, programmed cell death, and pathogenesis (25–29). Recently, much interest has developed in mechanisms of extracellular delivery of nucleic acids and proteins among virally infected and uninfected bystander cells, and exosomes have been shown to play an important role in viral pathogenesis and control of host immune responses to infection (28, 30–32).

First described in 1983 by Harding *et al.* (45), exosomes are nanovesicles between 30 and 120 nm in diameter and shed by a variety of different cell types, including those of hematological origin, such as B-cells, T-cells, dendritic cells, and non-hematological origin, such as epithelial cells, neuronal cells, and tumor-derived cells. Exosomes have been isolated from more complex physiological fluids, including saliva, urine, blood, and breast milk, where much effort has been dedicated to investigating the diagnostic potential of these vesicles as biomarkers (33–37). Importantly, heterogeneous populations of exosomes have been identified in various biofluid samples including seminal fluid and urine, potentially as a result of exosome production by various cell types. Depending upon the source, the exosome populations have been shown to range in size as well as protein content (38, 39). Heterogeneous populations of exosomes have also been identified from cancerous cell types, including colon cancer (40).

Exosome formation occurs via inward budding of endosomal membranes, which causes the accumulation of intraluminal vesicles (ILVs) within multivesicular bodies. These multivesicular bodies shuttle cargo either to lysosomes or to the plasma membrane, where the contents are exocytosed (41). In contrast, cells release other types of membrane vesicles, including apoptotic blebs and microparticles, which bud directly from the plasma membrane and represent a heterogeneous mixture of vesicles ranging in size from 100 to 1000 nm (42). In addition to the difference in size between exosomes and apoptotic blebs, several additional factors exist when distinguishing exosomes from apoptotic blebs. These include morphological traits of apoptotic blebs, which are denser, floating at a higher density on sucrose gradients, and do not appear cup-shaped under transmission electron microscopy (TEM). Furthermore, the apoptotic vesicles include very high levels of histones compared with levels seen in exosomes (43).

Because exosomes are generated through invagination of late endosomes, these vesicles incorporate a variety of host components, including Alix and TSG101, as well as proteins involved in membrane trafficking (Rabs and annexins), tetraspanins (CD63, CD81, and CD9), heat-shock proteins (HSP60, HSP70, and HSP90), and cytoskeletal components (actin); all of these proteins have been considered as consensus markers for exosomes (25, 42). Morphologically, exosomes have been shown to appear cup-shaped when visualized using TEM analysis (44). Currently, it is accepted that recipient cell uptake of exosomes is dependent, in part, upon ligand-receptor recognition, followed either by direct fusion of exosome and recipient cell plasma membranes or by endocytic processes involving dynamin2 and phosphatidylinositol 3-kinase (PI3K) (45, 46).

It has also been demonstrated that exosomes secreted from uninfected cells contain nucleic acids, including cellular mRNA and miRNA as well as functional proteins. However, infection can alter the levels and profiles of these cargo molecules contained in exosomes (47). With regard to viral infection, exosomes aid in the transfer of hepatitis C virus viral RNA from infected to uninfected plasmacytoid dendritic cells, inducing the production of type I IFN (48). Furthermore, HIV-1 Gag and p17 are incorporated into exosomes released from these infected cells (49). Regarding exosome-mediated transfer of miRNA, exosomes have been shown to deliver functional miRNA from infected donor cells to uninfected recipient cells during infection by the oncogenic Epstein-Barr virus (32). Exosome-mediated transfer of miRNAs has been implicated in HIV-associated neuronal disorders (50), and delivery of functional proteins to recipient cells has been shown in HIV-1-infected macrophages. Release of HIV-1 Nef within exosomes, onto B cells, may aid in viral immune evasion (51). Additionally, Nef stimulates its own release in exosomes, which can then cause apoptosis in resting $CD4^+$ T-cells (52).

To date, there are no studies describing a role of exosomes in HTLV-1 infection. It has been shown that soluble Tax can be taken up by recipient cells, whereas soluble Tax treatment of uninfected cells induces TNF-α gene expression and enhances the proliferation of phytohemagglutinin (PHA)-stimulated peripheral blood lymphocytes (18, 53). Tax has been detected in the cerebrospinal fluid of HTLV-1-infected patients, in HAM/TSP patients (54). However, the underlying mechanism for the secretion of Tax has not been clearly defined (55, 56). We reasoned that in order to be functional in circulation in bodily fluids, a more stable form of Tax may be present outside of a cell. Along these lines, we aimed to investigate whether Tax could exist in an extracellular vesicle, such as an exosome, secreted from HTLV-1-infected cells and thus contribute to viral pathogenesis.

We hypothesized that HTLV-1-infected T-cells produce exosomes, and these vesicles may contain unique molecules, including host and viral proteins. Herein we describe the characterization of exosomes secreted from uninfected and HTLV-1-infected T-cells. These exosomes displayed similar characteristics to the standard exosomes, demonstrating typical phenotypic and morphologic features. We also examined the proteomic profile of the exosomes and determined that exosomes from the HTLV-1-infected cells contain proinflammatory mediators as well as Tax protein. The HTLV-1 mRNA transcripts for *env*, *tax*, and *hbz* were also present within them. When we evaluated the functional significance of treating naive recipient T-cells with exosomes secreted from HTLV-1 infected cells, we determined that the exosomes were capable of inducing transcription in the recipient cells, which may contribute to an enhanced survival under stress conditions. Therefore, our data implicate a role for Tax-containing exosomes in the protection of recipient cells from apoptosis. Collectively, our results implicate exosomes as an important means of extracellular delivery of functional HTLV-1 proteins to uninfected recipient cells.

EXPERIMENTAL PROCEDURES

Cell Culture—The C8166-45 (C81) cells, which are HTLV-1-infected but do not produce infectious virus, were obtained through the AIDS Research and Reference Reagent Program, Division of AIDS, NIAID, National Institutes of Health (catalog no. 404). The HTLV-1-infected MT2 cells, which produce high levels of infectious virus, were obtained from Dr. Douglas Richman. Both the IL-2-independent C81 (producing only the Tax protein) and MT2 cell lines are derived from the fusion of normal cord blood cells with T-cells isolated from adult T-cell leukemia-infected patients (57, 58). Uninfected CEM-T4 was a kind gift from Dr. J. P. Jacobs. The HTLV-1-infected, Tax-negative ED40515(−) (ED(−)) cells were a generous gift from Dr. Cynthia Pise-Masison (NCI, National Institutes of Health, Bethesda, MD). This IL-2-dependent HTLV-1-infected cell line retains a nonsense mutation, rendering the virus defective for expression of the viral gene Tax (59). These T-cell lines and Jurkat T-cells (ATCC) were maintained in RPMI 1640 supplemented with exosome-depleted (see below) 10% fetal bovine serum (FBS), 1% streptomycin/penicillin antibiotics, and 1% L-glutamine (Quality Biological) and incubated in 5% CO_2 at 37 °C. HEK-293T cells were maintained in Dulbecco's modified Eagle's medium supplemented with 10% FBS, 1% streptomycin/penicillin antibiotics, 1% L-glutamine. Stable Jurkat transfectants were also treated with 200 μg/ml G418 (Sigma-Aldrich). The HEK-293-based reporter cell line HEK-Blue hTLR3 containing a secreted embryonic alkaline phosphatase reporter gene was obtained from InvivoGen and cultured following the manufacturer's protocol. PBMCs were stimulated with PHA and recombinant human IL-2 (10 units/ml; Roche Applied Science) for 3 days. Mouse T-cells, CTLL-2 (IL-2-dependent; 2 nM), were cultured in RPMI, 10% FBS, IL-2 supplemented with 55 μM 2-mercaptoethanol. Exosome-depleted FBS was generated by centrifugation at 31,000 rpm for 2 h at 4 °C, and the supernatant was considered clear of exosomes.

Transfection, Electroporation, and Plasmids—To generate exosomes from HTLV-1-infected cells, Jurkat T-cells (5×10^7 cells) were washed twice with PBS, reconstituted in RPMI (250 μl), and then transfected with pACH (30 μg), an infectious HTLV-1 molecular clone, graciously provided by Dr. Lee Ratner (60), by electroporation as described previously (61). Briefly, electroporations were conducted using a pulse voltage of 1,325 V, pulse width of 10 ms, and a pulse number of 3 using a Invitrogen electroporator.

Purification of Exosomes—Exosomes were isolated from cell supernatants as described previously (43) with a few modifications. Briefly, 50–100 ml of cell culture supernatants were subjected to low speed centrifugation at 2,000 rpm for 10 min at room temperature to remove whole cells. Next, the cell-free supernatants were centrifuged at 4,000 rpm for 10 min at room temperature to remove cell debris and then subjected to filtration through a 0.22-μm polyethersulfone membrane (Corning Inc.). These membranes were blocked with 0.5% BSA in PBS/Tween (10 ml) prior to use. Clarified supernatants were subjected to high-speed centrifugation at 10,000 × *g* for 30 min at 4 °C to remove any remaining cell debris. This supernatant was then spun at 100,000 × g for 70 min at 4 °C, and the exosome pellets were washed and reconstituted in Dulbecco's phosphate-buffered saline without calcium or magnesium (22 ml) (D-PBS without Ca^{2+}/Mg^{2+}; Quality Biological). These pellets were centrifuged again at 100,000 × *g* for 70 min at 4 °C, resuspended in D-PBS (25 μl), and stored at 4 °C until further use.

Cell Lysate Preparation—Using a sterile technique, fresh cell pellets (5×10^6) were collected from culture and spun at 1,800 rpm for 5 min at 4 °C. Cell pellets were washed twice with D-PBS without Ca^{2+} or Mg^{2+} and resuspended in 50 μl of lysis buffer (50 mM Tris-HCl, pH 7.5, 120 mM NaCl, 5 mM EDTA, 0.5% Nonidet P-40 (Nonidet P-40), 50 mM NaF, 0.2 mM Na_3VO_4, 1 mM dithiothreitol (DTT) containing protease inhibitors (one complete protease mixture tablet/50 ml of lysis buffer). This suspension was incubated on ice for 20 min, with gentle vortexing every 5 min. Cell lysates were centrifuged at 10,000 rpm for 10 min, and protein concentrations in the supernatants were determined using Bradford protein assay (Bio-Rad, catalog no. 500-0006).

Western Blot and Staining—CEM, C81, MT2, and ED(−)-derived exosomes and corresponding cell extracts were loaded on a 4–20% Tris/glycine gel (Invitrogen), run at 200 V, and transferred onto Immobilon PVDF membranes (Millipore) at 250 mA for 2 h. Membranes were blocked with D-PBS containing 0.1% Tween 20 and milk (5%) and incubated overnight at 4 °C with the appropriate primary antibody (α-actin (ab49900), α-Alix (sc-49268), α-CD63 (ab8219), α-cytochrome *c* (ab13575), α-HSP70 (sc-33575), α-MDR-1 (sc-55510), α-cFLIP (sc-H150), α-Rb (sc-C-15), α-AKT S473 (sc-33437), and α-Tax (monoclonal mouse, generous gift of Dr. Scott Gitlin, University of Michigan)). Antiserum to HTLV-I was obtained from the National Institutes of Health AIDS Reagent Program, Division of AIDS, NIAID/NIH (from Drs. P. Szecsi, H. Halgreen, and J. Tang). Membranes were incubated with the appropriate secondary antibody. Then HRP luminescence was activated with Super Signal West Dura Extended Duration Substrate (Pierce) and visualized by the Bio-Rad Molecular Imager ChemiDoc XRS system (Bio-Rad). Raw densitometry counts were obtained using ImageJ software.

For Coomassie staining, CEM, C81, MT2, and ED(−) exosomes (10 μg) were separated on 4–20% Tris/glycine gels and Coomassie-stained as per standard protocol with 40% methanol, 7% glacial acetic acid, and Coomassie Brilliant Blue (Bio-Rad, R-250). For silver staining, CEM, C81, and MT2-derived exosomes (3 μg) isolated from cell culture supernatants were resolved on a 4–20% Tris/glycine gel and silver-stained according to manufacturer's instructions (Pierce Silver Stain for Mass Spectrometry, catalog no. 24600).

Inhibition and Capturing of Exosomes—The presence of Tax within exosomes was confirmed by treating cells with exosomal inhibitors and capturing exosomes by nanotrap particles. The drugs manumycin A (Enzo Life Sciences) and brefeldin A (Selleckchem.com) were used at 1 μM concentration each in the culture medium of C81 cells for 48 h before harvesting exosomes as per the protocol described earlier. Harvested exosomal pellets were treated for Western blot analysis as described earlier. The nanotrap particles were provided by Ceres Nanosciences (Manassas, VA). Their production and method of use has been described previously (62). Briefly, a 30%

slurry (30 μl) of each type of nanotrap particles NT080 (nanotrap particle that captures exosomes) and NT086 (nanotrap particle that captures viruses) was washed twice with exosome-free culture medium and then incubated with 1 ml of 5-day-old culture media from CEM or MT2 cells for 1 h with rotation at room temperature. Nanotrap particles were then pelleted by gentle centrifugation at 12,000 $\times$ *g* for 10 min, washed to remove unbound exosomes or virus, respectively, and similarly treated for Western blot analysis as for exosomal inhibitor-treated pellets and as described earlier. Western blots were incubated overnight at 4 °C with anti-Tax monoclonal antibodies (Tabs 169, 170, 171, and 172) followed by appropriate HRP-conjugated secondary antibody and developed the next day using enhanced chemiluminescence.

Ca^{2+}-mediated Release of Exosomal Contents—Release of cytokines and Tax within exosomes was evaluated by first incubating a 25-μl buffer-suspended exosomal pellet with 100 μM Ca^{2+} for 1 h at 37 °C. After the incubation, the exosomes were trapped using nanotrap particles, which resulted in any cytokines or other exosomal content being released into the supernatant. Briefly, a 30% slurry (30 μl) of either NT080 or NT074 (nanotrap particle that captures either exosomes and free IL-6 or exosomes alone, respectively) was washed twice with exosome-free culture medium and then incubated with the Ca^{2+}-incubated exosomal pellet. Nanotrap particles were then pelleted by gentle centrifugation at 12,000 $\times$ *g* for 10 min. The resulting supernatant was treated for Western blot analysis by the addition of Laemmli buffer, as described earlier. Western blots were incubated overnight at 4 °C with anti-Tax monoclonal antibodies (Tabs 169, 170, 171, and 172) and anti-IL-6, anti-Alix, and anti-actin antibodies followed by appropriate HRP-conjugated secondary antibody and developed the next day using enhanced chemiluminescence.

Transmission Electron Microscopy—Samples were prepared as follows: CEM, C81, and MT2 exosomes (2 μg) were adsorbed onto 300-mesh Formvar-coated grids, stabilized with evaporated carbon film (Electron Microscopy Science, catalog no. FCF300-Ni), and fixed in 4% glutaraldehyde (5 μl) (Electron Microscopy Sciences, catalog no. 16210) at 4 °C for 5 min. After four quick rinses with autoclaved deionized water, fixed samples were stained for 2 min with uranium acetate (10 μl), dried for 20 min, and imaged with the transmission electron microscope (JEOL JEM 1200EX) at a magnification of $\times$75,000.

LC-MS/MS Analysis—Whole exosome preparations (10 μg), in duplicate, were first lysed in 8 M urea, after which they were reduced using DTT and acetylated using iodoacetamide by standard procedures. The reduced and alkylated proteins were trypsin-digested (Promega) overnight at 37 °C. The digested peptides were eluted using ZipTip purification (Millipore), and identification of the peptides was performed by LTQ-tandem MS/MS equipped with a reverse-phase liquid chromatography nanospray (Thermo Fisher Scientific). The reverse phase column was slurry-packed in house with 5 μM, 200-A pore size C18 resin (Michrom BioResources) in a 100 μm $\times$ 10-cm fused silica capillary (Polymicro Technologies) with a laser-pulled tip. After sample injection, the column was washed for 5 min at 200 nl/min with 0.1% formic acid; peptides were eluted using a 50-min linear gradient from 0 to 40% acetonitrile and an additional step of 80% acetonitrile (all in 0.1% formic acid) for 5 min. The LTQ-MS was operated in a data-dependent mode in which each full MS scan was followed by five MS-MS scans, where the five most abundant molecular ions were dynamically selected and fragmented by collision-induced dissociation using normalized collision energy (35%). Tandem mass spectra were matched against the National Center for Biotechnology Information (NCBI) mouse database by SequestBioworks software (Thermo Fisher Scientific) using full tryptic cleavage constraints and static cysteine alkylation by iodoacetamide as well as by searching the peptides against a human protein database using Bioworks Browser software. For a peptide to be considered accurately detected, it had to be the top number one match and achieve cross-correlation scores of 1.9 for $[M + H]^{1+}$, 2.2 for $[M + 2H]^{2+}$, 3.5 for $[M + 3H]^{3+}$, $\Delta Cn > 0.1$, and a maximum probability of randomized identification of 0.01. The peptide hits were scanned for HTLV proteins based on a compilation of HTLV protein sequences from the NCBI protein database.

Laser Ablation Electrospray Ionization (LAESI) Mass Spectrometry to Detect Metabolites—The lipid metabolites in both HTLV-1-infected C81 and uninfected CEM cell exosomes were analyzed by LAESI-MS as described previously (63, 64). Briefly, laser ablation was performed by a mid-IR laser system. An optical parametric oscillator (Opolette 100, Opotek, Carlsbad, CA) converted the output of a 100-Hz repetition rate Nd:YAG laser to mid-IR pulses of 5-ns duration at 2,940-nm wavelength. Beam steering and focusing were accomplished by gold-coated mirrors (PF10-03-M01, Thorlabs, Newton, NJ) and a 150-mm focal length CaF_2 lens (Infrared Optical Products, Farmingdale, NY), respectively. At ~5–6 mm downstream from the tip of the spray capillary, the laser beam with average output energy of 0.3 mJ/pulse was used to ablate the tissue sample at a right angle. Optical microscopy of the burn pattern produced on a photographic paper indicated that the laser spot size was ~300 μm in diameter. Twenty micrograms of exosomes were used for LAESI, where the ion source was mounted on a Q-TOF Premier mass spectrometer (Waters, Milford, MA). Full scan mass spectra were recorded over the mass range of m/z 50–2,000 using a time-of-flight (TOF) analyzer at a resolution of 8,000 (full width at half-maximum). For structure identification of the metabolites, collision-induced dissociation spectra were recorded by selecting the precursor ion using a quadruple analyzer (transmission window 2 Da), and the product ions were resolved by the TOF analyzer. Argon was used as the collision gas at a typical collision cell pressure of 4×10^{-3} millibars and collision energy set between 5 and 25 eV. Accurate masses were determined using the internal standard method. Glycine, methionine, *N*-acetyl phenylalanine, leucine enkephalin, and glufibrinopeptide were dissolved at the appropriate concentrations (50–200 μM) in the electrospray solution and used as internal standards. Averages of the LAESI spectra collected under similar experimental conditions for a fixed time window were considered so that the approximate number of exosomes used for obtaining LAESI spectra was the same for all of the studied exosomes. The human metabolome database, the MassBank high resolution mass spectral database, the NIST/EPA/NIH mass spectral library, and the MetaCyc database were used with

a mass tolerance ranging from 0.1 to 0.01 Da for the metabolite searches and identifications.

Quantitative RT-PCR Analysis—For quantitative analysis of HTLV-1 RNA, total RNA was isolated from the exosome fraction of cell culture supernatants. RNA was isolated using TRI Reagent-LS (MRC, Cincinnati, OH) according to the manufacturer's protocol. A total of 0.5 μg of RNA from the RNA fraction was treated with 0.25 mg/ml DNase I RNase-free (Roche Applied Science) for 60 min in the presence of 5 mM $MgCl_2$, followed by heat inactivation at 65 °C for 15 min. A 250-ng aliquot of total RNA was used to generate cDNA with the GoScript Reverse Transcription System (Promega, Madison, WI) using oligo(dT) reverse primers. Subsequent quantitative real-time PCR analysis was performed with 2 μl of undiluted and 10^{-1} and 10^{-2} diluted aliquots of RT reaction mixes using iQ SYBR Green Supermix (Bio-Rad) with the following pairs of primers: 1) Tax-specific primers Tax-F (5′-CCCACTTCCCAGGGTTTGGACAGAG-3′) and Tax-R (5′-CTGTAGAGCTGAGCCGATAACGCG-3′); 2) 5′LTR-specific primers 5′-LTR-F (5′-AAGGTCAGGGCCCAGACTAAG-3′) and 5′-LTR-R (5′-GAGGTGAGGGGTTGTCGTCAA-3′); 3) HBZ-specific primers HBZ-F (5′-AACTGTCTAGTATAGCCATCA-3′) and HBZ-R (5′-CAAGGAGGAGGAGGAAGCTGTGC-3′); and 4) Env-specific primers Env-F (5′-CCATCGTTAGCGCTTCCAGCCCC-3′) and Env-R (5′-CGGGATCCTAGCGTGGGAACAGGT-3′). Serial dilutions of DNA from MT2 cells (T-cell line containing three integrated copies of HTLV-1 provirus per cell) were used as the quantitative standards. The β-globin gene was also quantified by real-time PCR using a set of β-globin-specific primers: forward primer BGF1 (5′-CAACCTCAAACAGACACCATGG-3′) and reverse primer BGR1 (5′-TCCACGTTCACCTTGCCC-3′). Real-time PCRs were carried out at least in triplicate using the PTC-200 Peltier thermal cycler with a Chromo4 continuous fluorescence detector (both from MJ Research) and Opticon Monitor version 2.03 software.

Reverse Transcriptase Assay—Exosome fraction (1 μg) from filtered cell culture supernatants (undiluted and 10^{-1} dilution) were incubated in a 96-well plate with RT reaction mixture containing 1× RT buffer (50 mM Tris-Cl, 1 mM DTT, 5 mM $MgCl_2$, and 20 mM KCl), 0.1% Triton, poly(A) (1 unit/ml), pd(T) (1 unit/ml), and [^{3}H]TTP. The mixture was incubated overnight at 37 °C, and 10 μl of the reaction mix was spotted on a diethylaminoethyl Filtermat paper, washed four times with 5% Na_2HPO_4 and three times with water, and then dried completely. RT activity was measured in a Betaplate counter (Wallac, Gaithersburg, MD).

Cytokine Array—Analysis of exosome cytokine profiles was conducted utilizing the RayBio® Human Cytokine Array 1 (RayBiotech, Norcross, GA) as per the manufacturer's instructions. Briefly, exosome fractions from filtered cell culture supernatants (7 μg) were lysed and incubated with blocked membranes for 2 h. After a series of washes at room temperature, biotin-conjugated primary antibody was added to the membrane for 2 h and washed, and membranes were developed using SuperSignal West Femto chemiluminescent substrate (Thermo Fisher Scientific) and visualized by a Bio-Rad molecular imager ChemiDoc XRS system (Bio-Rad).

Chloramphenicol Acetyltransferase (CAT) Assay—Plasmid (PU_3R-CAT) (5 μg) was transfected by electroporation using a Bio-Rad Gene Pulser at 960 microfarads and 230 V. This construct, which has been described previously, contains CAT cDNA positioned downstream of the HTLV-1 LTR (65). After 48 h, cells were collected, washed twice in PBS, and then lysed via two successive freeze-thaw cycles. Samples were heated for 3 min at 65 °C prior to centrifugation. Supernatants were used for enzymatic assays. CAT activity was determined using a standard reaction by adding acetyl coenzyme A to a microcentrifuge tube containing cell extract (5 μg) and radiolabeled (^{14}C) chloramphenicol (2 μl) in a final volume of 25 μl and incubating the mixture at 37 °C for 1 h. The reaction mixture was then extracted with ethyl acetate and separated by thin layer chromatography on silica gel plates (Baker-flex silica gel thin layer chromatography plates) in a chloroform/methanol (19:1) solvent. The resolved reaction products were exposed to a PhosphorImager cassette and imaged using the Storm 860 Molecular Imager (GE Healthcare).

Metabolic Labeling and Immunoprecipitation—Labeling experiments were performed on HEK-293T cells (1×10^6). Twelve hours postseeding, cells were treated in duplicate with either CEM or C81 exosomes (5 or 25 μg) in a reaction volume of 200 μl. Immediately following exosome treatment, cells were treated with 55 μCi/ml [^{35}S]methionine/cysteine for 6 h. After removal of the reaction volume, cellular extracts from corresponding treatments were collected as described above. Extracts (250 μl) were then incubated with IgG, α-Tax, α-HBZ (generous gift of Dr. Pat Green), or antiserum to HTLV-1, rotating overnight at 4 °C. The next day, 30 μl of a 30% slurry of Protein A + G beads (Calbiochem) was added to the reaction and incubated for 2 h, rotating at 4 °C. The immunoprecipitates were spun briefly, and beads were washed with radioimmune precipitation assay buffer, followed by two washes with TNE_{50} + 0.1% Nonidet P-40. Proteins were eluted off of the beads with Laemmli buffer and resolved in 4–20% Tris/glycine gels. Dried gels were exposed for 7 days and imaged using the PhosphorImager (GE Healthcare).

Apoptosis Protection Assay—Jurkat cells were seeded (3×10^4 cells) in exosome-free culture medium and pretreated with exosomes from CEM, C81, and ED(−) cells (0.5 μg) for 2 h. Next, α-FAS (0.5 μg) (clone CH11-05-201, which recognizes the human cell surface antigen Fas expressed in various human cells, including myeloid cells, T lymphoblastoid cells, and diploid fibroblasts) was added. After 24 h, cell viability was measured using the CellTiter-Glo cell luminescence viability kit (Promega) as per the manufacturer's instructions. Briefly, an equal volume of CellTiter-Glo reagent (100 μl) was added to the cell suspension (100 μl). The plate was shaken for ~10 min on an orbital shaker at room temperature, following which luminescence was detected using the GLOMAX multidetection system (Promega).

Testing Functionality of Exosomal-Tax in Primary Human Dendritic Cells—PBMCs from normal donors were processed to obtain fresh $CD1c^+$ myeloid dendritic cells using Miltenyi's kit as described (56). Purity of the cells was confirmed by flow cytometry, and 3×10^5 myeloid dendritic cells were cultured in 0.5 ml of AIM-V medium (Invitrogen) in a 24-well plate and

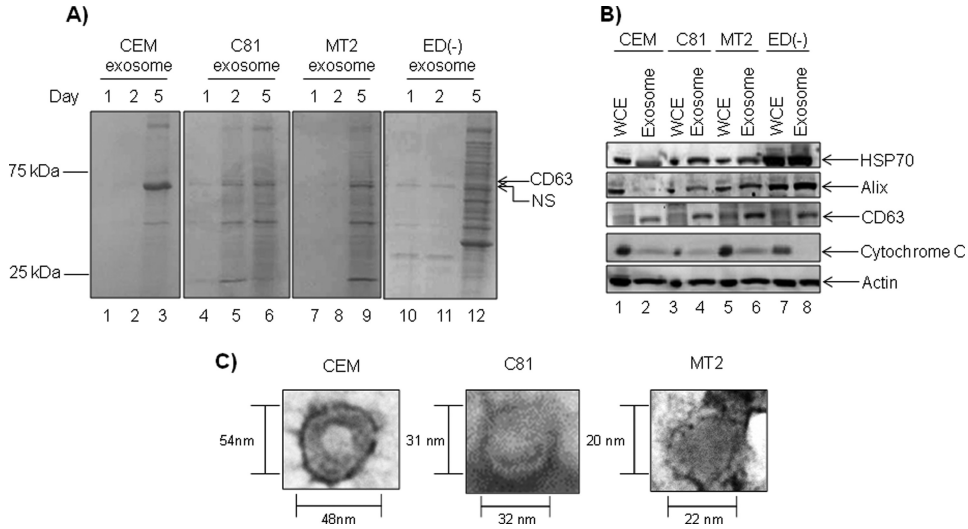

FIGURE 1. **Characterization of unfiltered exosomes derived from HTLV-infected cells.** *A*, exosome fractions were collected from cell culture supernatants 1, 2, and 5 days post-seeding in exosome-free medium. Equivalent amounts of exosomes isolated from uninfected CEM and HTLV-1-positive C81, MT2, and ED(−) cells were resolved on 4–20% Tris/glycine gels and analyzed by Coomassie Blue staining. *B*, CEM, C81, MT2, and ED(−)-derived exosomes (10 μg) and corresponding WCE collected 5 days postseeding were analyzed via Western blot using antibodies against HSP70, Alix, CD63, cytochrome *c*, and β-actin. *C*, transmission electron microscopy image analysis of CEM-, C81-, and MT2-derived exosomes are shown at ×75,000 magnification.

either left untreated or treated with exosomes from C81, CEM, and ED(−) cells (5 μg of total protein) for 48 h. Cell-free Tax was also included at (50 nM) as per previously published studies (56, 66–68). Culture supernatants from triplicate sample sets were used to measure the concentration (pg/ml) of a panel of 12 cytokines (IL-2, IL-4, IL-5, IL-6, IL-10, IL-12, IL-13, IL-17A, IFN-γ, TNF-α, G-CSF, and TGF-β1) using a human Th1/Th2/Th17 cytokine multianalyte ELISArray according to the manufacturer's protocol (SABiosciences, Frederick, MD) and as described (69).

Statistical Analysis—Significance between groups was determined by Student's *t* test.

RESULTS

Characterization of Exosomes Derived from HTLV-1-infected Cells—To characterize the exosome population secreted by CEM, C81, MT2, and ED(−) cell lines, we first examined the kinetics of exosome release. To determine the optimal time point for exosome collection, we cultured each cell type in exosome-depleted medium and isolated exosomes from the supernatants after 1, 2, and 5 days. We followed this time scale due to our previous experience at collecting exosomes from T-cell lines, including Jurkat and HIV-1-infected J1.1 cells (70). First, a series of low speed centrifugation steps was employed to remove whole cells and cellular debris from cell culture supernatants prior to ultracentrifugation, followed by a series of ultracentrifugation steps without filtration to enrich for all possible vesicles, including exosomes from cell culture supernatants. The enriched exosomal content, as well as corresponding whole cell extracts (WCEs), was resolved on a 4–20% Tris/glycine gel and stained with Coomassie Blue to illustrate total protein yields (Fig. 1*A*). This demonstrated that cell culture supernatants collected on the 5th day contained the highest levels of total protein in the exosome fraction from CEM, C81, MT2, and ED(−) cells (Fig. 1*A*, *lanes 3*, *6*, *9*, and *12*). Therefore, all of our subsequent experiments utilized day 5 for the time point of exosome collection.

It is established that the budding of exosomes from invaginations of late endosomal membranes allows for the incorporation of specific host components into exosomes, such as exosomal marker proteins HSP70, Alix, CD63, and β-actin (71). Therefore, we asked whether the 5-day-old exosomes enriched from cell culture supernatants contained these proteins. As a negative control, these exosome vesicles should exclude cell-specific proteins, such as cytochrome *c*. Western blot analysis of exosomes and corresponding WCEs demonstrate that CEM, C81, and MT2 exosomes incorporated HSP70, Alix, CD63, and β-actin and mostly excluded cytochrome *c* (Fig. 1*B*). Western blot analysis revealed increasing levels of Alix in C81 and MT2 exosomes compared with CEM exosomes, whereas ED(−) exosomes contained the highest levels of Alix. A similar trend was observed with HSP70, indicating that HTLV-1 infection could play a role in the incorporation of host proteins into exosomes. Levels of β-actin remained comparable between exosomes from the cell lines investigated. The exclusion of cytochrome *c* indicated that our exosome preparations contain low levels of contamination from cellular debris or other vesicles (Fig. 1*B*, *lanes 2*, *4*, *6*, and *8*). Also, the cellular proteins incorporated in HTLV-1-infected exosomes correlate with our previous findings that exosomes produced by HIV-infected cells incorporate increased levels of tetraspanins, such as CD45 and CD63 (70). Taken together, these results imply that infection could increase the incorporation of certain host proteins into released exosomes.

Finally, to confirm that the vesicles enriched in our preparations display standard morphological features, such as cup-shaped vesicles with a diameter range of 30–100 nm, TEM images were obtained of our CEM, C81, and MT2 exosome preparations (Fig. 1*C*). After measuring the diameter of multiple CEM, C81, and MT2 vesicles from the purified fractions, we found that CEM exosomes were slightly larger in size than the C81 and MT2 exosomes. The CEM exosomes measured approximately between 31 and 72 nm in diameter, C81 exo-

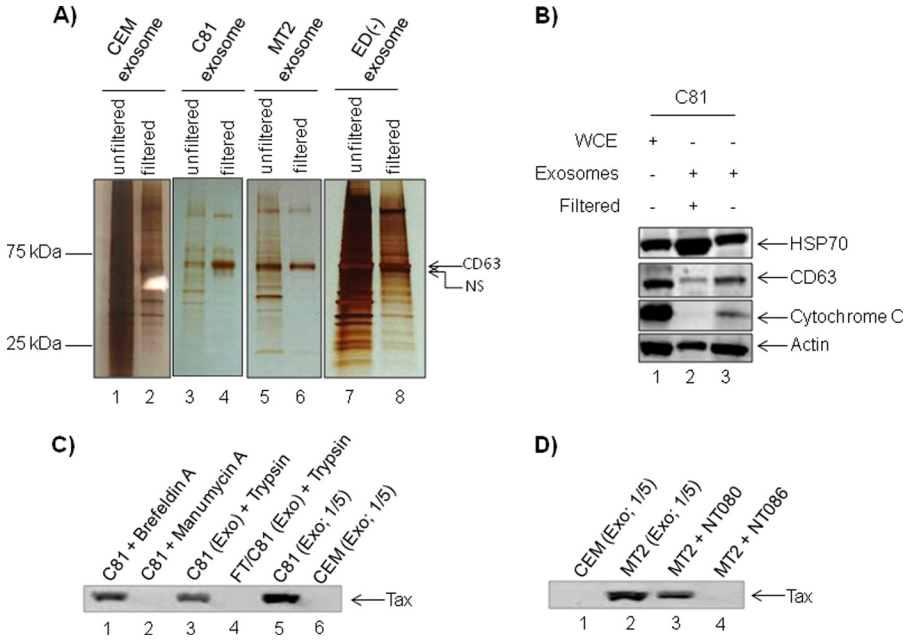

FIGURE 2. **Specific enrichment of exosomes.** *A*, aliquots of 50 ml (5-day-old cultures) of CEM, C81, MT2, and ED(−) cell culture supernatants were clarified by filtration (0.22 μm), whereas 50 ml of each supernatant were left unfiltered. Exosomes (1 μg) isolated from both filtered and unfiltered supernatants were resolved on 4–20% Tris/glycine gels and analyzed by silver staining. *B*, C81 exosomes from both filtered (9 μg) and unfiltered (7 μg) supernatants and corresponding WCE (10 μg) were evaluated for the incorporation of common exosome markers by Western blot using HSP70, CD63, cytochrome *c*, and actin antibodies. *C*, cells were treated with brefeldin A or manumycin A, and the resulting supernatant was collected after 48 h for exosomal preparation (*lanes 1* and *2*), or exosomes obtained from C81 cells were trypsin-treated or freeze/thawed (*F/T*) and then trypsin-treated (*lanes 3* and *4*). *Lanes 5* and *6*, input exosome controls from C81 or CEM cells, respectively. Resulting exosomes were assayed for the presence of Tax by Western blotting. *D*, exosomes from MT2 cells were enriched by trapping with nanotrap particles NT080 (*lane 3*) or NT086 (*lane 4*) to enrich for virions. *Lanes 1* and *2*, are exosomal controls from CEM or MT2 cells, respectively. The trapped exosomes were assayed for the presence of Tax by Western blotting.

somes averaged 31 nm in diameter, and MT2 exosomes averaged 21 nm in diameter. The representative TEM image analysis of exosomes from each cell type revealed the typical cup-shaped morphology, with an electron-dense lipid bilayer and concave interior (Fig. 1*C*). Thus, regardless of infection status, the isolated vesicles display diameter sizes and morphologies consistent with the currently accepted standards for exosomes (25, 43, 72). Collectively, these results indicated that exosomes can be enriched from both uninfected and HTLV-1-infected unfiltered T-cell culture supernatants.

Specific Enrichment of Exosomes by Filtration Method—In response to various environmental stimuli, cells produce heterogeneous populations of apoptotic blebs and microparticles, which could potentially be co-enriched during ultracentrifugation (73). In addition, the presence of histones and low levels of cytochrome *c* observed in our previous exosome preparations prompted us to address our enrichment methods. We therefore modified our protocol and subjected cell culture supernatants to filtration using 0.22-μm hydrophilic polyethersulfone membranes to remove contaminating cell debris and larger vesicles, particularly apoptotic blebs ranging in diameter from 100 to 1000 nm (42). Based on size exclusion of vesicles over 220 nm, which includes a large subset of apoptotic blebs, as well as the hydrophilic nature of polyethersulfone membranes, this filtration step permits the passage of exosomes (74, 75).

To determine the extent of vesicular enrichment, we collected 5-day-old cell culture supernatants from CEM, C81, MT2, and ED(−) cells, subjected half of the supernatant volume to 0.22-μm filtration, and left the remaining volume unfiltered. Postultracentrifugation, we reconstituted the enriched exosomes in equal volumes of PBS. After loading equal volumes of each exosome preparation, the silver-stained gels demonstrated a reduction in the amount of total proteins for each of the exosome preparations after filtration (Fig. 2*A*, *lanes 2*, *4*, *6*, and *8*) as compared with the unfiltered counterparts (Fig. 2*A*, *lanes 1*, *3*, *5*, and *7*). We observed an enhancement of CD63 band in most preparations. To determine the specificity of filtration, we next examined protein levels of HSP70, CD63, cytochrome *c*, and β-actin in C81 exosomes produced with or without filtration (Fig. 2*B*). Western blot analysis of filtered and unfiltered C81 exosomes revealed the presence of HSP70, CD63, and β-actin in both filtered and unfiltered exosomes. Whereas HSP70 levels appeared elevated in filtered C81 exosomes (Fig. 2*B*, *lane 2*), the levels of CD63, cytochrome *c*, and β-actin were somewhat reduced as compared with the unfiltered counterpart (Fig. 2*B*, *lanes 2* and *3*). These findings are consistent with our reduction in total protein after filtration (Fig. 2*A*). Levels of HSP70, Alix, CD63, β-actin, and cytochrome *c* in unfiltered exosomes closely agree with the previously observed levels of these proteins (Fig. 1*B*, *lane 4*). Taken together, these results indicate that a simple filtration of cell culture supernatants removes contaminating cell debris and other larger microvesicles, ultimately yielding a more uniform exosome population. We therefore used filtration of cell culture supernatants for all subsequent exosome preparations.

Exosomal Inhibitors and Nanotrap Particles Confirm Presence of Tax within Exosomes—After screening exosomes for the presence of Tax, we carried out experiments to show that Tax was indeed internal and exosomal. Because we have previously used exosomal inhibitor (manumycin A to inhibit exosomes

production) and protein trafficking inhibitor (brefeldin A to inhibit virus budding),[4] we used these two reagents to confirm the presence of Tax within exosomal and not viral particles. As we have previously observed, brefeldin A did not inhibit exosomal/Tax release, but manumycin A treatment inhibited exosome formation and by inference the absence of Tax in exosomes (Fig. 2*C*, compare *lane 1* with *lane 2*). We next attempted to determine whether Tax was either in free form or nonspecifically attached to the outer membrane of exosomes. As a control, we freeze-thawed exosomes to release its contents and asked whether Tax would be susceptible to protease treatment (*i.e.* trypsin). Results in Fig. 2*C* indicate that Tax is protected from trypsin when exosomes are intact (Fig. 2*C*, compare *lanes 3* and *4*). Exosomal samples in *lanes 5* and *6* served as control input. Finally, we asked whether exosomes could be separated from virus from cells that produce both exosomes and virus (*i.e.* MT2 cells). We have recently shown that specific nanoparticles can be used to separate exosomes from virus in complex fluids (62). We therefore utilized supernatant from MT2 cells, which contains both virus and exosomes, for binding to two different nanoparticles. Results in Fig. 2*D* indicate that NT080 particles, which specifically trap exosomes, contained Tax, whereas NT086 particles, which normally trap virus, did not show the presence of Tax. Collectively, these data indicate that Tax is present within exosomes and protected from extracellular proteases.

Exosomes Released by HTLV-1-infected Cells Contain Unique Host Proteins—Exosomes released by HIV-1-infected cells contain different proteomic profiles, specifically with the incorporation of viral proteins including Nef (51, 52). Our previous data indicated that HIV-1 infection alters the incorporation of host proteins into exosomes (70). Because our results also indicated that HTLV-1 infection altered the levels of HSP70 and Alix incorporated into exosomes (Figs. 1*B* and 2*B*), we hypothesized that HTLV-1 infection could influence the incorporation of both host and viral proteins into exosomes. Therefore, we next characterized the proteome of exosomes from CEM, C81, and MT2 exosomes via LC-MS/MS.

Approximately 180 host proteins were present in these exosomes, as determined by LC-MS/MS analysis. The complete proteomic profiles of exosomes from CEM, C81, MT2, and ED(−) cells are included in supplemental Table 1. We successfully identified 6 of the 11 proteins documented for T-cell exosomes in the ExoCarta database, including MHCII, integrin β2, MCHI, CD81, CD63, and FASLG. However, we found more than 160 proteins that have not yet been reported in T-cell-derived exosomes in the Exocarta database. The total number of proteins identified in the T-cell line-derived exosomes appears to be approximately half the number documented for exosomes derived from various other cancer cells, including colon and bladder cancer (72, 76).

On average, we identified 90–100 commonly incorporated proteins based upon the following individual comparisons: C81 *versus* CEM, MT2 *versus* CEM, and ED(−) *versus* CEM exosomes. Among exosomes from all cell lines, 54 proteins were found to be common. This represents a much larger body of standard proteins incorporated into exosomes derived from T-cells than previously documented. Functional classification of these 54 proteins revealed an abundance of nucleic acid binding components, followed by proteins involved in regulating cytoskeletal dynamics, cellular metabolism, protein folding, ion transport, and signaling (Fig. 3*A*).

We next investigated the incorporation of host proteins into exosomes as a result of HTLV-1 infection. We therefore excluded all host proteins common to CEM exosomes as compared with C81, MT2, and ED(−) exosomes because these proteins were present in uninfected exosomes. For further analysis, we generated a three-way Venn diagram to compare the protein content among exosomes from HTLV-1-infected, Tax-positive C81 and MT2 cells and HTLV-1-infected, Tax-negative ED(−) cells (Fig. 3*B*).

Importantly, we have identified two proteins, major histocompatibility class I A precursor and F isoform 2 precursor, common to exosomes from all HTLV-1-infected cell lines investigated, indicating that these two host proteins were specifically incorporated due to HTLV-1 infection. Furthermore, six proteins were common between C81 and MT2 exosomes but not ED(−) exosomes (Fig. 3*B*). These proteins included cofilin 2, eukaryotic translation elongation factor 1 α1, major histocompatibility complex class I E precursor, ribosomal protein L23, Thy-1 cell surface antigen preprotein, and tryptophanyl-tRNA synthetase isoform α. Interestingly, five other proteins were found to be common between MT2 and ED(−) exosomes. These proteins include β-2-microglobulin precursor, bisphosphoglycerate mutase 1, major histocompatibility complex class I B and C precursors, and tubulin. Comparison between C81 and ED(−) exosomes revealed six shared proteins, including α-fetoprotein precursor, H2A histone family member Y2, histone cluster 2ab, ribosomal proteins P1 isoform 1 and S26, and tyrosine 3/tryptophan 5-monooxygenase activation protein, θ-polypeptide (Fig. 3*B*).

Functionally, half of the proteins, shared among C81 or MT2 exosomes, are involved in transcription and translation, whereas the remaining proteins function in a variety of processes, including antigen processing and presentation, cytoskeletal dynamics, and T-cell receptor signaling. Collectively, these results indicate that specific subsets of host proteins incorporated into HTLV-1-derived exosomes may be Tax-dependent.

Finally, to determine whether the lipid contents of exosomes may also provide some pathophysiological differences in HTLV-1 infection, the lipid metabolites of exosomes from HTLV-1-infected C81 and uninfected CEM cells were analyzed by LAESI MS (see supplemental Table 1) and Fig. 3*C*) (63, 64). The unique feature of this method is that the samples do not have to be processed, and no front-end purifications are required to analyze the samples. Interestingly, a number of lipid metabolites, such as diacylglycerol, phosphatidylethanolamine, phosphatidylcholine, and phosphatidylglycerol, were identified from both types of exosomes with varying molecular weights. These apparent changes in the HTLV-1 exosomes may point

[4] E. Jaworski, A. Narayanan, R. Van Duyne, S. Shabbeer-Meyering, S. Iordanskiy, M. Saifuddin, R. Das, P. V. Afonso, G. C. Sampey, M. Chung, A. Popratiloff, B. Shrestha, M. Sehgal, P. Jain, A. Vertes, R. Mahieux, and F. Kashanchi, unpublished results.

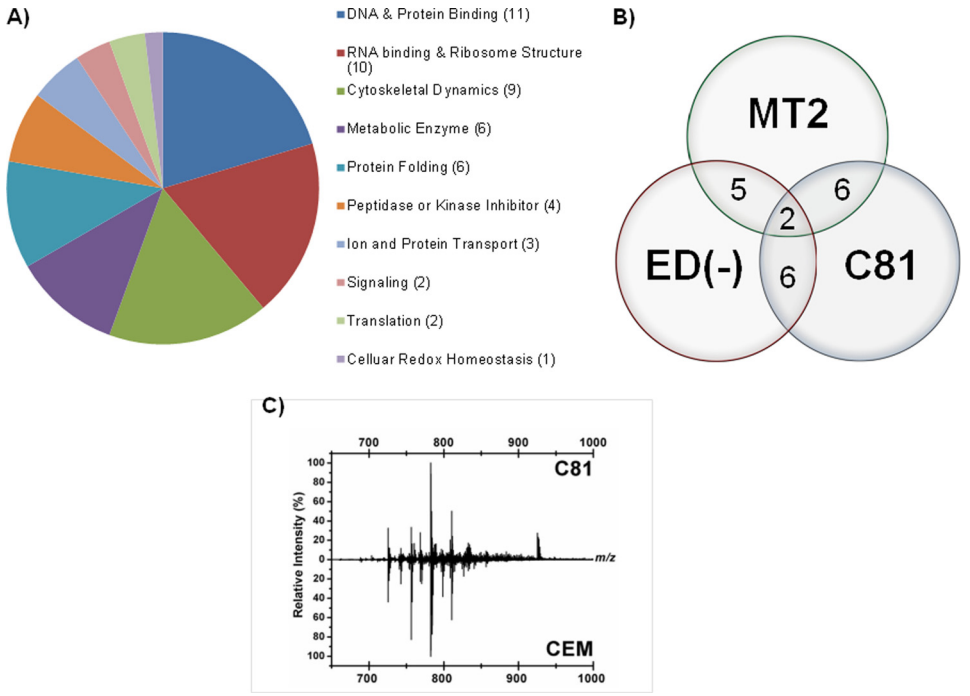

FIGURE 3. **Exosomes released by HTLV-1-infected cells contain unique host proteins and lipids.** *A*, exosomes derived from uninfected CEM and HTLV-1-positive C81, MT2, and ED(−) cell culture supernatants were analyzed by LC-MS/MS to determine the host proteomic profile. A total of 54 proteins were common to exosomes from all uninfected and infected cell types tested. Classification of shared host proteins according to function are included. *B*, after discounting exosomal host proteins common to exosomes from both uninfected and infected cell types, the numbers of specific host proteins incorporated into exosomes released from three HTLV-1-infected cell lines (C81, MT2, and ED(−)) are shown. *C*, relative intensities of various lipid metabolites present in the HTLV-1-infected C81 and uninfected CEM cell exosomes were measured by LAESI-MS.

toward their involvement in maturation and/or release of their virions. Collectively, these results imply that HTLV-1-infected cells and exosomes from these cells may have altered lipid content, as evident from the lower levels of phosphatidylserine and phosphatidylinositol in infected exosomes.

Validation of Viral Proteins Incorporated into Exosomes—In the case of oncogenic viral infections, Epstein-Barr virus-associated nasopharyngeal cancer (NPC) (77), it has been shown that infected cells produce exosomes, which deliver functional viral proteins and ultimately influence signal transduction pathways in target cells (30, 78). We therefore evaluated the preferential inclusion of viral proteins into the HTLV-1-derived exosomes, which could then function to support viral infection. Our LC-MS/MS analysis for viral proteins within the exosomes revealed the presence of envelope surface glycoprotein (gp46) and Gag, Gag-Pro, and Gag-Pro-Pol polyprotein within the MT2 exosomes only. However, we were unable to detect reasonable peptide hits corresponding to other viral proteins in C81 and ED(−) exosomes. For greater sensitivity, we performed a Western blot analysis, which revealed the presence of Tax in exosomes from C81 and MT2 (Fig. 4*A*, *lanes 4* and *6*). As expected, CEM and ED(−) exosomes failed to contain Tax (Fig. 4*A*, *lanes 2* and *8*).

Additionally, the presence of gp46 in MT2 exosomes only (Fig. 4*A*, *lane 6*) but not in exosomes from C81 and ED(−) confirmed our LC-MS/MS data (Fig. 4*A*, compare *lane 6* with *lanes 2* and *8*). We found that MT2 exosomes, but not C81 or ED(−), incorporated HTLV-1 capsid protein (p24) at levels detectable by Western blot (Fig. 4*A*, *lane 6*). In addition, we were unable to detect HBZ protein in the exosomes (data not shown).

To confirm that the incorporation of viral proteins is a direct result of infection and not a cell type phenomenon, we electroporated Jurkat T-cells (5×10^7 cells/ml) with an infectious HTLV-1 clone, pACH, and enriched for exosomes. Transfected cells were maintained in exosome-free medium for 5 days, at which time cell culture supernatants were collected for isolation of exosomes. Western blot analysis demonstrated the inclusion of Tax in exosomes released from infected Jurkat cells, albeit at low levels compared with other exosome proteins (Fig. 4*B*, *lane 2*). To better evaluate the effect of HTLV-1 infection on protein incorporation into exosomes, we obtained raw densitometry counts of Tax, Alix, HSP70, CD63, and β-actin (Fig. 4*C*). Other than Tax, none of the other proteins showed a dramatic difference between transfected and untransfected cells.

To determine the functional impacts of exosomal Tax, we set out to discern whether Tax could transactivate the HTLV-1 LTR in target recipient cells. To detect Tax-mediated HTLV-LTR transcription, we conducted a CAT reporter assay with extracts collected from CEM cells (5×10^6 cells) transfected with PU_3R-CAT and titrated with CEM or C81 exosomes (0.1, 1.0, or 10 μg) (Fig. 4*D*). As a positive control experiment, we utilized *Escherichia coli* purified Tax protein. We did not detect viral LTR transcription above basal levels after treatment with CEM exosomes (Fig. 4*D*, *lanes 4–6*). However, we observed a dose-dependent response in Tax-mediated LTR transcription upon treatment with C81 exosomes (Fig. 4*D*, *lanes 7–9*). To

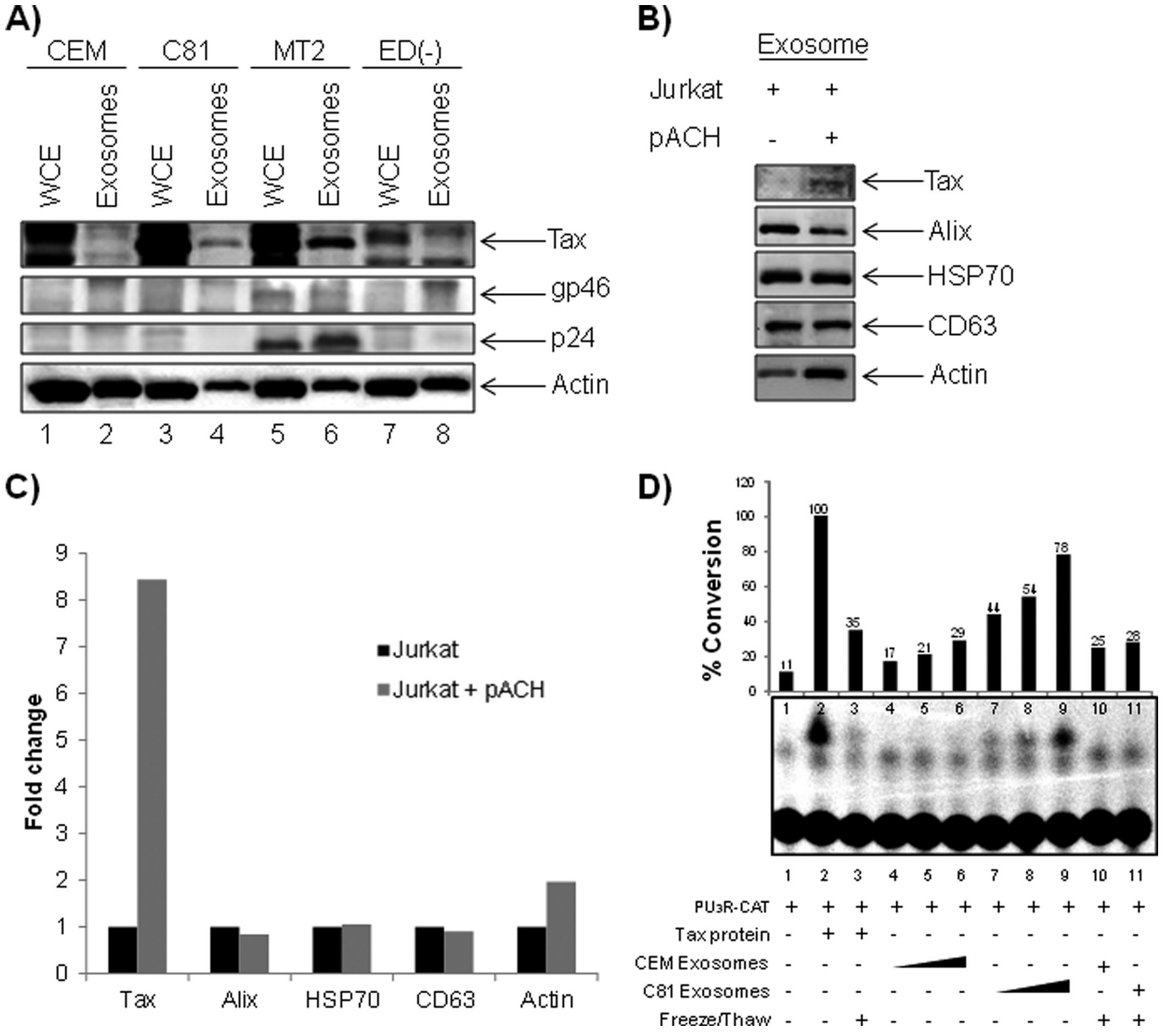

FIGURE 4. **Validation of viral proteins incorporated into exosomes.** *A*, exosomes from HTLV-1-infected cells were evaluated for the presence of viral proteins by LC-MS/MS analysis, and the results were validated by Western blot using α-Tax monoclonal antibody and antiserum to HTLV-I (which reacts with gp46 and p24). *B*, Jurkat cells (1×10^6 cells/ml) were transfected with 30 μg of pACH (an infectious HTLV-1 clone), and exosomes were isolated 5 days post-transfection. Exosome samples (10 μg) were assayed for the presence of HTLV-1 Tax, Alix, HSP70, CD63, and actin via Western blot. *C*, Raw densitometry counts were obtained from the Western blot analysis of *B*. *D*, uninfected CEM cells (5×10^6) were transfected with PU_3R-CAT plasmid by electroporation and then exposed to CEM- or C81-derived exosomes (0.1, 1.0, and 10 μg) or Tax protein. Samples were kept in complete medium for 48 h. The transfected CEM cells were also treated with Tax protein or each exosome following inactivation by three cycles of freeze and thaw. Detection of Tax-mediated transactivation of the HTLV-LTR promoter was measured via a chloramphenicol transferase assay.

confirm that this transcription was a direct result of functional Tax, we subjected the CEM and C81 exosomes to five sequential freeze-thaw cycles before incubation with target cells. This step rendered the Tax protein non-functional (Fig. 4*D*, *lanes 3* and *11*). Accordingly, we observed a reduction in LTR transcription in samples treated with inactivated C81 exosomes. Collectively, these data indicate that Tax present in exosomes may be functional by activating a responsive promoter.

Exosomes Derived from HTLV-1-infected Cells Contain Viral mRNA Transcripts—Previous reports have shown the presence of functional mRNA in exosomes isolated from cancer cells (79–82). Therefore, we next attempted to investigate the presence of viral mRNA transcripts in exosomes derived from HTLV-1-infected cells. We carried out quantitative RT-PCR analysis for the presence of HTLV-1 *env*, *tax*, *hbz*, and 5′-LTR transcripts within exosomes derived from CEM, C81, MT2, and ED(−) cells. After normalizing the data to β-globin within the samples, our results show that C81 and ED(−) exosomes each contained less than 10 total copies of *tax*, *hbz*, and 5′-LTR mRNA, whereas MT2 exosomes contained a vast excess of these transcripts (5 logs) for *tax*, *hbz*, and 5′-LTR mRNAs (Fig. 5*A*). As expected, we failed to observe the presence of viral transcripts in the exosomes from uninfected CEM cells.

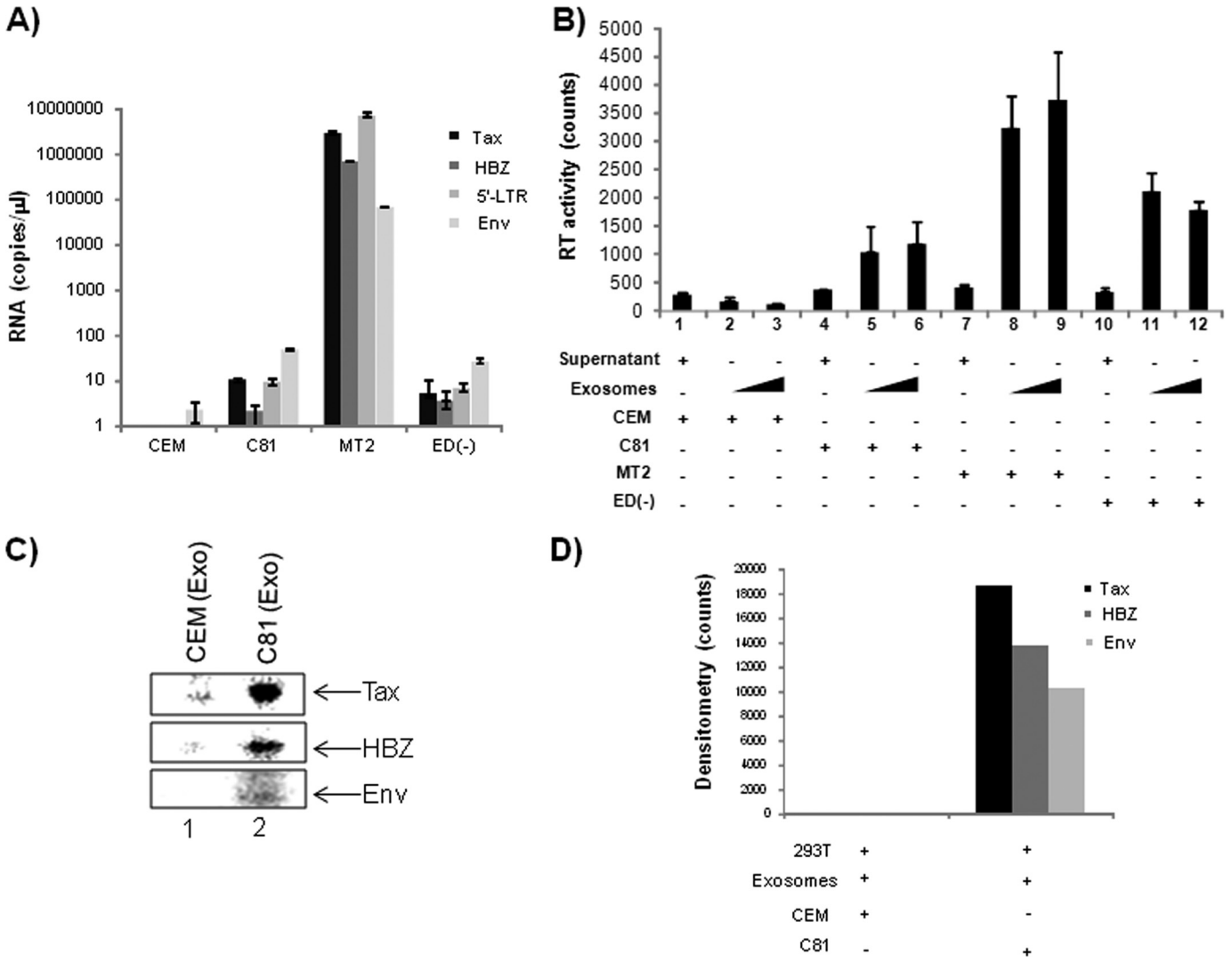

FIGURE 5. **Exosomes derived from HTLV-1-infected cells contain viral mRNA transcripts.** *A*, total RNA was isolated from exosomes derived from CEM, C81, MT2, and ED(−) cells and subjected to quantitative RT-PCR in triplicate using primers specific for HTLV-1 Tax, HBZ, 5′-LTR, and Env. Results presented are mean ± S.D. (*error bars*) after normalization to β-globin. *B*, both cell culture supernatants and exosomes (undiluted and 10^{-1}) derived from CEM, C81, MT2, and ED(−) cells were analyzed for RT activity. *C*, 293T cells (1×10^6 cells) were seeded for 12 h, exposed to CEM- or C81-derived exosomes (10 μg) for 2 h, and then labeled with ^{35}S label for 4 h. After lysis, cellular extracts were subjected to co-immunoprecipitation using IgG, α-Tax, α-HBZ, or α-Env antibody (3 μg each) overnight at 4 °C. The next day, Protein A + G was added, and samples were washed with radioimmune precipitation assay buffer and then TNE50 + 0.1% Nonidet P-40. Washed immunoprecipitated complexes were resolved on 4–20% Tris/glycine gels, dried, and imaged using a PhosphorImager. *D*, raw densitometry counts of images from the PhosphorImager were obtained using ImageJ, and results were normalized to IgG counts before plotting.

The high levels of *tax*, *hbz*, and 5′-LTR present in MT2 exosomes indicated the potential contamination of MT2 exosome preparations with HTLV-1 virions. To address this possibility, we performed a reverse transcriptase assay of undiluted and 10^{-1} diluted exosome samples to evaluate the presence of virus in these preparations (Fig. 5*B*). When analyzing for RT activity, we consistently observed higher levels of RT in exosomes from MT2 cells, indicating that our MT2 preparations may be contaminated with virus. Unlike other viral proteins, which can be freely present in the extracellular environment, RT is normally used to detect functional viral particles. The RT activity in C81 and ED(−) cells may be an indication of RT incorporation into exosomes. Neither of these two cell types contains wild type virus in its genome. Collectively, our results indicate the absence of full-length viral transcripts in C81 and ED(−) exosomes while demonstrating abundant viral mRNA transcripts of *tax*, *hbz*, and 5′-LTR in MT2 exosomes. The lack of 5′-LTR transcripts in C81 and ED(−) exosomes further supports the absence of virus (genomic RNA) in these exosomes, whereas the virions produced by MT2 cells may be co-enriched with exosomes from MT2 cells.

In order to evaluate the functional capacity of the viral transcripts contained within exosomes, we conducted metabolic pulse labeling experiments. 293T cells were treated with CEM or C81 exosomes, followed by the addition of [^{35}S]methionine/cysteine to label new protein synthesis. Labeled cells were then lysed and used for co-immunoprecipitation with α-Tax, α-HBZ, α-Env, and IgG control. The co-immunoprecipitated material was washed and run on a 4–20% SDS-polyacrylamide gel and dried, and bands were quantified using densitometry (Fig. 5*C*). We observed significant counts from all three ORFs in C81 exosomes but more from Tax protein (Fig. 5*D*). As

expected, there were small counts in CEM exosomes, which were considered as background. This indicates that the Tax mRNA in C81 exosomes may be translated in the recipient cells.

C81, MT2, and ED(−) Cell Lines Contain Inflammatory Mediators—Many of the pathological effects observed from HTLV-1 infection result from chronic inflammation, particularly degeneration of the neuronal cells in the central nervous system (CNS), as observed in HAM/TSP patients. To explain the mechanism underlying this neurodegeneration, the "bystander damage" hypothesis suggests that HTLV-1 infected $CD4^+$ cells are activated, migrate across the blood-brain barrier, enter the central nervous system, and begin to express viral antigens. This triggers the production and secretion of proinflammatory cytokines and chemokines (5, 83–85). Furthermore, it has been reported that serum from HAM/TSP patients contains a proinflammatory cytokine signature different from those of asymptomatic carriers (86, 87). Because it has been demonstrated that exosomes secreted by astrocytoma brain tumor cells contain cytokines, including TGF-β, we next asked whether exosomes released from HTLV-1-infected cells contained cytokines (88, 89).

To evaluate the capacity in which exosomes are involved in cytokine signaling, we first asked whether the exosomes derived from HTLV-1-infected cells contained proinflammatory cytokines. Because we were unable to detect the reasonable peptide hits corresponding to cytokines in our LC-MS/MS analysis (data not shown), we further explored the incorporation of these inflammatory mediators via a specific antigen-antibody reaction. We collected exosomes from CEM, C81, MT2, and ED(−) cell culture supernatants and then employed the RayBio® human cytokine array, a detection method utilizing a sandwich enzyme-linked immunosorbent assay (ELISA) using a mixture of biotinylated primary cytokine-specific antibodies and HRP-conjugated streptavidin. Based on signal intensities, our initial analysis revealed distinct cytokine profiles for CEM, C81, MT2, and ED(−) exosomes. We noted elevated levels of GM-CSF and IL-6 in exosomes released from infected cells. We then observed a drastic reduction in levels of MCP-1 (monocyte chemotactic protein 1) and RANTES (regulated upon activation normal T-cell-expressed and secreted) in exosomes derived from C81, MT2, and ED(−) cells as compared with those of CEM. Furthermore, levels of IL-1a and IL-8 remained consistent in exosomes collected from all cell types.

In order to more accurately evaluate the levels of cytokine incorporation within the exosomes, we obtained and compared raw densitometry counts for each cytokine-specific signal in CEM, C81, MT2, and ED(−) exosomes (Fig. 6, *A* and *B*). We then grouped the cytokines based upon the following parameters: Tax-dependent expression, HTLV-1 infection-dependent expression, and whether these cytokines were up- or down-regulated in each case. Cytokines that were present at more than 2-fold of the level found in CEM exosomes were considered to be up-regulated, whereas cytokines present at less than 1-fold of CEM levels were considered as down-regulated. To establish the subset of cytokines that remained unchanged, we considered only signal intensities that fell between 0.9- and 1.2-fold of the mean value for CEM, C81, MT2 and ED(−) exosomes. Along these lines, we confirmed that IL-1a and IL-8 levels remained unchanged in exosomes from all cell types (Fig. 6*A*, *Group 1*). We observed a greater than 2-fold increase of Gro, Gro-α, and GM-CSF in C81 and MT2 exosomes but not ED(−), potentially indicating a Tax-dependent inclusion in exosomes (Fig. 6*A*, *Group 2*). We further detected enhanced IL-6 incorporation into C81, MT2, and ED(−) exosomes, indicating that these cytokines were incorporated into exosomes in an HTLV-1 infection-dependent manner (Fig. 6*A*, *Group 3*).

It has been shown that co-culturing human umbilical vein endothelial cells with MT2 cells induces the production of GM-CSF and that Tax may play a role in GM-CSF production via transactivation of the GM-CSF promoter. Furthermore, elevated levels of GM-CSF are found within tail tumors of Tax-transgenic mice (90–92). Although elevated levels of GM-CSF present in ED(−) exosomes indicate a Tax-independent mechanism of incorporation, our results suggest that HTLV-1 infection alters the profile of inflammatory mediators within cytokines.

Importantly, we observed a drastic reduction in the abundance of MCP-1 and RANTES contained within exosomes derived from all HTLV-1-infected cells (Fig. 6*B*, *Group 2*). Previously, it has been reported that serum levels of MCP-1 are diminished in infected patients (93). However, enhanced levels of RANTES production and secretion have been documented in adult T-cell leukemia cell lines and PBMCs collected from HAM/TSP patients (94, 95). Although it appears that exosomes do not contribute to the increased abundance of RANTES during HTLV-1 infection, it is possible that HTLV-1 infection or Tax expression could influence the production and secretion of other proinflammatory cytokines, including IL-6, via exosomes.

We next addressed a possible mechanism by which the intra-exosomal cytokines could be released into the extracellular space in order to act on recipient target cells. Our reasoning for asking this question was that cytokines act as extracellular signaling proteins, where they bind to specific receptors on recipient cells and induce intracellular transduction. The sequestration of cytokines inside an exosome would presumably defeat the general purpose of cytokines because they would not come into contact with the extracellular domain of their corresponding receptor on a target cell. Therefore, we focused on the possible role of active transporters of cytokines that could be present in exosomes. Recently, ATP-binding cassette (ABC) transporters have been implicated in neurodegenerative disorders with the capability of releasing chemokines into the extracellular milieu (96, 97). We therefore hypothesized that these inflammatory molecules could be released from the exosomes into the extracellular space to then bind membrane-associated receptors on target cells. To explore this possibility, we subjected exosomes from CEM, C81, MT2, and ED(−) cells to Western blot analysis for a number of receptors, including MDR-1 (multidrug resistance protein 1), an ABC transporter shown to be present in T-cells (Fig. 6*C*). Results indicated the presence of MDR-1 in exosomes from all cell types (Fig. 6*C*, *lanes 2*, *4*, *6*, and *8*), regardless of infection.

To determine whether the MDR-1 or any other transport mechanism that will allow the intracellular components to be

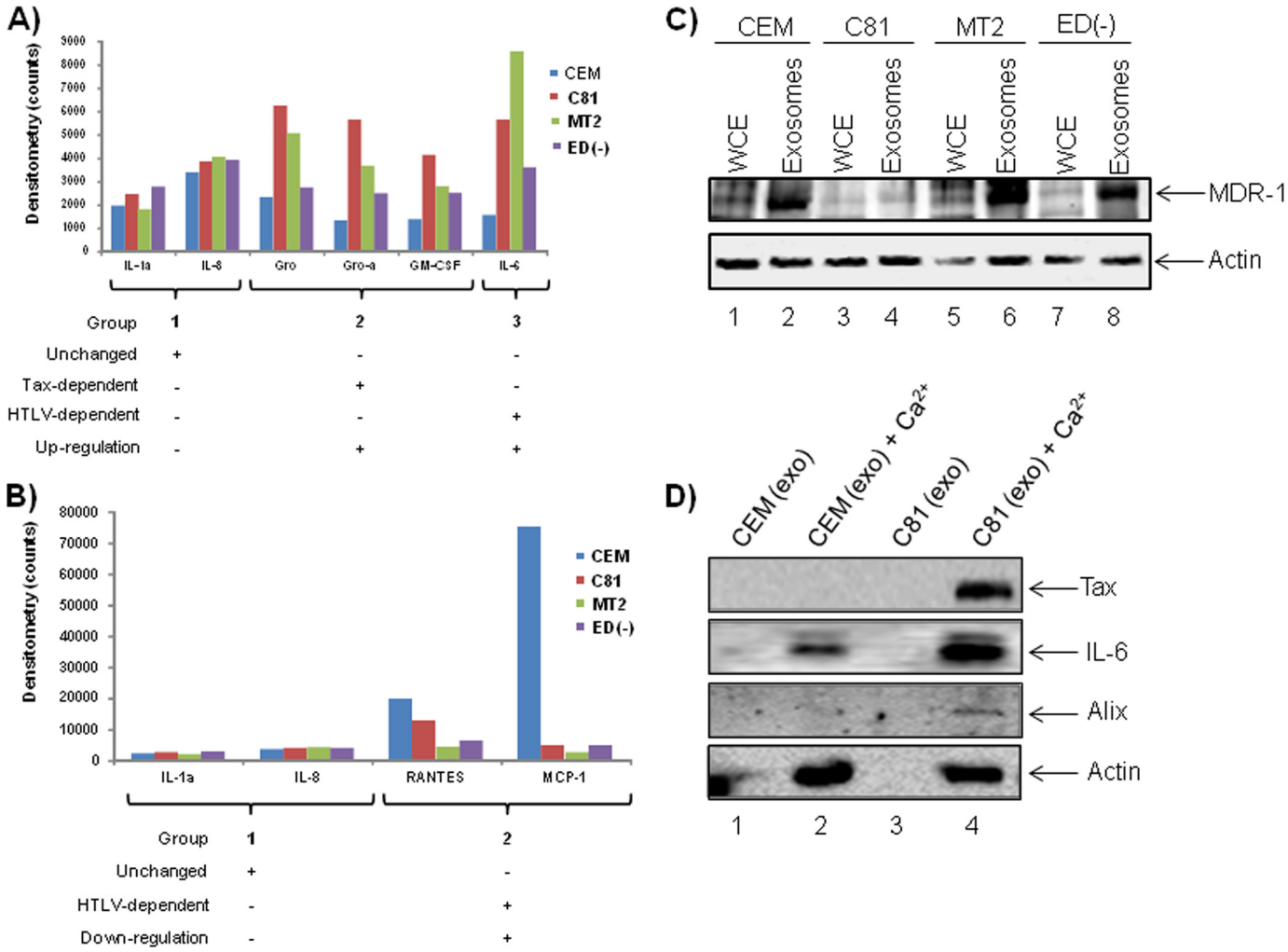

FIGURE 6. **Exosomes from HTLV-1-infected C81, MT2, and ED(−) cell lines contain inflammatory mediators.** CEM, C81, MT2, and ED(−) exosomes (7 μg) were assayed for the presence of proinflammatory cytokines using RayBio® Human Cytokine Array 1. *A*, the subset of cytokines was considered unchanged if the signal intensities observed were between 0.9- and 1.2-fold of the mean value for exosomes from all cell types, CEM, C81, MT2, and ED(−). Cytokines were considered up-regulated if they were present at greater than 2-fold of the levels in CEM exosomes and were classified depending upon Tax expression or HTLV-1 infection. *B*, cytokines were considered down-regulated if they were present at levels less than half of those in CEM exosomes. *C*, Western blot analysis was performed using CEM, C81, MT2, and ED(−) exosomes and corresponding cell lysates (10 μg) to evaluate for the presence of the ABC transporter MDR-1 (multidrug resistance protein 1). *D*, exosomes concentrated within nanotrap particles were treated with 100 μM Ca^{2+} to release various exosomal proteins. Western blot analysis was performed for the presence of Tax, IL-6, Alix, and β-actin protein.

released is active in exosomes, we carried out Ca^{2+} treatment of the exosomal pellet and then surveyed the resulting supernatant for the presence of released cytokines. We did this by trapping exosomes (after Ca^{2+} treatment) using nanotrap particles as described for Fig. 2. We first used NT080 to trap the exosomes and assayed the resulting supernatant by Western blot. We observed the presence of Tax, Alix, and actin proteins in this supernatant (Fig. 6*D*). However, the Western blot for IL-6 showed a negative result. This was because NT080 also traps some cytokines, including IL-6. We then tried another nanotrap particle, NT074, which would not trap the cytokine IL-6 but would still trap exosomes. The supernatant resulting from this assay showed the presence of IL-6 in the supernatant by Western blot (Fig. 6*D*). Thus, by the use of nanotrap particles, we were able to demonstrate that Ca^{2+} allows intracellular exosomal content, including the cytokine IL-6 that was tested, to be released into the extracellular space.

Collectively, these results imply that exosomes are important mediators of inflammation during HTLV-1 infection and suggest a potential mechanism for the delivery of intraexosomal cytokines to target cells. Furthermore, these results may provide an explanation for elevated serum levels of molecules such as IL-6 and TNF-α in infected patients.

Exosomes Containing Tax Protect Cells from FAS-mediated Apoptosis—Fas-associated death domain links CD95 and procaspase-8 by undergoing homotypic protein-protein interactions with the CD95, causing apoptosis of cells. It has also previously been demonstrated that Tax is able to inhibit Fas-mediated apoptosis by up-regulating cFLIP expression and regulation of NF-κB (98, 99). We therefore asked whether recipient cells that received Tax-containing exosomes were more resistant to apoptosis through FAS signaling. Jurkat cells were treated with exosomes derived from CEM, C81, and ED(−) cells and then treated with Fas antibody. After 24 h, cell viability was measured using the CellTiter-Glo Cell luminescence viability kit. Results indicate that exosome treatment alone did not promote apoptosis (Fig. 7*A*, *lanes 2*, *4*, and *6*), whereas cells treated with either CEM or ED(−) exosomes and

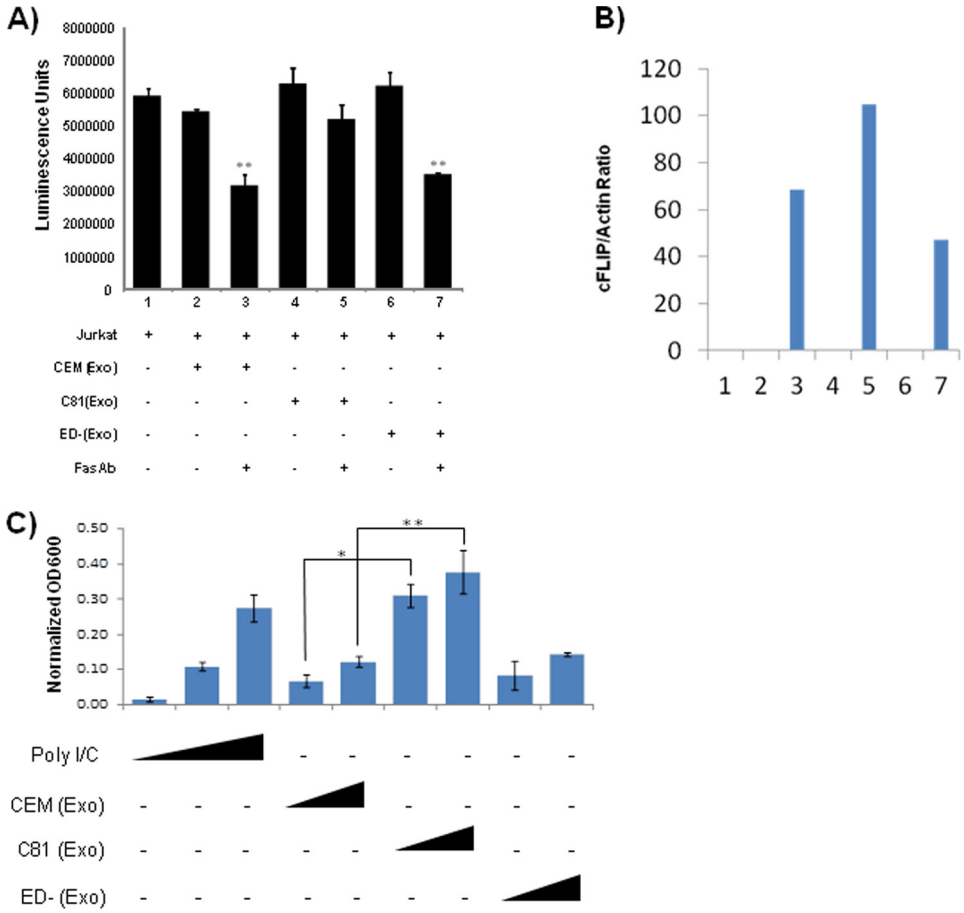

FIGURE 7. **Exosomes from HTLV-1 infected cells protect target cells from Fas antibody-mediated killing.** *A*, Jurkat cells were treated with exosomes derived from CEM, C81, and ED(−) cells, followed by the addition of FAS antibody. After 24 h, cell viability was measured using the CellTiter-Glo cell luminescence viability kit. *B*, Jurkat cells were treated with various exosomes, and then whole cell extracts were analyzed for cFLIP expression by Western blotting using a specific antibody. The level of cFLIP expression was then quantified by measuring the band intensity ratio between cFLIP and actin. *C*, HEK-Blue hTLR3 cells (5×10^4 cells/well) containing a secreted embryonic alkaline phosphatase reporter gene were incubated in a secreted embryonic alkaline phosphatase detection medium with 5 and 30 μg of exosomes from HTLV-1-infected C81 (Tax-positive) or ED(−) (Tax-negative) cells or uninfected CEM cells in a 96-well plate. Similarly, poly(I/C) (10, 50, and 250 ng/ml) was also incubated with the HEK-Blue hTLR3 cells as a positive control of NF-κB activator. After 18 h of incubation at 37 °C, cells were lysed, and the absorbance ($A_{600\,nm}$) was measured using the GloMax multidetection system (Promega). Readings from all positive controls and experimental samples were normalized using the mean value from three PBS-negative controls. All samples were tested in triplicate, and the mean ± S.D. (*error bars*) was calculated. Student's *t* test was used to calculate *p* values between control and treatment groups. *, $p \leq 0.002$; **, $p \leq 0.02$.

Fas antibody displayed a decrease in cell viability. However, exosomes from C81 cells showed better protection against apoptosis compared with treatment with exosomes from either uninfected CEM or ED(−) cells lacking Tax protein (*lanes 3*, *5*, and *7*). To determine whether exosomal Tax induces cFLIP expression to protect cells from Fas-mediated apoptosis, Jurkat cells were similarly treated with various exosomes and Fas antibody as in *A*. Cells were then lysed, and the WCE was analyzed for cFLIP expression by Western blotting. Results in Fig. 7*B* show that all of the Fas antibody-treated Jurkat cells expressed cFLIP; however, the level of cFLIP expression in C81 exosome-treated cells was higher (*lane 5*) than in the cells treated with exosomes from either uninfected CEM or ED(−) cells lacking Tax protein. These results indicate that exosomal Tax protein induces cFLIP, which in turn may protect cells from Fas-mediated apoptosis (98–100).

Finally, we asked whether Tax in the exosomes was functional in an NF-κB activation assay using a TLR readout. HEK-Blue hTLR3 cells containing a secreted embryonic alkaline phosphatase reporter gene were incubated in a secreted embryonic alkaline phosphatase detection medium with various concentrations of exosomes from C81, CEM, or ED(−) exosomes in a 96-well plate. Poly(I/C) was also incubated with the HEK-Blue hTLR3 cells as a positive control of NF-κB activator. After 18 h, cells were lysed, and the absorbance was measured using the GloMax multidetection system (Promega). Results in Fig. 7*C* indicate that although all three exosomes were able to activate the TLR system, the C81 exosomes was able to activate much more strongly as compared with the controls. Therefore, these results imply that Tax not only is able to activate its own promoter, but it also may work through NF-κB to activate other cellular genes important for survival of recipient cells.

Exosomes Containing Tax Increase Survival of Target Cells—We next asked whether Tax-containing exosomes could contribute to the survival of recipient cells. We tested the survival of IL-2-dependent CTLL-2 cells and PBMCs following treatment with each of the HTLV-1-infected T-cell line-derived exosomes. The CTLL-2 cells normally require IL-2 for survival. Here, we removed IL-2 from these cells and asked whether Tax could functionally replace the IL-2 requirement (101, 102).

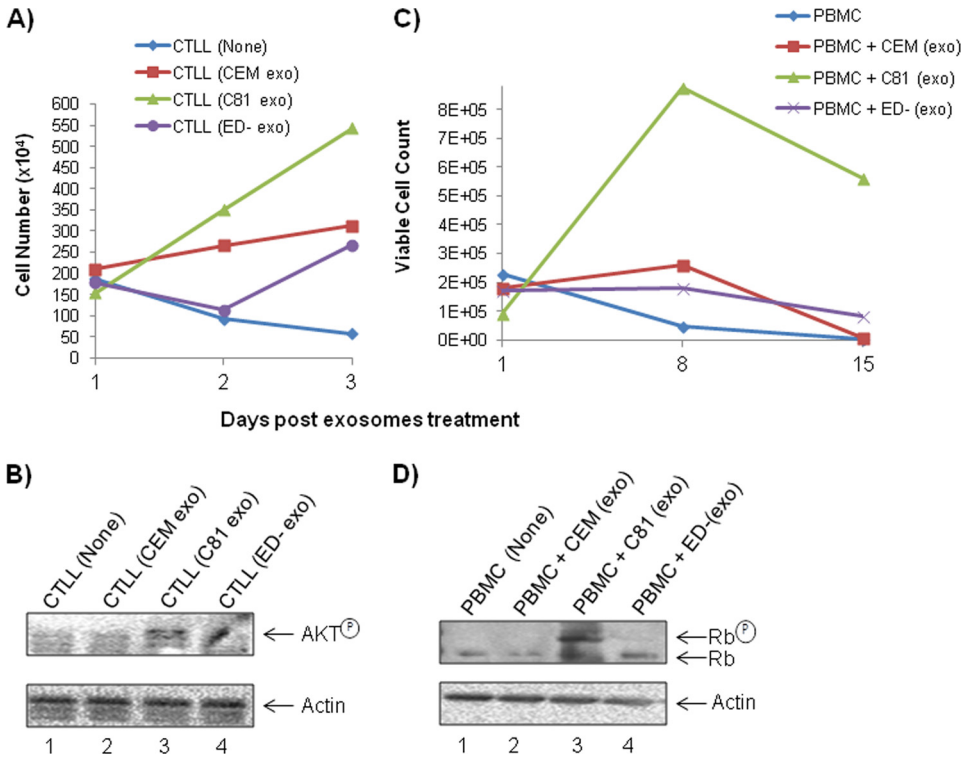

FIGURE 8. **Exosomes containing Tax increase survival of target cells.** *A*, CTLL-2 cells were grown in the presence of IL-2 to log phase of growth. They were subsequently washed and plated at ~10^6/100 μl and treated with various exosomal preparations, including CEM, C81, and ED(−) (5 μg each). Cells were counted using trypan blue at days 1, 2, and 3. *B*, CTLL-2 cells were treated with exosomes, and then WCEs were analyzed by Western blotting for AKT expression. The amount of total protein loading was monitored by comparing with actin expression. *C*, PBMCs were cultured with PHA/IL-2 for 3 days and subsequently removed and washed with PBS. Fresh medium (~90 μl) and exosomes (~10 μl, 5 μg) were added to each sample and left at 37 °C for 15 days. Live cells were counted using trypan blue at days 1, 8, and 15. An average of two experiments are shown for both *A* and *C*. *D*, similar to *C*, where cells were treated with exosomes, and then WCEs were analyzed for Rb (retinoblastoma) protein expression using Western blotting. The amount of total protein loading was monitored by comparing with actin expression.

Results in Fig. 8*A* indicate that CTLL-2 cells die out in 3 days or less in the absence of IL-2. However, when they are incubated with C81, but not with CEM or ED(−), exosomes, the survival rate increased dramatically. Survival has been known to be associated with AKT regulation in HTLV-infected cells (22, 103, 104). Therefore, we tested the IL-2-depleted and exosome-treated cells for the presence of phosphorylated AKT. Western blot results in *B* show that the phosphorylated AKT was up-regulated in the C81 exosome-treated cells compared with the cells treated with exosomes from either uninfected CEM or ED(−) lacking Tax protein. These results imply that Tax-containing exosomes may contribute to the survival of the recipient cells. Similarly, PHA/IL-2-stimulated PBMCs were washed and cultured with exosomes for 15 days. Results in Fig. 8*C* show that PBMCs treated with C81 exosome survived better in the absence of exogenous PHA or IL-2. We then asked whether survival of these cells was associated with increased Rb phosphorylation due to the presence of Tax (105–107). Results in Fig. 8*D* indicate that the PBMCs treated with C81, and not with CEM or ED(−), exosomes contain high levels of phosphorylated Rb protein in treated cells (Fig. 8*D*), indicating that Tax was able to regulate Rb phosphorylation and growth in these treated cells. Collectively, these results imply that Tax-containing exosomes enhance cell survival in both cell lines and primary cells possibly through up-regulation of prosurvival signaling molecules, including AKT and Rb (108, 109).

Tax-containing Exosomes Have Immunomodulatory Effects on Dendritic Cells—Finally, we asked whether exosomal Tax could alter the cytokine profile in the recipient cells. Among pleiotropic properties of Tax, its immunomodulatory activities have been primarily reported with the cell-free form (56, 66–68), the form that is most likely to be contained within exosomes from the HTLV-1-infected patient samples. Therefore, we hypothesized that Tax-bearing exosomes could potentially exert immunity stimulating properties, suggestive of their functional status. We tested this effect on the most potent antigen-presenting cells by utilizing freshly prepared myeloid dendritic cells and assessing for Th1 (IL-2, IL-10, IL-12, IFN-γ, and TNF-α), Th2 (IL-2, IL-4, IL-5, IL-10, and IL-13), and Th17 (IL-6, IL-17A, TNFα, G-CSF, and TGF-β1) cytokines. Results from CEM- and ED(−)-derived exosomes provided a basal cytokine profile from T-cells in the absence of HTLV-1 infection or Tax protein (Fig. 9). Exosomal Tax results from C81-treated samples were compared with control and free Tax protein. Exosomal Tax from C81 cells demonstrated a significant increase in the levels of IL-2, IL-5, and IL-6. TGF-β1 levels were also higher in C81 exosome-treated samples but not at a significant level. Compared with control, cell-free Tax was able to induce the secretion of IL-10, IL-12, IL-17A, IFN-γ, and G-CSF from dendritic cells. Taken together, these results are in agreement with previous observations made with Tax or samples from patients with regard to modulation of proinflammatory

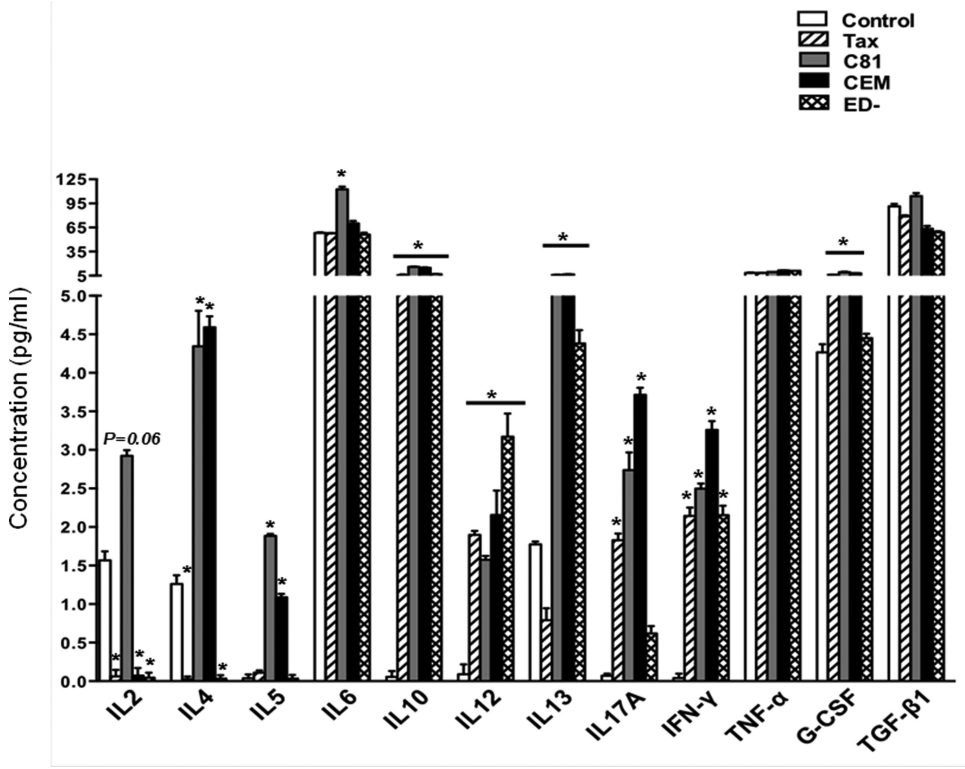

FIGURE 9. **Primary human myeloid dendritic cells were either untreated (control) or treated with cell-free Tax (50 nM) and each of the indicated exosome preparations (5 μg) for 48 h.** Cell culture supernatants were assayed for Th1/Th2/Th17 cytokines as described under "Materials and Methods." Data represent cumulative response from three donors ± S.D. (*error bars*) Student's *t* test was used to calculate *p* values between control and treatment groups. *, $p \leq 0.05$.

cytokines and demonstrate the functionality of Tax contained within exosomes.

DISCUSSION

Recently, exosomes have emerged as critical components of intercellular communication during viral infection and in a variety of disease states, including those associated with cancer and viral infections where these vesicles function in antigen presentation, cellular inflammation, and transfer of functional proteins and nucleic acids (42, 48, 50, 71, 110–114). Previous studies have demonstrated the involvement of exosomes in viral pathogenesis, particularly with respect to the ability of exosomes to modulate gene expression in recipient cells via delivery of miRNA and functional proteins (32, 52, 78, 115). In the context of retroviral infection, we have previously observed that naive recipient cells exposed to HIV-1-derived exosomes containing TAR miRNA resulted in increased susceptibility to viral infection (70). Because the role of exosomes in HTLV-1 infections is poorly understood, we aimed to identify how exosomes secreted from HTLV-1-infected cells might contribute to a possible phenotype. Our preliminary data suggest a role for HIV-1 exosomes in the transfer of unique host proteins and viral miRNA to recipient cells, ultimately modulating cellular processes, including apoptosis (70). However, with respect to HTLV-1 infection and pathogenesis, the role of exosomes remains largely unexplored and poorly understood. Our rationale for completing these studies stems from the fact that HTLV-1 Tax has been known to be detected in cell culture supernatants. We therefore explored the possibility that Tax could be incorporated into exosomes derived from HTLV-1-infected cells (53, 116, 117). In this work, we observed that exosomes derived from HTLV-1-infected T-cell lines incorporate host and viral proteins as well as a few copies of viral mRNA transcripts. More importantly, these exosomes deliver the viral transactivator Tax to target cells where it can activate transcription (*i.e.* HTLV-LTR).

After determining that exosomes released from uninfected and HTLV-1-infected T-cell lines display a few of the standard phenotypic features, such as CD63, HSP70, and actin, our TEM imaging analysis revealed the typically accepted size and morphology accepted for these vesicles (Fig. 1). Although we observed that HTLV-1-infected cells produce higher levels of exosomes at earlier time points than uninfected cells (Fig. 1*A*), we did not detect any significant differences in the presence of exosome marker proteins among uninfected or infected exosomes (Fig. 1*B*). We next validated that 0.22-μm filtration of cell culture supernatants produced a more uniform exosome preparation devoid of contamination by cellular debris and larger apoptotic vesicles. In doing so, we noticed a reduction in total protein after filtration of supernatants (Fig. 2*A*). In these postfiltrates, we detected usual markers, including HSP70 and CD63 in the exosomes. This step may be critical when utilizing low volume sample (*i.e.* serum, CSF, etc.) as compared with large volumes obtained from *in vitro* cell culture.

Because Tax has been shown to be present in an extracellular form, we immunoblotted C81 and MT2 exosomes (10 μg) for the presence of Tax (53, 117, 118). We further explored the host

and viral proteomic profiles of the exosomes derived from CEM, C81, MT2, and ED(−) T-cell lines. Overall, T-cell line exosomes contain approximately half the number of proteins documented for exosomes released by other cancerous cells (72, 76). Importantly, we detected 54 proteins shared among exosomes from all cell types, indicating that these host components were not incorporated as a result of infection, although there is no clear indication of quantitative differences at this time. Our LC-MS/MS analysis further enabled us to discern two proteins incorporated into exosomes in an HTLV-dependent manner, namely major histocompatibility complex class I A precursor and F isoform. We were also able to identify six proteins included in exosomes in a Tax-dependent manner: cofilin 2, eukaryotic translation elongation factor 1 α1, major histocompatibility complex class I E precursor, ribosomal protein L23, Thy-1 cell surface antigen preprotein, and tryptophanyl-tRNA synthetase isoform α. It is possible that the MHCI molecules incorporated into exosomes are responsible for the presentation of viral antigens, which contributes to the overall proinflammatory response associated with symptomatic HTLV-1 infection (5).

Furthermore, our initial LC-MS/MS analysis detected the surface domain of envelope glycoprotein (gp46), Gag, Gag-Pro, and Gag-Pro-Pol polyprotein only in MT2 exosomes. Although we validated the presence of gp46 in MT2 exosomes, our specific interest in Tax prompted us to use a more antigen-specific Western blot analysis to demonstrate the inclusion of Tax within both C81 and MT2 exosomes (Fig. 4*B*). To ensure that this incorporation was specifically a result of viral infection, we transfected Jurkat cells with the pACH HTLV-1 infectious molecular clone and successfully detected Tax present in exosomes collected from these cells (Fig. 4*C*). We next explored the functional relevance of intraexosomal Tax by activating viral promoter in recipient cells and found specific activation of LTR in reporter cells.

To address the discrepancies between the inclusion of viral proteins in C81 *versus* MT2 exosomes, it is important to note that two of the three integrated proviral genomes in C81 cells contain internal deletions spanning most of the Gag-Env region and thus do not produce structural viral proteins, such as gp46 or p24 (119). Also, MT2 cells produce and shed free virions, which could potentially be co-purified with the exosomes and allow for the detection of p24.

In the context of viral infections, exosomes have been shown to contain various mRNA, miRNA, and lipids. We therefore investigated the inclusion of viral *tax*, *hbz*, and *env* mRNA transcripts into exosomes. Our results show that <40 copies of each transcript were contained within C81 and ED(−) cells, whereas 10^6 copies were present in MT2 exosomes (Fig. 5*A*). Our subsequent RT assay revealed the presence of contaminating virus in MT2 exosomes while confirming the absence of virus in C81 exosome preparations (Fig. 5*B*).

We also examined the lipid metabolite contents in exosomes from both infected and uninfected cells. Lipid metabolites play important roles in many aspects of mammalian cell biology, such as cytoskeletal organization, protein localization, membrane transport, and cell proliferation, by acting as secondary messengers and by regulating various signal transduction pathways (120). Although some members are exclusively located in the plasma membrane, others or their specific kinases or phosphatases are found in the cytoplasm or in the cell organelles, such as mitochondria or endoplasmic reticulum. Cell surface lipids are also known to be involved in retrovirus life cycles. Some are directly associated with viral entry to target cells, replication, virion maturation, or release from the host cells, whereas others act as cofactors or second messengers and may affect target cell activation, apoptosis, or mitogenic growth through signal transduction. For example, glycosylphosphatidylinositol-linked complement control proteins, such as CD55 and CD59, present on activated T-cells are incorporated onto HIV-1 and HTLV-1 virions to protect them from complement (innate immunity)-mediated destruction and also to enhance infectivity of virions (121, 122). More interestingly, plasma membrane phosphatidylinositol 4,5-biphosphate directly interacts with HIV-1 Gag matrix and facilitates virion maturation and release (123). However, on the contrary, maturation of HTLV-1 Gag matrix and the release of virions are shown to be less dependent on the plasma membrane phosphatidylinositol 4,5-biphosphate.

Physiologically important lipid metabolites, such as diacylglycerol, phosphatidylethanolamine, phosphatidylcholine, and phosphatidylglycerol, were identified in both types of exosomes (infected and uninfected), although the molecular weights of these lipids were different between the two groups. However, two other lipid moieties, phosphatidylserine and phosphatidylinositol, were found to be more prevalent in the uninfected, but not in the HTLV-1 infected, exosomes. We therefore speculate that phosphatidylserine, being a hallmark of apoptosis and cell death (associated with HIV-1 infection) (124), is not important in an oncogenic HTLV-1 infection and as such was not found in the exosomes from the infected C81 cells (supplemental Table 1). Regarding the absence of phosphatidylinositol in HTLV-1-infected exosomes, a study by Inlora *et al.* (123) has shown that maturation of HTLV-1 Gag matrix and release of virions are not as dependent on this lipid moiety as is maturation of the HIV-1 virion, thus supporting our finding that phosphatidylinositol may be absent from the HTLV-1-infected exosomes.

It has previously been demonstrated that the release of proinflammatory mediators contributes to the neurodegeneration observed in symptomatic HAM/TSP patients (5). Taking this into consideration, we examined our LC-MS/MS results for the detection of various proinflammatory cytokines in exosomes. Although we failed to identify cytokines in this system (possibly due to lack of sufficient peptide coverage), we opted for a more specific antigen-antibody interaction to identify these molecules within exosomes using a cytokine array. In doing so, we successfully identified the enhanced incorporation of cytokines, including Gro, Gro-α GM-CSF, and IL-6, whereas we noted a drastic reduction in the presence of MCP-1 and RANTES (Fig. 6*B*). Several of these proteins, including IL-6, have been reported as elevated in serum collected from HAM/TSP patients (86, 125).

Furthermore, we have identified a potential mechanism in which ABC transporters are required for the targeted delivery of cytokines to recipient cells. ABC transporters, specifically

MDR-1, have recently emerged as key players in neuroinflammation, particularly due to their ability to transport and release certain inflammatory mediators, including cytokines (96, 97). The inclusion of the ABC transporter MDR-1 in exosomes presents an important means by which the proinflammatory molecules may be specifically targeted and delivered via exosomes. Although it is not known if these transporters are active (and are the means of delivery of exosomal cytokines to recipient cells), it is known that calcium can activate some protein kinases (*e.g.* PKA and CaMKIIs) that can phosphorylate some receptors/channels (*e.g.* NMDA receptors, AMPA receptors, and voltage-gated ion channels), which could increase their activity. Our calcium induced-experiments show that increasing extracellular Ca^{2+} can induce the cells to release enclosed cytokines into the extracellular space. Thus, our results indicate that exosomes could, at least in part, play a role in the secretion and targeted delivery of cytokines (through MDR-1 activity or in the presence of stimulators such as Ca^{2+}), potentially to areas outside of infection, including the CNS compartments, and therefore contribute to neurological abnormalities observed in HAM/TSP.

In our current study, we have utilized a few novel reagents to validate the relevance of exosomal material and confirm the presence of its intracellular components. We used two drugs, namely manumycin A and brefeldin A, which have been demonstrated to down-regulate release of proteins such as TNFR1, CD63, and CD81 in exosomes (126, 127). Manumycin A is an nSMase2 inhibitor and therefore inhibits exosome production (127, 128); brefeldin A specifically inhibits extracellular release of viruses (129, 130) but not exosome production (127). These two well validated reagents confirm the presence of extracellular Tax within exosomes and not within other particles. Further confirmation of extracellular Tax present in a protected environment comes from the fact that Tax is protected from tryptic digestion but not after a freeze thaw cycle. The characteristic lipid bilayer composition of exosomes protects its components from trypsin, but a freeze-thaw cycle can rupture this membrane and make intracellular components susceptible to external factors (131). Similarly, we have utilized the versatile properties of nanotrap particles of various shells and dye baits to differentiate between an exosome that contains Tax and virions. This is in agreement with our recent report utilizing the nanotrap particle NT080 to trap HIV-1-associated exosomes and NT086 to capture HIV-1 particles (62).

Finally, we asked whether Tax-containing exosomes could function by allowing recipient cells to survive under stress conditions. Results in both Figs. 7 and 8 indicate that Tax is able to work through the TLR pathway and aid in survival of cells when treated with the Fas antibody as well as withdrawal of stimulus, such as cytokines. Along these lines, both IL-2-dependent and PBMC-treated cells had a better survival rate (through both AKT and Rb pathways) when treated with Tax-containing exosomes. The functional abilities of the viral transactivator Tax to contribute to pathogenesis have been extensively studied (1, 8, 132–134). More specifically, Tax is a critical component for regulating the dynamics of the viral life cycle and deregulation of many cellular genes.

Taken together, our results implicate exosomes as critical mediators of signal transduction and possibly contribute to the pathogenesis of HTLV-1 infection and disease progression. Understanding the significance of the Tax and cytokine-containing exosomes *in vivo* may also contribute to better treatment of both HAM/TSP and adult T-cell leukemia in infected patients.

Acknowledgments—We thank the members of the Kashanchi laboratory for helpful discussions and critical review of the manuscript and Dianna Martin for careful editing. Dr. Tim McCaffery (George Washington University) generously donated the FAS antibody, and Dr. Scott Gitlin (University of Michigan) generously contributed the Tax polyclonal antibody.

REFERENCES

1. Yasunaga, J., and Matsuoka, M. (2011) Molecular mechanisms of HTLV-1 infection and pathogenesis. *Int. J. Hematol.* **94,** 435–442
2. Watanabe, T. (2011) Current status of HTLV-1 infection. *Int. J. Hematol.* **94,** 430–434
3. Gessain, A., and Cassar, O. (2012) Epidemiological Aspects and World Distribution of HTLV-1 Infection. *Front. Microbiol.* **3,** 388
4. Kamoi, K., and Mochizuki, M. (2012) HTLV-1 uveitis. *Front. Microbiol.* **3,** 270
5. Yamano, Y., and Sato, T. (2012) Clinical pathophysiology of human T-lymphotropic virus-type 1-associated myelopathy/tropical spastic paraparesis. *Front. Microbiol.* **3,** 389
6. Cook, L. B., Elemans, M., Rowan, A. G., and Asquith, B. (2013) HTLV-1: persistence and pathogenesis. *Virology* **435,** 131–140
7. Proietti, F. A., Carneiro-Proietti, A. B., Catalan-Soares, B. C., and Murphy, E. L. (2005) Global epidemiology of HTLV-I infection and associated diseases. *Oncogene* **24,** 6058–6068
8. Currer, R., Van Duyne, R., Jaworski, E., Guendel, I., Sampey, G., Das, R., Narayanan, A., and Kashanchi, F. (2012) HTLV tax: a fascinating multifunctional co-regulator of viral and cellular pathways. *Front. Microbiol.* **3,** 406
9. Grassmann, R., Aboud, M., and Jeang, K. T. (2005) Molecular mechanisms of cellular transformation by HTLV-1 Tax. *Oncogene* **24,** 5976–5985
10. Grassmann, R., Dengler, C., Müller-Fleckenstein, I., Fleckenstein, B., McGuire, K., Dokhelar, M. C., Sodroski, J. G., and Haseltine, W. A. (1989) Transformation to continuous growth of primary human T lymphocytes by human T-cell leukemia virus type I X-region genes transduced by a *Herpesvirus saimiri* vector. *Proc. Natl. Acad. Sci. U.S.A.* **86,** 3351–3355
11. Norris, P. J., Hirschkorn, D. F., DeVita, D. A., Lee, T. H., and Murphy, E. L. (2010) Human T cell leukemia virus type 1 infection drives spontaneous proliferation of natural killer cells. *Virulence* **1,** 19–28
12. Boxus, M., Twizere, J. C., Legros, S., Dewulf, J. F., Kettmann, R., and Willems, L. (2008) The HTLV-1 Tax interactome. *Retrovirology* **5,** 76
13. Chandhasin, C., Ducu, R. I., Berkovich, E., Kastan, M. B., and Marriott, S. J. (2008) Human T-cell leukemia virus type 1 tax attenuates the ATM-mediated cellular DNA damage response. *J. Virol.* **82,** 6952–6961
14. Kehn, K., Fuente Cde, L., Strouss, K., Berro, R., Jiang, H., Brady, J., Mahieux, R., Pumfery, A., Bottazzi, M. E., and Kashanchi, F. (2005) The HTLV-I Tax oncoprotein targets the retinoblastoma protein for proteasomal degradation. *Oncogene* **24,** 525–540
15. Vajente, N., Trevisan, R., and Saggioro, D. (2009) HTLV-1 Tax protein cooperates with Ras in protecting cells from apoptosis. *Apoptosis* **14,** 153–163
16. Majone, F., and Jeang, K. T. (2012) Unstabilized DNA breaks in HTLV-1 Tax expressing cells correlate with functional targeting of Ku80, not PKcs, XRCC4, or H2AX. *Cell Biosci.* **2,** 15
17. Belgnaoui, S. M., Fryrear, K. A., Nyalwidhe, J. O., Guo, X., and Semmes, O. J. (2010) The viral oncoprotein tax sequesters DNA damage response factors by tethering MDC1 to chromatin. *J. Biol. Chem.* **285,**

32897–32905
18. Kinjo, T., Ham-Terhune, J., Peloponese, J. M., Jr., and Jeang, K. T. (2010) Induction of reactive oxygen species by human T-cell leukemia virus type 1 tax correlates with DNA damage and expression of cellular senescence marker. *J. Virol.* **84,** 5431–5437
19. Durkin, S. S., Guo, X., Fryrear, K. A., Mihaylova, V. T., Gupta, S. K., Belgnaoui, S. M., Haoudi, A., Kupfer, G. M., and Semmes, O. J. (2008) HTLV-1 Tax oncoprotein subverts the cellular DNA damage response via binding to DNA-dependent protein kinase. *J. Biol. Chem.* **283,** 36311–36320
20. Yang, L., Kotomura, N., Ho, Y. K., Zhi, H., Bixler, S., Schell, M. J., and Giam, C. Z. (2011) Complex cell cycle abnormalities caused by human T-lymphotropic virus type 1 Tax. *J. Virol.* **85,** 3001–3009
21. Kim, Y. M., Geiger, T. R., Egan, D. I., Sharma, N., and Nyborg, J. K. (2010) The HTLV-1 tax protein cooperates with phosphorylated CREB, TORC2 and p300 to activate CRE-dependent cyclin D1 transcription. *Oncogene* **29,** 2142–2152
22. Liu, M., Yang, L., Zhang, L., Liu, B., Merling, R., Xia, Z., and Giam, C. Z. (2008) Human T-cell leukemia virus type 1 infection leads to arrest in the G1 phase of the cell cycle. *J. Virol.* **82,** 8442–8455
23. Chlichlia, K., and Khazaie, K. (2010) HTLV-1 Tax: linking transformation, DNA damage and apoptotic T-cell death. *Chem. Biol. Interact.* **188,** 359–365
24. Saito, K., Saito, M., Taniura, N., Okuwa, T., and Ohara, Y. (2010) Activation of the PI3K-Akt pathway by human T cell leukemia virus type 1 (HTLV-1) oncoprotein Tax increases Bcl3 expression, which is associated with enhanced growth of HTLV-1-infected T cells. *Virology* **403,** 173–180
25. Pant, S., Hilton, H., and Burczynski, M. E. (2012) The multifaceted exosome: biogenesis, role in normal and aberrant cellular function, and frontiers for pharmacological and biomarker opportunities. *Biochem. Pharmacol.* **83,** 1484–1494
26. Wahlgren, J., Karlson Tde, L., Glader, P., Telemo, E., and Valadi, H. (2012) Activated human T cells secrete exosomes that participate in IL-2 mediated immune response signaling. *PLoS One* **7,** e49723
27. Xin, H., Li, Y., Buller, B., Katakowski, M., Zhang, Y., Wang, X., Shang, X., Zhang, Z. G., and Chopp, M. (2012) Exosome-mediated transfer of miR-133b from multipotent mesenchymal stromal cells to neural cells contributes to neurite outgrowth. *Stem Cells* **30,** 1556–1564
28. Testa, J. S., Apcher, G. S., Comber, J. D., and Eisenlohr, L. C. (2010) Exosome-driven antigen transfer for MHC class II presentation facilitated by the receptor binding activity of influenza hemagglutinin. *J. Immunol.* **185,** 6608–6616
29. Wang, G., Dinkins, M., He, Q., Zhu, G., Poirier, C., Campbell, A., Mayer-Proschel, M., and Bieberich, E. (2012) Astrocytes secrete exosomes enriched with proapoptotic ceramide and prostate apoptosis response 4 (PAR-4): potential mechanism of apoptosis induction in Alzheimer disease (AD). *J. Biol. Chem.* **287,** 21384–21395
30. Meckes, D. G., Jr., Shair, K. H., Marquitz, A. R., Kung, C. P., Edwards, R. H., and Raab-Traub, N. (2010) Human tumor virus utilizes exosomes for intercellular communication. *Proc. Natl. Acad. Sci. U.S.A.* **107,** 20370–20375
31. Gourzones, C., Gelin, A., Bombik, I., Klibi, J., Vérillaud, B., Guigay, J., Lang, P., Témam, S., Schneider, V., Amiel, C., Baconnais, S., Jimenez, A. S., and Busson, P. (2010) Extra-cellular release and blood diffusion of BART viral micro-RNAs produced by EBV-infected nasopharyngeal carcinoma cells. *Virol. J.* **7,** 271
32. Pegtel, D. M., Cosmopoulos, K., Thorley-Lawson, D. A., van Eijndhoven, M. A., Hopmans, E. S., Lindenberg, J. L., de Gruijl, T. D., Würdinger, T., and Middeldorp, J. M. (2010) Functional delivery of viral miRNAs via exosomes. *Proc. Natl. Acad. Sci. U.S.A.* **107,** 6328–6333
33. Ohno, S., Ishikawa, A., and Kuroda, M. (2013) Roles of exosomes and microvesicles in disease pathogenesis. *Adv. Drug Deliv. Rev.* **65,** 398–401
34. Keller, S., Ridinger, J., Rupp, A. K., Janssen, J. W., and Altevogt, P. (2011) Body fluid derived exosomes as a novel template for clinical diagnostics. *J. Transl. Med.* **9,** 86
35. Michael, A., Bajracharya, S. D., Yuen, P. S., Zhou, H., Star, R. A., Illei, G. G., and Alevizos, I. (2010) Exosomes from human saliva as a source of microRNA biomarkers. *Oral Dis.* **16,** 34–38
36. Chen, C. L., Lai, Y. F., Tang, P., Chien, K. Y., Yu, J. S., Tsai, C. H., Chen, H. W., Wu, C. C., Chung, T., Hsu, C. W., Chen, C. D., Chang, Y. S., Chang, P. L., and Chen, Y. T. (2012) Comparative and targeted proteomic analyses of urinary microparticles from bladder cancer and hernia patients. *J. Proteome Res.* **11,** 5611–5629
37. Lässer, C., Alikhani, V. S., Ekström, K., Eldh, M., Paredes, P. T., Bossios, A., Sjöstrand, M., Gabrielsson, S., Lötvall, J., and Valadi, H. (2011) Human saliva, plasma and breast milk exosomes contain RNA: uptake by macrophages. *J. Transl. Med.* **9,** 9
38. Dear, J. W., Street, J. M., and Bailey, M. A. (2013) Urinary exosomes: a reservoir for biomarker discovery and potential mediators of intrarenal signalling. *Proteomics* **13,** 1572–1580
39. Poliakov, A., Spilman, M., Dokland, T., Amling, C. L., and Mobley, J. A. (2009) Structural heterogeneity and protein composition of exosome-like vesicles (prostasomes) in human semen. *Prostate* **69,** 159–167
40. Tauro, B. J., Greening, D. W., Mathias, R. A., Mathivanan, S., Ji, H., and Simpson, R. J. (2013) Two distinct populations of exosomes are released from LIM1863 colon carcinoma cell-derived organoids. *Mol. Cell Proteomics* **12,** 587–598
41. Mathivanan, S., Ji, H., and Simpson, R. J. (2010) Exosomes: extracellular organelles important in intercellular communication. *J. Proteomics* **73,** 1907–1920
42. Simpson, R. J., Jensen, S. S., and Lim, J. W. (2008) Proteomic profiling of exosomes: current perspectives. *Proteomics* **8,** 4083–4099
43. Thery, C., Amigorena, S., Raposo, G., and Clayton, A. (2006) Isolation and characterization of exosomes from cell culture supernatants and biological fluids. *Curr. Protoc. Cell Biol.* **Chapter 3,** Unit 3.22
44. György, B., Szabó, T. G., Pásztói, M., Pál, Z., Misják, P., Aradi, B., László, V., Pállinger, E., Pap, E., Kittel, A., Nagy, G., Falus, A., and Buzás, E. I. (2011) Membrane vesicles, current state-of-the-art: emerging role of extracellular vesicles. *Cell Mol. Life Sci.* **68,** 2667–2688
45. Harding, C., Heuser, J., and Stahl, P. (1983) Receptor-mediated endocytosis of transferrin and recycling of the transferrin receptor in rat reticulocytes. *J. Cell Biol.* **97,** 329–339
46. Wurdinger, T., Gatson, N. N., Balaj, L., Kaur, B., Breakefield, X. O., and Pegtel, D. M. (2012) Extracellular vesicles and their convergence with viral pathways. *Adv. Virol.* **2012,** 767694
47. Vlassov, A. V., Magdaleno, S., Setterquist, R., and Conrad, R. (2012) Exosomes: current knowledge of their composition, biological functions, and diagnostic and therapeutic potentials. *Biochim. Biophys. Acta* **1820,** 940–948
48. Dreux, M., Garaigorta, U., Boyd, B., Décembre, E., Chung, J., Whitten-Bauer, C., Wieland, S., and Chisari, F. V. (2012) Short-range exosomal transfer of viral RNA from infected cells to plasmacytoid dendritic cells triggers innate immunity. *Cell Host Microbe* **12,** 558–570
49. Columba Cabezas, S., and Federico, M. (2013) Sequences within RNA coding for HIV-1 Gag p17 are efficiently targeted to exosomes. *Cell Microbiol.* **15,** 412–429
50. Hu, G., Yao, H., Chaudhuri, A. D., Duan, M., Yelamanchili, S. V., Wen, H., Cheney, P. D., Fox, H. S., and Buch, S. (2012) Exosome-mediated shuttling of microRNA-29 regulates HIV Tat and morphine-mediated neuronal dysfunction. *Cell Death Dis.* **3,** e381
51. Xu, W., Santini, P. A., Sullivan, J. S., He, B., Shan, M., Ball, S. C., Dyer, W. B., Ketas, T. J., Chadburn, A., Cohen-Gould, L., Knowles, D. M., Chiu, A., Sanders, R. W., Chen, K., and Cerutti, A. (2009) HIV-1 evades virus-specific IgG2 and IgA responses by targeting systemic and intestinal B cells via long-range intercellular conduits. *Nat. Immunol.* **10,** 1008–1017
52. Lenassi, M., Cagney, G., Liao, M., Vaupotic, T., Bartholomeeusen, K., Cheng, Y., Krogan, N. J., Plemenitas, A., and Peterlin, B. M. (2010) HIV Nef is secreted in exosomes and triggers apoptosis in bystander $CD4^+$ T cells. *Traffic* **11,** 110–122
53. Marriott, S. J., Lindholm, P. F., Reid, R. L., and Brady, J. N. (1991) Soluble HTLV-I Tax1 protein stimulates proliferation of human peripheral blood lymphocytes. *New Biol.* **3,** 678–686
54. Cartier, L., and Ramirez, E. (2005) Presence of HTLV-I Tax protein in cerebrospinal fluid from HAM/TSP patients. *Arch. Virol.* **150,** 743–753
55. Alefantis, T., Jain, P., Ahuja, J., Mostoller, K., and Wigdahl, B. (2005)

HTLV-1 Tax nucleocytoplasmic shuttling, interaction with the secretory pathway, extracellular signaling, and implications for neurologic disease. *J. Biomed. Sci.* **12,** 961–974
56. Jain, P., Mostoller, K., Flaig, K. E., Ahuja, J., Lepoutre, V., Alefantis, T., Khan, Z. K., and Wigdahl, B. (2007) Identification of human T cell leukemia virus type 1 tax amino acid signals and cellular factors involved in secretion of the viral oncoprotein. *J. Biol. Chem.* **282,** 34581–34593
57. Salahuddin, S. Z., Markham, P. D., Wong-Staal, F., Franchini, G., Kalyanaraman, V. S., and Gallo, R. C. (1983) Restricted expression of human T-cell leukemia–lymphoma virus (HTLV) in transformed human umbilical cord blood lymphocytes. *Virology* **129,** 51–64
58. Popovic, M., Lange-Wantzin, G., Sarin, P. S., Mann, D., and Gallo, R. C. (1983) Transformation of human umbilical cord blood T cells by human T-cell leukemia/lymphoma virus. *Proc. Natl. Acad. Sci. U.S.A.* **80,** 5402–5406
59. Maeda, Y., Sasakawa, A., Hirase, C., Yamaguchi, T., Morita, Y., Miyatake, J., Urase, F., Nomura, S., and Matsumura, I. (2011) Senescence induction therapy for the treatment of adult T-cell leukemia. *Leuk. Lymphoma* **52,** 150–152
60. Kimata, J. T., Wong, F. H., Wang, J. J., and Ratner, L. (1994) Construction and characterization of infectious human T-cell leukemia virus type 1 molecular clones. *Virology* **204,** 656–664
61. Kashanchi, F., Duvall, J. F., and Brady, J. N. (1992) Electroporation of viral transactivator proteins into lymphocyte suspension cells. *Nucleic Acids Res.* **20,** 4673–4674
62. Jaworski, E., Saifuddin, M., Sampey, G., Shafagati, N., Van Duyne, R., Iordanskiy, S., Kehn-Hall, K., Liotta, L., Petricoin, E., 3rd, Young, M., Lepene, B., and Kashanchi, F. (2014) The use of nanotrap particles technology in capturing HIV-1 virions and viral proteins from infected cells. *PLoS One* **9,** e96778
63. Sripadi, P., Shrestha, B., Easley, R. L., Carpio, L., Kehn-Hall, K., Chevalier, S., Mahieux, R., Kashanchi, F., and Vertes, A. (2010) Direct detection of diverse metabolic changes in virally transformed and tax-expressing cells by mass spectrometry. *PLoS One* **5,** e12590
64. Shrestha, B., Sripadi, P., Walsh, C. M., Razunguzwa, T. T., Powell, M. J., Kehn-Hall, K., Kashanchi, F., and Vertes, A. (2012) Rapid, non-targeted discovery of biochemical transformation and biomarker candidates in oncovirus-infected cell lines using LAESI mass spectrometry. *Chem. Commun.* (*Camb.*) **48,** 3700–3702
65. Jin, D. Y., and Jeang, K. T. (1997) HTLV-I Tax self-association in optimal trans-activation function. *Nucleic Acids Res.* **25,** 379–387
66. Ahuja, J., Kampani, K., Datta, S., Wigdahl, B., Flaig, K. E., and Jain, P. (2006) Use of human antigen presenting cell gene array profiling to examine the effect of human T-cell leukemia virus type 1 Tax on primary human dendritic cells. *J. Neurovirol.* **12,** 47–59
67. Ahuja, J., Lepoutre, V., Wigdahl, B., Khan, Z. K., and Jain, P. (2007) Induction of pro-inflammatory cytokines by human T-cell leukemia virus type-1 Tax protein as determined by multiplexed cytokine protein array analyses of human dendritic cells. *Biomed. Pharmacother.* **61,** 201–208
68. Manuel, S. L., Schell, T. D., Acheampong, E., Rahman, S., Khan, Z. K., and Jain, P. (2009) Presentation of human T cell leukemia virus type 1 (HTLV-1) Tax protein by dendritic cells: the underlying mechanism of HTLV-1-associated neuroinflammatory disease. *J. Leukoc. Biol.* **86,** 1205–1216
69. Rahman, S., Quann, K., Pandya, D., Singh, S., Khan, Z. K., and Jain, P. (2012) HTLV-1 Tax mediated downregulation of miRNAs associated with chromatin remodeling factors in T cells with stably integrated viral promoter. *PLoS One* **7,** e34490
70. Narayanan, A., Iordanskiy, S., Das, R., Van Duyne, R., Santos, S., Jaworski, E., Guendel, I., Sampey, G., Dalby, E., Iglesias-Ussel, M., Popratiloff, A., Hakami, R., Kehn-Hall, K., Young, M., Subra, C., Gilbert, C., Bailey, C., Romerio, F., and Kashanchi, F. (2013) Exosomes derived from HIV-1-infected cells contain trans-activation response element RNA. *J. Biol. Chem.* **288,** 20014–20033
71. Luga, V., Zhang, L., Viloria-Petit, A. M., Ogunjimi, A. A., Inanlou, M. R., Chiu, E., Buchanan, M., Hosein, A. N., Basik, M., and Wrana, J. L. (2012) Exosomes mediate stromal mobilization of autocrine Wnt-PCP signaling in breast cancer cell migration. *Cell* **151,** 1542–1556
72. Mathivanan, S., Lim, J. W., Tauro, B. J., Ji, H., Moritz, R. L., and Simpson, R. J. (2010) Proteomics analysis of A33 immunoaffinity-purified exosomes released from the human colon tumor cell line LIM1215 reveals a tissue-specific protein signature. *Mol. Cell Proteomics* **9,** 197–208
73. Rood, I. M., Deegens, J. K., Merchant, M. L., Tamboer, W. P., Wilkey, D. W., Wetzels, J. F., and Klein, J. B. (2010) Comparison of three methods for isolation of urinary microvesicles to identify biomarkers of nephrotic syndrome. *Kidney Int.* **78,** 810–816
74. Bobrie, A., Colombo, M., Krumeich, S., Raposo, G., and Thery, C. (2012) Diverse subpopulations of vesicles secreted by different intracellular mechanisms are present in exosome preparations obtained by differential ultracentrifugation. *J. Extracell. Vesicles* 10.3402/jev.v1i0.18397
75. Giri, P. K., and Schorey, J. S. (2008) Exosomes derived from M. Bovis BCG infected macrophages activate antigen-specific $CD4^+$ and $CD8^+$ T cells *in vitro* and *in vivo*. *PLoS One* **3,** e2461
76. Welton, J. L., Khanna, S., Giles, P. J., Brennan, P., Brewis, I. A., Staffurth, J., Mason, M. D., and Clayton, A. (2010) Proteomics analysis of bladder cancer exosomes. *Mol. Cell Proteomics* **9,** 1324–1338
77. Principe, S., Jones, E. E., Kim, Y., Sinha, A., Nyalwidhe, J. O., Brooks, J., Semmes, O. J., Troyer, D. A., Lance, R. S., Kislinger, T., and Drake, R. R. (2013) In-depth proteomic analyses of exosomes isolated from expressed prostatic secretions in urine. *Proteomics* **13,** 1667–1671
78. Meckes, D. G., Jr., and Raab-Traub, N. (2011) Microvesicles and viral infection. *J. Virol.* **85,** 12844–12854
79. Valadi, H., Ekström, K., Bossios, A., Sjöstrand, M., Lee, J. J., and Lötvall, J. O. (2007) Exosome-mediated transfer of mRNAs and microRNAs is a novel mechanism of genetic exchange between cells. *Nat. Cell Biol.* **9,** 654–659
80. Chiba, M., Kimura, M., and Asari, S. (2012) Exosomes secreted from human colorectal cancer cell lines contain mRNAs, microRNAs and natural antisense RNAs, that can transfer into the human hepatoma HepG2 and lung cancer A549 cell lines. *Oncol. Rep.* **28,** 1551–1558
81. Xiao, D., Ohlendorf, J., Chen, Y., Taylor, D. D., Rai, S. N., Waigel, S., Zacharias, W., Hao, H., and McMasters, K. M. (2012) Identifying mRNA, microRNA and protein profiles of melanoma exosomes. *PLoS One* **7,** e46874
82. Borges, F. T., Melo, S. A., Özdemir, B. C., Kato, N., Revuelta, I., Miller, C. A., Gattone, V. H., 2nd, LeBleu, V. S., and Kalluri, R. (2013) TGF-β1-containing exosomes from injured epithelial cells activate fibroblasts to initiate tissue regenerative responses and fibrosis. *J. Am. Soc. Nephrol.* **24,** 385–392
83. Araya, N., Sato, T., Yagishita, N., Ando, H., Utsunomiya, A., Jacobson, S., and Yamano, Y. (2011) Human T-lymphotropic virus type 1 (HTLV-1) and regulatory T cells in HTLV-1-associated neuroinflammatory disease. *Viruses* **3,** 1532–1548
84. Ijichi, S., Ijichi, N., and Osame, M. (1997) [HTLV-I-associated myelopathy/tropical spastic paraparesis (HAM/TSP)]. *Nihon Rinsho* **55,** 926–933
85. Ijichi, S., Izumo, S., Eiraku, N., Machigashira, K., Kubota, R., Nagai, M., Ikegami, N., Kashio, N., Umehara, F., and Maruyama, I. (1993) An autoaggressive process against bystander tissues in HTLV-I-infected individuals: a possible pathomechanism of HAM/TSP. *Med. Hypotheses* **41,** 542–547
86. Starling, A. L., Martins-Filho, O. A., Lambertucci, J. R., Labanca, L., de Souza Pereira, S. R., Teixeira-Carvalho, A., Martins, M. L., Ribas, J. G., Carneiro-Proietti, A. B., and Gonçalves, D. U. (2013) Proviral load and the balance of serum cytokines in HTLV-1-asymptomatic infection and in HTLV-1-associated myelopathy/tropical spastic paraparesis (HAM/TSP). *Acta Trop.* **125,** 75–81
87. Nishimoto, N., Yoshizaki, K., Eiraku, N., Machigashira, K., Tagoh, H., Ogata, A., Kuritani, T., Osame, M., and Kishimoto, T. (1990) Elevated levels of interleukin-6 in serum and cerebrospinal fluid of HTLV-I-associated myelopathy/tropical spastic paraparesis. *J. Neurol. Sci.* **97,** 183–193
88. Banerjee, P., Rochford, R., Antel, J., Canute, G., Wrzesinski, S., Sieburg, M., and Feuer, G. (2007) Proinflammatory cytokine gene induction by human T-cell leukemia virus type 1 (HTLV-1) and HTLV-2 Tax in primary human glial cells. *J. Virol.* **81,** 1690–1700

89. Graner, M. W., Alzate, O., Dechkovskaia, A. M., Keene, J. D., Sampson, J. H., Mitchell, D. A., and Bigner, D. D. (2009) Proteomic and immunologic analyses of brain tumor exosomes. *FASEB J.* **23,** 1541–1557
90. Nimer, S. D., Gasson, J. C., Hu, K., Smalberg, I., Williams, J. L., Chen, I. S., and Rosenblatt, J. D. (1989) Activation of the GM-CSF promoter by HTLV-I and -II tax proteins. *Oncogene* **4,** 671–676
91. Grossman, W. J., and Ratner, L. (1997) Cytokine expression and tumorigenicity of large granular lymphocytic leukemia cells from mice transgenic for the tax gene of human T-cell leukemia virus type I. *Blood* **90,** 783–794
92. Takashima, H., Eguchi, K., Kawakami, A., Kawabe, Y., Migita, K., Sakai, M., Origuchi, T., and Nagataki, S. (1996) Cytokine production by endothelial cells infected with human T cell lymphotropic virus type I. *Ann. Rheum. Dis.* **55,** 632–637
93. Guerreiro, J. B., Santos, S. B., Morgan, D. J., Porto, A. F., Muniz, A. L., Ho, J. L., Teixeira, A. L., Jr., Teixeira, M. M., and Carvalho, E. M. (2006) Levels of serum chemokines discriminate clinical myelopathy associated with human T lymphotropic virus type 1 (HTLV-1)/tropical spastic paraparesis (HAM/TSP) disease from HTLV-1 carrier state. *Clin. Exp. Immunol.* **145,** 296–301
94. Mori, N., Krensky, A. M., Ohshima, K., Tomita, M., Matsuda, T., Ohta, T., Yamada, Y., Tomonaga, M., Ikeda, S., and Yamamoto, N. (2004) Elevated expression of CCL5/RANTES in adult T-cell leukemia cells: possible transactivation of the CCL5 gene by human T-cell leukemia virus type I tax. *Int. J. Cancer* **111,** 548–557
95. Montanheiro, P., Vergara, M. P., Smid, J., da Silva Duarte, A. J., de Oliveira, A. C., and Casseb, J. (2007) High production of RANTES and MIP-1α in the tropical spastic paraparesis/HTLV-1-associated myelopathy (TSP/HAM). *J. Neuroimmunol.* **188,** 138–142
96. Kooij, G., van Horssen, J., Bandaru, V. V., Haughey, N. J., and de Vries, H. E. (2012) The role of ATP-binding cassette transporters in neuroinflammation: relevance for bioactive lipids. *Front. Pharmacol.* **3,** 74
97. Kooij, G., Backer, R., Koning, J. J., Reijerkerk, A., van Horssen, J., van der Pol, S. M., Drexhage, J., Schinkel, A., Dijkstra, C. D., den Haan, J. M., Geijtenbeek, T. B., and de Vries, H. E. (2009) P-glycoprotein acts as an immunomodulator during neuroinflammation. *PLoS One* **4,** e8212
98. Okamoto, K., Fujisawa, J., Reth, M., and Yonehara, S. (2006) Human T-cell leukemia virus type-I oncoprotein Tax inhibits Fas-mediated apoptosis by inducing cellular FLIP through activation of NF-κB. *Genes Cells* **11,** 177–191
99. Krueger, A., Fas, S. C., Giaisi, M., Bleumink, M., Merling, A., Stumpf, C., Baumann, S., Holtkotte, D., Bosch, V., Krammer, P. H., and Li-Weber, M. (2006) HTLV-1 Tax protects against CD95-mediated apoptosis by induction of the cellular FLICE-inhibitory protein (c-FLIP). *Blood* **107,** 3933–3939
100. Kawakami, A., Nakashima, T., Sakai, H., Urayama, S., Yamasaki, S., Hida, A., Tsuboi, M., Nakamura, H., Ida, H., Migita, K., Kawabe, Y., and Eguchi, K. (1999) Inhibition of caspase cascade by HTLV-I tax through induction of NF-κB nuclear translocation. *Blood* **94,** 3847–3854
101. Iwanaga, Y., Tsukahara, T., Ohashi, T., Tanaka, Y., Arai, M., Nakamura, M., Ohtani, K., Koya, Y., Kannagi, M., Yamamoto, N., and Fujii, M. (1999) Human T-cell leukemia virus type 1 tax protein abrogates interleukin-2 dependence in a mouse T-cell line. *J. Virol.* **73,** 1271–1277
102. de la Fuente, C., Gupta, M. V., Klase, Z., Strouss, K., Cahan, P., McCaffery, T., Galante, A., Soteropoulos, P., Pumfery, A., Fujii, M., and Kashanchi, F. (2006) Involvement of HTLV-I Tax and CREB in aneuploidy: a bioinformatics approach. *Retrovirology* **3,** 43
103. Bellon, M., and Nicot, C. (2008) Central role of PI3K in transcriptional activation of hTERT in HTLV-I-infected cells. *Blood* **112,** 2946–2955
104. Jeong, S. J., Dasgupta, A., Jung, K. J., Um, J. H., Burke, A., Park, H. U., and Brady, J. N. (2008) PI3K/AKT inhibition induces caspase-dependent apoptosis in HTLV-1-transformed cells. *Virology* **370,** 264–272
105. Santiago, F., Clark, E., Chong, S., Molina, C., Mozafari, F., Mahieux, R., Fujii, M., Azimi, N., and Kashanchi, F. (1999) Transcriptional up-regulation of the cyclin D2 gene and acquisition of new cyclin-dependent kinase partners in human T-cell leukemia virus type 1-infected cells. *J. Virol.* **73,** 9917–9927
106. Iwanaga, R., Ohtani, K., Hayashi, T., and Nakamura, M. (2001) Molecular mechanism of cell cycle progression induced by the oncogene product Tax of human T-cell leukemia virus type I. *Oncogene* **20,** 2055–2067
107. Haller, K., Wu, Y., Derow, E., Schmitt, I., Jeang, K. T., and Grassmann, R. (2002) Physical interaction of human T-cell leukemia virus type 1 Tax with cyclin-dependent kinase 4 stimulates the phosphorylation of retinoblastoma protein. *Mol. Cell Biol.* **22,** 3327–3338
108. Jeong, S. J., Pise-Masison, C. A., Radonovich, M. F., Park, H. U., and Brady, J. N. (2005) Activated AKT regulates NF-κB activation, p53 inhibition and cell survival in HTLV-1-transformed cells. *Oncogene* **24,** 6719–6728
109. Schmitt, I., Rosin, O., Rohwer, P., Gossen, M., and Grassmann, R. (1998) Stimulation of cyclin-dependent kinase activity and G_1- to S-phase transition in human lymphocytes by the human T-cell leukemia/lymphotropic virus type 1 Tax protein. *J. Virol.* **72,** 633–640
110. Suetsugu, A., Honma, K., Saji, S., Moriwaki, H., Ochiya, T., and Hoffman, R. M. (2013) Imaging exosome transfer from breast cancer cells to stroma at metastatic sites in orthotopic nude-mouse models. *Adv. Drug. Deliv. Rev.* **65,** 383–390
111. Peinado, H., Alečković, M., Lavotshkin, S., Matei, I., Costa-Silva, B., Moreno-Bueno, G., Hergueta-Redondo, M., Williams, C., García-Santos, G., Ghajar, C., Nitadori-Hoshino, A., Hoffman, C., Badal, K., Garcia, B. A., Callahan, M. K., Yuan, J., Martins, V. R., Skog, J., Kaplan, R. N., Brady, M. S., Wolchok, J. D., Chapman, P. B., Kang, Y., Bromberg, J., and Lyden, D. (2012) Melanoma exosomes educate bone marrow progenitor cells toward a pro-metastatic phenotype through MET. *Nat. Med.* **18,** 883–891
112. Honegger, A., Leitz, J., Bulkescher, J., Hoppe-Seyler, K., and Hoppe-Seyler, F. (2013) Silencing of human papillomavirus (HPV) E6/E7 oncogene expression affects both the contents and the amounts of extracellular microvesicles released from HPV-positive cancer cells. *Int. J. Cancer* **133,** 1631–1642
113. Kadiu, I., Narayanasamy, P., Dash, P. K., Zhang, W., and Gendelman, H. E. (2012) Biochemical and biologic characterization of exosomes and microvesicles as facilitators of HIV-1 infection in macrophages. *J. Immunol.* **189,** 744–754
114. Khatua, A. K., Taylor, H. E., Hildreth, J. E., and Popik, W. (2009) Exosomes packaging APOBEC3G confer human immunodeficiency virus resistance to recipient cells. *J. Virol.* **83,** 512–521
115. Ceccarelli, S., Visco, V., Raffa, S., Wakisaka, N., Pagano, J. S., and Torrisi, M. R. (2007) Epstein-Barr virus latent membrane protein 1 promotes concentration in multivesicular bodies of fibroblast growth factor 2 and its release through exosomes. *Int. J. Cancer* **121,** 1494–1506
116. Lindholm, P. F., Marriott, S. J., Gitlin, S. D., Bohan, C. A., and Brady, J. N. (1990) Induction of nuclear NF-kappa B DNA binding activity after exposure of lymphoid cells to soluble tax1 protein. *New Biol.* **2,** 1034–1043
117. Cowan, E. P., Alexander, R. K., Daniel, S., Kashanchi, F., and Brady, J. N. (1997) Induction of tumor necrosis factor alpha in human neuronal cells by extracellular human T-cell lymphotropic virus type 1 Tax. *J. Virol.* **71,** 6982–6989
118. Lindholm, P. F., Reid, R. L., and Brady, J. N. (1992) Extracellular Tax1 protein stimulates tumor necrosis factor-β and immunoglobulin κ light chain expression in lymphoid cells. *J. Virol.* **66,** 1294–1302
119. Bhat, N. K., Adachi, Y., Samuel, K. P., and Derse, D. (1993) HTLV-1 gene expression by defective proviruses in an infected T-cell line. *Virology* **196,** 15–24
120. Vance, J. E., and Tasseva, G. (2013) Formation and function of phosphatidylserine and phosphatidylethanolamine in mammalian cells. *Biochim. Biophys. Acta* **1831,** 543–554
121. Saifuddin, M., Parker, C. J., Peeples, M. E., Gorny, M. K., Zolla-Pazner, S., Ghassemi, M., Rooney, I. A., Atkinson, J. P., and Spear, G. T. (1995) Role of virion-associated glycosylphosphatidylinositol-linked proteins CD55 and CD59 in complement resistance of cell line-derived and primary isolates of HIV-1. *J. Exp. Med.* **182,** 501–509
122. Spear, G. T., Lurain, N. S., Parker, C. J., Ghassemi, M., Payne, G. H., and Saifuddin, M. (1995) Host cell-derived complement control proteins CD55 and CD59 are incorporated into the virions of two unrelated enveloped viruses. Human T cell leukemia/lymphoma virus type I (HTLV-I) and human cytomegalovirus (HCMV). *J. Immunol.* **155,**

4376–4381
123. Inlora, J., Chukkapalli, V., Derse, D., and Ono, A. (2011) Gag localization and virus-like particle release mediated by the matrix domain of human T-lymphotropic virus type 1 Gag are less dependent on phosphatidylinositol-(4,5)-bisphosphate than those mediated by the matrix domain of HIV-1 Gag. *J. Virol.* **85,** 3802–3810
124. Callahan, M. K., Popernack, P. M., Tsutsui, S., Truong, L., Schlegel, R. A., and Henderson, A. J. (2003) Phosphatidylserine on HIV envelope is a cofactor for infection of monocytic cells. *J. Immunol.* **170,** 4840–4845
125. Carvalho, E. M., Bacellar, O., Porto, A. F., Braga, S., Galvão-Castro, B., and Neva, F. (2001) Cytokine profile and immunomodulation in asymptomatic human T-lymphotropic virus type 1-infected blood donors. *J. Acquir. Immune. Defic. Syndr.* **27,** 1–6
126. Islam, A., Shen, X., Hiroi, T., Moss, J., Vaughan, M., and Levine, S. J. (2007) The brefeldin A-inhibited guanine nucleotide-exchange protein, BIG2, regulates the constitutive release of TNFR1 exosome-like vesicles. *J. Biol. Chem.* **282,** 9591–9599
127. Mittelbrunn, M., Gutiérrez-Vázquez, C., Villarroya-Beltri, C., González, S., Sánchez-Cabo, F., González, M. Á., Bernad, A., and Sánchez-Madrid, F. (2011) Unidirectional transfer of microRNA-loaded exosomes from T cells to antigen-presenting cells. *Nat. Commun.* **2,** 282
128. Arenz, C., Thutewohl, M., Block, O., Waldmann, H., Altenbach, H. J., and Giannis, A. (2001) Manumycin A and its analogues are irreversible inhibitors of neutral sphingomyelinase. *Chembiochem.* **2,** 141–143
129. Pal, R., Mumbauer, S., Hoke, G. M., Takatsuki, A., and Sarngadharan, M. G. (1991) Brefeldin A inhibits the processing and secretion of envelope glycoproteins of human immunodeficiency virus type 1. *AIDS Res. Hum. Retroviruses* **7,** 707–712
130. Macovei, A., Zitzmann, N., Lazar, C., Dwek, R. A., and Branza-Nichita, N. (2006) Brefeldin A inhibits pestivirus release from infected cells, without affecting its assembly and infectivity. *Biochem. Biophys. Res. Commun.* **346,** 1083–1090
131. Schneider, A., and Simons, M. (2013) Exosomes: vesicular carriers for intercellular communication in neurodegenerative disorders. *Cell Tissue Res.* **352,** 33–47
132. Macaire, H., Riquet, A., Moncollin, V., Biémont-Trescol, M. C., Duc Dodon, M., Hermine, O., Debaud, A. L., Mahieux, R., Mesnard, J. M., Pierre, M., Gazzolo, L., Bonnefoy, N., and Valentin, H. (2012) Tax protein-induced expression of antiapoptotic Bfl-1 protein contributes to survival of human T-cell leukemia virus type 1 (HTLV-1)-infected T-cells. *J. Biol. Chem.* **287,** 21357–21370
133. Cheng, H., Ren, T., and Sun, S. C. (2012) New insight into the oncogenic mechanism of the retroviral oncoprotein Tax. *Protein Cell* **3,** 581–589
134. Matsuoka, M., and Jeang, K. T. (2011) Human T-cell leukemia virus type 1 (HTLV-1) and leukemic transformation: viral infectivity, Tax, HBZ and therapy. *Oncogene* **30,** 1379–1389

Supplemental Table 1. Characteristics of exosomal proteins and lipids.

Proteomics analysis of CEM exosomes.

	Reference	Peptide (prob)	Protein Score	MW (Da)	Accession Number
1	actin, beta-like 2	1.00E+00	10.19	41976.0	63055057
2	actin, gamma 1 propeptide	1.00E-30	120.43	41765.8	4501887
3	actin, gamma 2 propeptide	7.55E-11	120.23	41849.8	4501889
4	activated RNA polymerase II transcription cofactor 4	2.02E-04	10.13	14386.4	217330646
5	adenosylhomocysteinase isoform 1	5.06E-05	10.16	47685.3	9951915
6	adenylyl cyclase-associated protein	5.03E-06	10.17	51640.7	5453595
7	albumin preproprotein	5.73E-07	30.22	69321.6	4502027
8	alpha 2 globin	1.43E-11	40.24	15247.9	4504345
9	alpha-2-HS-glycoprotein	7.46E-07	20.21	39315.7	156523970
10	ankyrin repeat domain 32	2.67E-04	10.14	120972.5	188219549
11	annexin VI isoform 1	4.02E-06	20.21	75825.7	71773329
12	ATP-dependent DNA helicase II	2.29E-04	20.15	82652.4	10863945
13	beta tubulin 1, class VI	7.05E-07	20.25	50294.6	13562114
14	bisphosphoglycerate mutase 4	8.65E-09	10.27	28758.8	71274132
15	carboxypeptidase N, polypeptide 1 precursor	1.82E-07	10.23	52253.4	4503011
16	CD40 antigen isoform 2 precursor	6.68E-11	20.19	22244.1	23312371
17	chaperonin containing TCP1, subunit 2	3.22E-06	10.17	57452.3	5453603
18	chaperonin containing TCP1, subunit 3 isoform a	6.47E-06	40.17	60495.4	63162572
19	chaperonin containing TCP1, subunit 4 (delta)	1.66E-07	30.19	57887.9	38455427
20	chaperonin containing TCP1, subunit 5 (epsilon)	4.91E-10	10.26	59632.9	24307939
21	chaperonin containing TCP1, subunit 7 isoform a	1.11E-15	20.26	59329.0	5453607
22	chaperonin containing TCP1, subunit 8 (theta)	7.46E-09	30.23	59582.6	48762932
23	chloride intracellular channel 1	1.00E-30	20.20	26905.8	14251209
24	clathrin heavy chain 1	1.67E-13	290.29	191491.7	4758012
25	coagulation factor II preproprotein	4.40E-12	60.25	69992.2	4503635
26	coagulation factor V precursor	6.58E-10	20.18	251543.8	105990535
27	cofilin 1 (non-muscle)	1.21E-11	20.19	18490.7	5031635
28	coronin, actin binding protein, 1A	1.54E-10	20.18	50993.9	5902134
29	enolase 1	1.15E-12	80.30	47139.4	4503571
30	enolase 2	2.22E-15	20.20	47239.1	5803011
31	epsilon globin	4.00E-07	10.14	16192.5	4885393
32	eukaryotic translation elongation factor 1 alpha 2	4.51E-10	40.25	50438.4	4503475

33	eukaryotic translation elongation factor 2	1.35E-12	140.33	95277.1	4503483
34	eukaryotic translation initiation factor 2, subunit 1 alpha, 35kDa	3.98E-06	10.16	36089.4	4758256
35	eukaryotic translation initiation factor 3, subunit 10 theta, 150/170kDa	5.85E-04	10.15	166467.5	4503509
36	eukaryotic translation initiation factor 4A isoform 1	4.15E-06	10.13	46124.6	4503529
37	eukaryotic translation initiation factor 4A, isoform 3	4.86E-05	10.14	46841.2	7661920
38	fatty acid synthase	1.02E-09	40.17	273251.6	41872631
39	filamin A, alpha isoform 1	4.67E-06	10.17	279841.1	116063573
40	fructose-bisphosphate aldolase A	3.84E-09	20.20	39395.3	193794814
41	fructose-bisphosphate aldolase C	4.67E-07	10.19	39431.3	4885063
42	galectin-1	3.90E-09	20.18	14706.2	4504981
43	gelsolin isoform b	1.21E-08	40.19	80590.6	189083772
44	glucose phosphate isomerase	4.68E-10	10.22	63107.3	18201905
45	glyceraldehyde-3-phosphate dehydrogenase	4.44E-15	150.29	36030.4	7669492
46	glyceraldehyde-3-phosphate dehydrogenase, spermatogenic	1.01E-05	10.17	44472.8	7657116
47	guanine nucleotide binding protein (G protein), beta polypeptide 2-like 1	1.10E-08	30.16	35054.6	5174447
48	H2A histone family, member V isoform 1	1.37E-08	10.19	13500.5	6912616
49	H2A histone family, member V isoform 2	3.41E-12	30.29	12138.7	20357599
50	H2A histone family, member Y isoform 1	1.69E-12	40.23	39159.2	20336746
51	H3 histone family, member H	1.00E-30	60.26	15394.5	4504291
52	heat shock 70kDa protein 2	7.62E-06	10.19	69978.0	13676857
53	heat shock 70kDa protein 4	2.60E-07	10.19	94271.1	38327039
54	heat shock 70kDa protein 8 isoform 1	1.91E-07	50.22	70854.4	5729877
55	heat shock 90kDa protein 1, alpha isoform 1	5.99E-12	10.21	98099.4	153792590
56	heat shock 90kDa protein 1, beta	6.34E-12	50.26	83212.2	20149594
57	heterogeneous nuclear ribonucleoprotein L isoform a	3.00E-04	10.15	64092.4	52632383
58	heterogeneous nuclear ribonucleoprotein U isoform a	1.89E-10	20.25	90528.0	74136883
59	histone cluster 1, H1b	1.83E-13	50.24	22566.5	4885381
60	histone cluster 1, H1c	2.25E-06	20.20	21351.8	4885375
61	histone cluster 1, H1t	8.22E-11	10.23	22005.7	20544168
62	histone cluster 1, H2ad	8.97E-13	50.21	14098.9	10800130
63	histone cluster 1, H2ae	1.74E-09	20.21	14127.0	10645195
64	histone cluster 1, H2bb	1.25E-05	20.20	13941.6	10800140
65	histone cluster 1, H2bi	5.73E-12	70.24	13897.6	4504271
66	histone cluster 1, H4a	4.98E-10	160.25	11360.4	4504301
67	histone cluster 2, H2aa3	9.23E-12	10.23	14086.9	4504251
68	inter-alpha globulin inhibitor H2	1.34E-09	40.27	106396.8	70778918

	polypeptide				
69	intercellular adhesion molecule 1 precursor	1.03E-05	10.12	57789.0	167466198
70	macrophage migration inhibitory factor	2.12E-05	10.16	12468.2	4505185
71	major histocompatibility complex, class II, DP beta 1 precursor	1.09E-04	10.19	29140.8	24797076
72	major histocompatibility complex, class II, DR alpha precursor	5.52E-05	10.23	28602.7	52426774
73	major vault protein	1.11E-15	100.22	99266.1	19913412
74	moesin	9.99E-15	50.25	67777.9	4505257
75	myosin IG	8.88E-08	20.21	116367.2	54873627
76	myosin, heavy polypeptide 10, non-muscle	1.55E-09	60.24	228856.9	41406064
77	myosin, heavy polypeptide 9, non-muscle	8.88E-15	180.28	226390.6	12667788
78	nucleophosmin 1 isoform 1	7.77E-15	10.20	32554.9	10835063
79	nucleosome assembly protein 1-like 1	1.06E-09	50.22	45346.0	4758756
80	nucleosome assembly protein 1-like 4	5.29E-04	10.16	42797.0	5174613
81	peptidylprolyl isomerase A	9.68E-10	20.25	18000.9	10863927
82	peroxiredoxin 1	8.37E-06	10.15	22096.3	4505591
83	phosphoglycerate kinase 1	2.80E-13	60.24	44586.2	4505763
84	phosphoglycerate kinase 2	3.55E-09	20.20	44767.4	31543397
85	PREDICTED: similar to complement component C3, partial	1.77E-12	40.22	144718.0	169218213
86	PREDICTED: similar to major histocompatibility complex, class II, DR beta 3 isoform 2	6.14E-08	20.20	30101.1	239740857
87	PREDICTED: similar to protein kinase, DNA-activated, catalytic polypeptide	6.92E-05	20.20	465164.9	113430845
88	PREDICTED: similar to pyruvate kinase, muscle	1.44E-09	150.27	39567.3	169218111
89	pregnancy-zone protein	5.36E-08	20.17	163759.1	162809334
90	profilin 1	5.38E-09	50.22	15044.6	4826898
91	proteasome activator subunit 2	1.08E-07	10.19	27384.3	30410792
92	pyruvate kinase, muscle isoform M1	5.55E-15	30.26	58025.1	33286420
93	pyruvate kinase, muscle isoform M2	3.33E-14	30.25	57900.2	33286418
94	RAP1B, member of RAS oncogene family-like	9.33E-14	40.20	20911.6	148227764
95	ras-related C3 botulinum toxin substrate 2	1.93E-06	10.16	21415.1	4506381
96	ras-related nuclear protein	9.51E-08	40.20	24407.6	5453555
97	ribosomal protein L10	1.73E-09	20.31	24587.9	223890243
98	ribosomal protein L10a	3.05E-07	10.19	24815.5	15431288
99	ribosomal protein L10-like protein	1.68E-06	30.15	24502.7	18152783
100	ribosomal protein L11	6.41E-08	20.20	20239.7	15431290
101	ribosomal protein L13	1.33E-04	10.13	24246.5	15431295
102	ribosomal protein L13a	1.00E-05	20.20	23562.4	6912634
103	ribosomal protein L14	1.89E-08	30.21	23417.0	78000181

104	ribosomal protein L15	3.62E-11	40.20	24131.1	15431293
105	ribosomal protein L17	1.81E-06	20.17	21383.3	4506617
106	ribosomal protein L18	1.16E-08	40.23	21621.1	4506607
107	ribosomal protein L18a	6.67E-07	20.20	20748.9	11415026
108	ribosomal protein L19	1.89E-14	10.26	23451.3	4506609
109	ribosomal protein L21	4.63E-11	20.23	18553.1	18104948
110	ribosomal protein L22 proprotein	3.09E-08	10.27	14777.8	4506613
111	ribosomal protein L24	3.17E-08	40.23	17767.9	4506619
112	ribosomal protein L27	1.67E-04	10.12	15787.8	4506623
113	ribosomal protein L27a	7.20E-09	20.20	16551.0	4506625
114	ribosomal protein L28 isoform 1	1.54E-06	20.18	18418.4	209915581
115	ribosomal protein L3 isoform b	1.19E-06	20.20	40126.6	76496472
116	ribosomal protein L30	3.19E-06	30.22	12775.7	4506631
117	ribosomal protein L32	1.22E-09	40.22	15849.8	4506635
118	ribosomal protein L4	2.03E-13	120.33	47667.5	16579885
119	ribosomal protein L5	4.68E-11	20.23	34340.7	14591909
120	ribosomal protein L6	9.99E-07	10.21	32707.6	16753227
121	ribosomal protein L7	7.83E-10	50.19	29207.2	15431301
122	ribosomal protein L7a	2.63E-11	50.28	29977.0	4506661
123	ribosomal protein L8	9.78E-06	10.18	28007.3	15431306
124	ribosomal protein P0	2.37E-06	10.17	34251.8	16933546
125	ribosomal protein S11	6.76E-08	10.15	18419.0	4506681
126	ribosomal protein S16	8.88E-04	10.14	16435.0	4506691
127	ribosomal protein S2	7.14E-11	50.25	31304.6	15055539
128	ribosomal protein S24 isoform a	5.67E-09	20.13	15059.2	14916501
129	ribosomal protein S3	5.76E-06	20.18	26671.4	15718687
130	ribosomal protein S3a	8.70E-06	40.20	29925.8	4506723
131	ribosomal protein S4, X-linked X isoform	2.42E-04	10.13	29579.1	4506725
132	ribosomal protein S5	2.15E-06	10.23	22862.1	13904870
133	ribosomal protein S6	1.94E-08	40.22	28663.0	17158044
134	ribosomal protein S8	1.86E-11	80.24	24190.2	4506743
135	ribosomal protein S9	1.77E-04	20.14	22577.6	14141193
136	septin 2	6.97E-07	10.19	41461.3	4758158
137	serine (or cysteine) proteinase inhibitor, clade F (alpha-2 antiplasmin, pigment epithelium derived factor), member 1	6.19E-09	50.21	46283.4	39725934
138	small nuclear ribonucleoprotein D1 polypeptide 16kDa	5.33E-14	20.21	13273.4	5902102
139	smooth muscle myosin heavy chain 11 isoform SM2A	1.93E-06	20.21	223438.2	13124875
140	talin 1	9.76E-07	20.16	269596.3	223029410
141	talin 2	4.33E-06	10.19	271440.8	156938343
142	T-complex protein 1 isoform a	2.02E-10	40.19	60305.7	57863257
143	thrombospondin 1 precursor	1.11E-08	70.19	129299.2	40317626

144	transgelin 2	1.44E-12	20.25	22377.2	4507357
145	transmembrane protein 35	2.06E-04	10.15	18428.3	11056012
146	triosephosphate isomerase 1 isoform 1	3.78E-11	30.25	26652.7	4507645
147	Trypsin_porcine	1.20E-13	10.31	24393.8	
148	tubulin alpha 6	4.06E-09	50.21	49863.5	14389309
149	tubulin, alpha 3e	2.09E-11	80.28	49884.6	46409270
150	tubulin, alpha 4a	1.39E-06	20.25	49892.4	17921989
151	tubulin, beta	1.75E-12	20.29	49639.0	29788785
152	tubulin, beta 2	2.23E-13	60.30	49875.0	4507729
153	tubulin, beta polypeptide 4, member Q	3.06E-08	10.16	48456.4	55770868
154	tubulin, beta, 2	5.64E-06	30.22	49799.0	5174735
155	tumor necrosis factor ligand superfamily, member 7	6.42E-07	20.17	21104.9	4507605
156	ubiquitin-activating enzyme E1	2.79E-05	30.17	117774.5	23510340
157	vitronectin precursor	3.33E-12	10.24	54271.2	88853069
158	WD repeat-containing protein 1 isoform 1	3.40E-13	20.25	66151.9	9257257

Proteomics analysis of C81 exosomes.

	Reference	Peptide (prob)	Protein Score	MW (Da)	Accession Number
1	actin, gamma 1 propeptide [Homo sapiens]	1.00E-30	110.43	41765.8	4501887
2	actin, gamma 2 propeptide [Homo sapiens]	9.00E-12	180.23	41849.8	4501889
3	albumin preproprotein [Homo sapiens]	8.32E-11	40.24	69321.6	4502027
4	alpha 2 globin [Homo sapiens]	2.65E-12	40.23	15247.9	4504345
5	alpha-2-HS-glycoprotein [Homo sapiens]	1.65E-07	20.19	39315.7	156523970
6	alpha-fetoprotein precursor [Homo sapiens]	8.26E-10	10.21	68633.1	4501989
7	ATP-dependent DNA helicase II, 70 kDa subunit [Homo sapiens]	4.69E-04	10.15	69799.2	4503841
8	barrier to autointegration factor 1 [Homo sapiens]	9.33E-13	40.30	10052.0	4502389
9	basigin isoform 2 precursor [Homo sapiens]	3.25E-08	50.23	29202.7	38372925
10	bisphosphoglycerate mutase 4 [Homo sapiens]	6.41E-09	20.26	28758.8	71274132
11	casein kinase II alpha 1 subunit isoform a [Homo sapiens]	6.22E-07	10.21	45114.9	29570791
12	CD5 molecule [Homo sapiens]	4.83E-07	40.19	54542.9	166197668
13	chaperonin containing TCP1, subunit 3 isoform a [Homo sapiens]	1.13E-06	20.23	60495.4	63162572
14	chaperonin containing TCP1, subunit 5 (epsilon) [Homo sapiens]	1.36E-08	30.22	59632.9	24307939
15	chaperonin containing TCP1, subunit 7	3.51E-06	20.19	59329.0	5453607

	isoform a [Homo sapiens]				
16	chaperonin containing TCP1, subunit 8 (theta) [Homo sapiens]	4.69E-07	10.20	59582.6	48762932
17	chloride intracellular channel 1 [Homo sapiens]	5.86E-12	50.25	26905.8	14251209
18	clathrin heavy chain 1 [Homo sapiens]	3.77E-11	180.26	191491.7	4758012
19	coagulation factor II preproprotein [Homo sapiens]	5.77E-11	30.25	69992.2	4503635
20	coagulation factor V precursor [Homo sapiens]	5.01E-09	20.18	251543.8	105990535
21	cofilin 2 [Homo sapiens]	9.78E-10	10.27	18724.9	33946278
22	enolase 1 [Homo sapiens]	2.82E-08	80.23	47139.4	4503571
23	enolase 2 [Homo sapiens]	1.76E-04	20.19	47239.1	5803011
24	eukaryotic translation elongation factor 1 alpha 1 [Homo sapiens]	1.22E-14	40.29	50109.2	4503471
25	eukaryotic translation elongation factor 1 alpha 2 [Homo sapiens]	9.37E-11	40.21	50438.4	4503475
26	eukaryotic translation elongation factor 2 [Homo sapiens]	6.66E-14	130.30	95277.1	4503483
27	eukaryotic translation initiation factor 4A2 [Homo sapiens]	9.12E-10	10.26	46372.8	83700235
28	fascin 1 [Homo sapiens]	2.28E-11	80.27	54496.1	4507115
29	filamin A, alpha isoform 1 [Homo sapiens]	1.47E-13	100.28	279841.1	116063573
30	galectin-1 [Homo sapiens]	7.53E-10	20.20	14706.2	4504981
31	glyceraldehyde-3-phosphate dehydrogenase [Homo sapiens]	2.22E-16	160.29	36030.4	7669492
32	guanine nucleotide binding protein (G protein), beta polypeptide 2-like 1 [Homo sapiens]	4.41E-08	30.23	35054.6	5174447
33	H2A histone family, member V isoform 1 [Homo sapiens]	7.98E-07	10.24	13500.5	6912616
34	H2A histone family, member Y isoform 1 [Homo sapiens]	1.98E-08	50.25	39159.2	20336746
35	H2A histone family, member Y2 [Homo sapiens]	6.87E-12	10.26	40033.4	8923920
36	H3 histone family, member H [Homo sapiens]	1.00E-30	60.37	15394.5	4504291
37	heat shock 70kDa protein 2 [Homo sapiens]	3.69E-12	70.24	69978.0	13676857
38	heat shock 70kDa protein 8 isoform 1 [Homo sapiens]	3.82E-07	80.22	70854.4	5729877
39	heat shock 90kDa protein 1, alpha isoform 1 [Homo sapiens]	3.74E-11	20.27	98099.4	153792590
40	heat shock 90kDa protein 1, beta [Homo sapiens]	3.82E-13	190.28	83212.2	20149594
41	heat shock protein beta-1 [Homo sapiens]	1.76E-09	30.21	22768.5	4504517
42	heterogeneous nuclear ribonucleoprotein	8.56E-07	10.18	33649.6	117189975

	C isoform a [Homo sapiens]				
43	heterogeneous nuclear ribonucleoprotein C-like 1 [Homo sapiens]	8.19E-05	20.19	32122.7	61966711
44	heterogeneous nuclear ribonucleoprotein L isoform a [Homo sapiens]	1.59E-08	10.19	64092.4	52632383
45	heterogeneous nuclear ribonucleoprotein U isoform a [Homo sapiens]	9.02E-10	50.25	90528.0	74136883
46	histone cluster 1, H1b [Homo sapiens]	1.52E-09	30.21	22566.5	4885381
47	histone cluster 1, H1c [Homo sapiens]	3.70E-09	30.22	21351.8	4885375
48	histone cluster 1, H2ad [Homo sapiens]	1.72E-10	70.25	14098.9	10800130
49	histone cluster 1, H2ae [Homo sapiens]	4.29E-08	20.26	14127.0	10645195
50	histone cluster 1, H2bb [Homo sapiens]	1.22E-06	20.25	13941.6	10800140
51	histone cluster 1, H2bi [Homo sapiens]	6.41E-11	70.24	13897.6	4504271
52	histone cluster 1, H4a [Homo sapiens]	1.10E-11	150.29	11360.4	4504301
53	histone cluster 2, H2aa3 [Homo sapiens]	9.46E-11	10.25	14086.9	4504251
54	histone cluster 2, H2ab [Homo sapiens]	3.05E-07	10.23	13986.8	28195394
55	integrin alpha L isoform a precursor [Homo sapiens]	7.16E-08	10.16	128688	167466215
56	integrin, beta 2 precursor [Homo sapiens]	7.16E-09	10.16	84726.1	89191865
57	inter-alpha globulin inhibitor H2 polypeptide [Homo sapiens]	1.74E-04	10.16	106396.8	70778918
58	major histocompatibility complex, class I, A precursor [Homo sapiens]	2.65E-12	60.23	40815.2	24797067
59	major histocompatibility complex, class I, E precursor [Homo sapiens]	1.86E-08	20.22	40032.8	62912479
60	major histocompatibility complex, class I, F isoform 2 precursor [Homo sapiens]	2.89E-12	20.22	39037.5	149158698
61	major vault protein [Homo sapiens]	1.12E-08	60.20	99266.1	19913412
62	milk fat globule-EGF factor 8 protein isoform a [Homo sapiens]	4.93E-13	100.28	43077.5	167830475
63	myosin IG [Homo sapiens]	6.88E-05	10.16	116367.2	54873627
64	myosin, heavy polypeptide 10, non-muscle [Homo sapiens]	8.88E-15	430.37	228856.9	41406064
65	myosin, heavy polypeptide 9, non-muscle [Homo sapiens]	1.23E-13	490.33	226390.6	12667788
66	neurolysin [Homo sapiens]	1.00E+00	20.16	80599.8	14149738
67	olfactory receptor, family 5, subfamily H, member 2 [Homo sapiens]	8.05E-05	10.14	35949.7	53828688
68	peptidylprolyl isomerase A [Homo sapiens]	8.65E-10	30.27	18000.9	10863927
69	peroxiredoxin 1 [Homo sapiens]	3.11E-04	10.11	22096.3	4505591
70	phosphoglycerate kinase 1 [Homo sapiens]	5.49E-12	70.25	44586.2	4505763
71	PREDICTED: similar to complement component C3, partial [Homo sapiens]	7.79E-08	20.19	144718.0	169218213
72	PREDICTED: similar to peptidylprolyl isomerase A isoform 2 [Homo sapiens]	2.93E-10	10.21	18013.8	88953813

73	PREDICTED: similar to protein kinase, DNA-activated, catalytic polypeptide [Homo sapiens]	6.41E-05	10.18	465164.9	113430845
74	PREDICTED: similar to pyruvate kinase, muscle [Homo sapiens]	6.77E-14	120.31	39567.3	169218111
75	pregnancy-zone protein [Homo sapiens]	2.00E-09	20.16	163759.1	162809334
76	profilin 1 [Homo sapiens]	6.18E-10	40.25	15044.6	4826898
77	PRP19/PSO4 pre-mRNA processing factor 19 homolog [Homo sapiens]	9.04E-06	10.12	55146.4	7657381
78	pyruvate kinase, muscle isoform M1 [Homo sapiens]	1.76E-11	60.25	58025.1	33286420
79	pyruvate kinase, muscle isoform M2 [Homo sapiens]	1.80E-10	20.22	57900.2	33286418
80	RAP1B, member of RAS oncogene family-like [Homo sapiens]	8.93E-12	20.23	20911.6	148227764
81	ras-related nuclear protein [Homo sapiens]	1.22E-06	30.22	24407.6	5453555
82	ribosomal protein L10a [Homo sapiens]	6.88E-10	30.20	24815.5	15431288
83	ribosomal protein L11 [Homo sapiens]	3.99E-07	10.21	20239.7	15431290
84	ribosomal protein L14 [Homo sapiens]	7.35E-09	30.21	23417.0	78000181
85	ribosomal protein L18 [Homo sapiens]	1.13E-06	20.17	21621.1	4506607
86	ribosomal protein L18a [Homo sapiens]	2.99E-09	30.19	20748.9	11415026
87	ribosomal protein L21 [Homo sapiens]	1.04E-10	20.27	18553.1	18104948
88	ribosomal protein L23 [Homo sapiens]	1.98E-10	10.21	14856.1	4506605
89	ribosomal protein L24 [Homo sapiens]	1.04E-05	10.15	17767.9	4506619
90	ribosomal protein L27a [Homo sapiens]	8.49E-08	20.20	16551.0	4506625
91	ribosomal protein L3 isoform b [Homo sapiens]	2.85E-13	50.29	40126.6	76496472
92	ribosomal protein L32 [Homo sapiens]	1.63E-10	20.24	15849.8	4506635
93	ribosomal protein L4 [Homo sapiens]	1.03E-05	40.28	47667.5	16579885
94	ribosomal protein L5 [Homo sapiens]	1.67E-12	50.23	34340.7	14591909
95	ribosomal protein L6 [Homo sapiens]	9.76E-11	30.22	32707.6	16753227
96	ribosomal protein L7 [Homo sapiens]	9.66E-09	60.20	29207.2	15431301
97	ribosomal protein L7a [Homo sapiens]	3.92E-12	40.23	29977.0	4506661
98	ribosomal protein P1 isoform 1 [Homo sapiens]	2.90E-04	10.14	11506.7	4506669
99	ribosomal protein S2 [Homo sapiens]	1.09E-05	40.18	31304.6	15055539
100	ribosomal protein S24 isoform a [Homo sapiens]	1.69E-07	20.17	15059.2	14916501
101	ribosomal protein S26 [Homo sapiens]	1.29E-07	20.21	13007.1	15011936
102	ribosomal protein S3 [Homo sapiens]	4.38E-08	40.23	26671.4	15718687
103	ribosomal protein S3a [Homo sapiens]	1.25E-06	30.22	29925.8	4506723
104	ribosomal protein S6 [Homo sapiens]	1.17E-06	10.22	28663.0	17158044
105	ribosomal protein S8 [Homo sapiens]	1.34E-12	80.21	24190.2	4506743
106	ribosomal protein S9 [Homo sapiens]	4.99E-06	40.18	22577.6	14141193

107	serine (or cysteine) proteinase inhibitor, clade F (alpha-2 antiplasmin, pigment epithelium derived factor), member 1 [Homo sapiens]	3.45E-09	10.19	46283.4	39725934
108	serine hydroxymethyltransferase 2 (mitochondrial) [Homo sapiens]	7.85E-07	40.20	55957.8	19923315
109	small nuclear ribonucleoprotein D1 polypeptide 16kDa [Homo sapiens]	3.12E-09	40.29	13273.4	5902102
110	smooth muscle myosin heavy chain 11 isoform SM2A [Homo sapiens]	1.18E-11	40.25	223438.2	13124875
111	solute carrier family 1 member 5 isoform 1 [Homo sapiens]	1.52E-09	20.19	56562.4	5032093
112	thrombospondin 1 precursor [Homo sapiens]	6.97E-08	70.23	129299.2	40317626
113	Thy-1 cell surface antigen preproprotein [Homo sapiens]	8.77E-14	30.30	17923.4	19923362
114	triosephosphate isomerase 1 isoform 1 [Homo sapiens]	4.28E-07	50.22	26652.7	4507645
115	Trypsin_porcine	2.52E-13	20.31	24393.8	
116	tryptophanyl-tRNA synthetase isoform a [Homo sapiens]	1.43E-05	30.16	53131.7	47419914
117	tubulin alpha 6 [Homo sapiens]	1.37E-12	80.36	49863.5	14389309
118	tubulin, alpha 3e [Homo sapiens]	8.60E-13	80.24	49884.6	46409270
119	tubulin, alpha 4a [Homo sapiens]	2.48E-07	30.21	49892.4	17921989
120	tubulin, beta [Homo sapiens]	7.77E-15	50.29	49639.0	29788785
121	tubulin, beta 2 [Homo sapiens]	1.22E-14	80.33	49875.0	4507729
122	tubulin, beta polypeptide 4, member Q [Homo sapiens]	2.99E-11	20.25	48456.4	55770868
123	tumor necrosis factor ligand superfamily, member 7 [Homo sapiens]	4.11E-08	30.18	21104.9	4507605
124	tyrosine 3/tryptophan 5 -monooxygenase activation protein, theta polypeptide [Homo sapiens]	1.26E-05	10.18	27746.8	5803227
125	ubiquitin-activating enzyme E1 [Homo sapiens]	2.86E-08	20.21	117774.5	23510340
126	vitronectin precursor [Homo sapiens]	1.05E-12	60.28	54271.2	88853069

Proteomics analysis of MT2 exosomes.

	Reference	Peptide (prob)	Protein Score	MW (Da)	Accession Number
1	actin, gamma 1 propeptide	1.89E-14	70.32	41765.8	4501887
2	actin, gamma 2 propeptide	3.19E-11	110.22	41849.8	4501889
3	albumin preproprotein	2.83E-09	30.18	69321.6	4502027
4	alpha 2 globin	1.54E-04	40.24	15247.9	4504345
5	alpha isoform of regulatory subunit A, protein phosphatase 2	2.21E-05	10.17	65267.1	21361399

6	alpha-2-HS-glycoprotein	2.65E-07	30.18	39315.7	156523970
7	annexin VI isoform 1	4.01E-11	40.24	75825.7	71773329
8	beta tubulin 1, class VI	4.31E-06	10.17	50294.6	13562114
9	beta-2-microglobulin precursor	1.71E-12	20.20	13705.9	4757826
10	bisphosphoglycerate mutase 1	7.15E-09	10.21	28785.9	4505753
11	bisphosphoglycerate mutase 4	6.17E-09	10.15	28758.8	71274132
12	CD81 antigen	1.44E-14	20.28	25792.1	4757944
13	chaperonin containing TCP1, subunit 2	3.11E-14	20.20	57452.3	5453603
14	chaperonin containing TCP1, subunit 5 (epsilon)	5.10E-09	10.22	59632.9	24307939
15	chaperonin containing TCP1, subunit 6A isoform a	1.57E-12	10.17	57987.7	4502643
16	chaperonin containing TCP1, subunit 8 (theta)	2.99E-07	10.19	59582.6	48762932
17	chloride intracellular channel 1	6.89E-08	30.22	26905.8	14251209
18	clathrin heavy chain 1	4.44E-15	120.32	191491.7	4758012
19	coagulation factor II preproprotein	2.05E-09	20.23	69992.2	4503635
20	cofilin 2	6.33E-06	20.19	18724.9	33946278
21	delta globin	4.19E-05	10.14	16045.3	4504351
22	DnaJ (Hsp40) homolog, subfamily A, member 1	1.36E-05	10.14	44839.5	4504511
23	EGF-like repeats and discoidin I-like domains-containing protein 3	1.51E-11	10.27	53730.0	31317224
24	enolase 1	4.24E-05	40.28	47139.4	4503571
25	epsilon globin	1.17E-05	10.13	16192.5	4885393
26	eukaryotic translation elongation factor 1 alpha 1	1.39E-09	30.28	50109.2	4503471
27	eukaryotic translation elongation factor 1 alpha 2	1.16E-04	30.17	50438.4	4503475
28	eukaryotic translation elongation factor 2	7.71E-12	60.28	95277.1	4503483
29	ezrin	2.08E-11	10.19	69369.8	21614499
30	fatty acid synthase	1.34E-05	30.14	273251.6	41872631
31	fructose-bisphosphate aldolase A	1.58E-07	30.22	39395.3	193794814
32	galectin-1	4.60E-09	30.26	14706.2	4504981
33	glyceraldehyde-3-phosphate dehydrogenase	1.54E-11	70.20	36030.4	7669492
34	H2A histone family, member V isoform 1	1.15E-05	10.15	13500.5	6912616
35	H3 histone family, member H	2.22E-15	20.38	15394.5	4504291
36	heat shock 70kDa protein 1A	3.82E-04	10.18	70009.2	194248072
37	heat shock 70kDa protein 2	2.18E-12	40.27	69978.0	13676857
38	heat shock 70kDa protein 5	1.11E-11	60.24	72288.5	16507237
39	heat shock 70kDa protein 8 isoform 1	1.80E-10	80.22	70854.4	5729877
40	heat shock 90kDa protein 1, alpha isoform 1	2.20E-06	10.18	98099.4	153792590

41	heat shock 90kDa protein 1, beta	5.00E-14	60.21	83212.2	20149594
42	heat shock protein 90kDa beta, member 1	2.91E-12	50.23	92411.2	4507677
43	histone cluster 1, H2ad	8.66E-09	60.23	14098.9	10800130
44	histone cluster 1, H2ae	5.43E-08	20.15	14127.0	10645195
45	histone cluster 1, H2bb	1.86E-04	10.15	13941.6	10800140
46	histone cluster 1, H2bi	3.18E-10	40.24	13897.6	4504271
47	histone cluster 1, H4a	1.04E-10	90.27	11360.4	4504301
48	inter-alpha (globulin) inhibitor H3 preproprotein	6.23E-09	20.16	99786.6	133925809
49	inter-alpha globulin inhibitor H2 polypeptide	2.72E-11	10.16	106396.8	70778918
50	intercellular adhesion molecule 1 precursor	6.07E-12	120.27	57789.0	167466198
51	interleukin 2 receptor, alpha chain precursor	1.10E-04	10.12	30798.7	4557667
52	macrophage migration inhibitory factor	4.71E-05	10.17	12468.2	4505185
53	major histocompatibility complex, class I, A precursor	2.48E-09	40.23	40815.2	24797067
54	major histocompatibility complex, class I, B precursor	1.66E-10	30.22	40435.0	17986001
55	major histocompatibility complex, class I, C precursor	6.58E-07	30.21	40623.0	52630342
56	major histocompatibility complex, class I, E precursor	1.29E-08	10.17	40032.8	62912479
57	major histocompatibility complex, class I, F isoform 2 precursor	9.21E-14	20.28	39037.5	149158698
58	major histocompatibility complex, class II, DQ alpha 1 precursor	5.42E-07	10.18	27982.0	18426975
59	major vault protein	2.92E-06	40.17	99266.1	19913412
60	moesin	4.03E-09	40.26	67777.9	4505257
61	myosin, heavy polypeptide 10, non-muscle	4.42E-09	80.23	228856.9	41406064
62	myosin, heavy polypeptide 9, non-muscle	3.55E-14	110.32	226390.6	12667788
63	myosin, light chain 6, alkali, smooth muscle and non-muscle isoform 1	1.03E-05	10.18	16919.1	17986258
64	nucleophosmin 1 isoform 1	2.05E-13	10.22	32554.9	10835063
65	peptidylprolyl isomerase A	1.54E-10	30.21	18000.9	10863927
66	peroxiredoxin 1	1.68E-05	10.15	22096.3	4505591
67	phosphoglycerate kinase 1	7.82E-09	10.22	44586.2	4505763
68	phosphoglycerate kinase 2	2.46E-10	10.17	44767.4	31543397
69	PREDICTED: similar to complement component C3, partial	7.98E-11	20.19	144718.0	169218213
70	PREDICTED: similar to pyruvate kinase, muscle	7.77E-15	70.28	39567.3	169218111
71	pregnancy-zone protein	2.17E-08	30.17	163759.1	162809334
72	profilin 1	5.88E-08	50.21	15044.6	4826898

73	prostaglandin-E synthase 3	1.26E-04	10.13	18685.4	23308579
74	protein disulfide-isomerase A3 precursor	1.43E-13	60.31	56746.8	21361657
75	pyruvate kinase, muscle isoform M1	1.00E-30	30.33	58025.1	33286420
76	pyruvate kinase, muscle isoform M2	1.33E-14	20.27	57900.2	33286418
77	radixin	3.56E-06	20.21	68521.5	4506467
78	ribosomal protein L14	2.31E-07	30.19	23417.0	78000181
79	ribosomal protein L18	6.12E-08	10.22	21621.1	4506607
80	ribosomal protein L21	2.30E-04	20.16	18553.1	18104948
81	ribosomal protein L23	8.99E-12	10.24	14856.1	4506605
82	ribosomal protein L29	6.70E-05	10.16	17741.1	4506629
83	ribosomal protein L30	4.83E-07	10.16	12775.7	4506631
84	ribosomal protein L32	9.96E-09	10.17	15849.8	4506635
85	ribosomal protein L4	9.03E-12	30.19	47667.5	16579885
86	ribosomal protein L7	1.43E-07	50.18	29207.2	15431301
87	ribosomal protein L7a	1.09E-06	10.18	29977.0	4506661
88	ribosomal protein S2	2.69E-05	10.16	31304.6	15055539
89	ribosomal protein S3a	6.64E-04	10.14	29925.8	4506723
90	ribosomal protein S5	5.75E-08	20.21	22862.1	13904870
91	ribosomal protein S6	6.72E-05	10.22	28663.0	17158044
92	ribosomal protein S8	1.00E-30	70.25	24190.2	4506743
93	serine (or cysteine) proteinase inhibitor, clade F (alpha-2 antiplasmin, pigment epithelium derived factor), member 1	4.78E-07	20.18	46283.4	39725934
94	smooth muscle myosin heavy chain 11 isoform SM2A	3.06E-08	10.24	223438.2	13124875
95	solute carrier family 3, member 2 isoform a	2.03E-06	20.17	71079.4	61744475
96	talin 1	3.66E-14	10.30	269596.3	223029410
97	thrombospondin 1 precursor	2.09E-05	30.17	129299.2	40317626
98	Thy-1 cell surface antigen preproprotein	2.44E-07	10.16	17923.4	19923362
99	transgelin 2	5.22E-10	10.26	22377.2	4507357
100	triosephosphate isomerase 1 isoform 1	1.30E-11	30.25	26652.7	4507645
101	Trypsin_porcine	1.67E-14	10.29	24393.8	
102	tryptophanyl-tRNA synthetase isoform a	8.97E-07	10.14	53131.7	47419914
103	tubulin alpha 6	1.38E-11	40.21	49863.5	14389309
104	tubulin, alpha 3e	1.67E-14	50.21	49884.6	46409270
105	tubulin, alpha 4a	1.60E-08	20.14	49892.4	17921989
106	tubulin, beta 2	7.39E-10	30.31	49875.0	4507729
107	tubulin, beta 6	2.71E-07	20.17	49825.0	14210536
108	tubulin, beta polypeptide 4, member Q	1.34E-11	10.18	48456.4	55770868
109	tubulin, beta, 2	3.07E-05	10.25	49799.0	5174735
110	tumor necrosis factor ligand superfamily, member 7	7.05E-07	20.18	21104.9	4507605

111	vimentin	1.11E-06	30.18	53619.2	62414289
112	vitronectin precursor	5.64E-11	20.23	54271.2	88853069

Proteomics analysis of ED(-) exosomes.

	Reference	Peptide (prob)	Protein Score	MW (Da)	Accession Number
1	actin, gamma 1 propeptide [Homo sapiens]	1.78E-14	60.34	41765.8	4501887
2	actin, gamma 2 propeptide [Homo sapiens]	7.55E-11	110.26	41849.8	4501889
3	activated RNA polymerase II transcription cofactor 4 [Homo sapiens]	2.22E-14	20.23	14386.4	217330646
4	adenosylhomocysteinase isoform 1 [Homo sapiens]	3.07E-07	30.26	47685.3	9951915
5	albumin preproprotein [Homo sapiens]	2.00E-08	20.21	69321.6	4502027
6	alpha 2 globin [Homo sapiens]	4.54E-12	40.26	15247.9	4504345
7	alpha-2-HS-glycoprotein [Homo sapiens]	1.63E-06	20.23	39315.7	156523970
8	alpha-2-macroglobulin precursor [Homo sapiens]	9.70E-08	10.17	163188.3	66932947
9	alpha-2-plasmin inhibitor [Homo sapiens]	2.29E-04	10.15	54531.2	115583663
10	alpha-fetoprotein precursor [Homo sapiens]	2.91E-11	10.23	68633.1	4501989
11	apolipoprotein E precursor [Homo sapiens]	1.48E-04	20.18	36131.8	4557325
12	ATP citrate lyase isoform 1 [Homo sapiens]	2.47E-05	30.19	120762.1	38569421
13	ATP-dependent DNA helicase II [Homo sapiens]	1.42E-05	20.15	82652.4	10863945
14	beta tubulin 1, class VI [Homo sapiens]	1.08E-04	40.25	50294.6	13562114
15	beta-2-microglobulin precursor [Homo sapiens]	4.68E-11	10.22	13705.9	4757826
16	bisphosphoglycerate mutase 1 [Homo sapiens]	1.55E-08	20.19	28785.9	4505753
17	bisphosphoglycerate mutase 2 [Homo sapiens]	2.89E-08	10.13	28747.9	50593010
18	bisphosphoglycerate mutase 4 [Homo sapiens]	1.31E-07	10.17	28758.8	71274132
19	chaperonin containing TCP1, subunit 2 [Homo sapiens]	1.14E-04	10.14	57452.3	5453603
20	chaperonin containing TCP1, subunit 3 isoform a [Homo sapiens]	5.77E-09	20.19	60495.4	63162572
21	chaperonin containing TCP1, subunit 5 (epsilon) [Homo sapiens]	1.67E-08	20.23	59632.9	24307939
22	chaperonin containing TCP1, subunit 7 isoform a [Homo sapiens]	2.62E-11	20.18	59329.0	5453607
23	chaperonin containing TCP1, subunit 8 (theta) [Homo sapiens]	6.52E-06	20.22	59582.6	48762932

24	chloride intracellular channel 1 [Homo sapiens]	1.17E-06	10.16	26905.8	14251209
25	clathrin heavy chain 1 [Homo sapiens]	1.00E-30	210.28	191491.7	4758012
26	coagulation factor II preproprotein [Homo sapiens]	2.59E-06	40.19	69992.2	4503635
27	coagulation factor V precursor [Homo sapiens]	1.62E-04	10.12	251543.8	105990535
28	DEAH (Asp-Glu-Ala-His) box polypeptide 9 [Homo sapiens]	6.31E-06	20.16	140868.9	100913206
29	enolase 1 [Homo sapiens]	4.15E-07	30.23	47139.4	4503571
30	enolase 2 [Homo sapiens]	2.61E-07	20.23	47239.1	5803011
31	epsilon globin [Homo sapiens]	9.26E-06	10.15	16192.5	4885393
32	eukaryotic translation elongation factor 1 alpha 2 [Homo sapiens]	2.14E-09	30.23	50438.4	4503475
33	eukaryotic translation elongation factor 1 gamma [Homo sapiens]	6.90E-08	20.21	50087.2	4503481
34	eukaryotic translation elongation factor 2 [Homo sapiens]	2.30E-10	90.31	95277.1	4503483
35	fatty acid synthase [Homo sapiens]	2.85E-11	200.26	273251.6	41872631
36	filamin A, alpha isoform 1 [Homo sapiens]	1.21E-06	20.16	279841.1	116063573
37	fructose-bisphosphate aldolase A [Homo sapiens]	3.29E-11	40.23	39395.3	193794814
38	gelsolin isoform b [Homo sapiens]	1.26E-08	50.22	80590.6	189083772
39	glutamyl-prolyl tRNA synthetase [Homo sapiens]	1.07E-04	10.17	170482.3	62241042
40	glyceraldehyde-3-phosphate dehydrogenase [Homo sapiens]	3.33E-15	130.31	36030.4	7669492
41	glyceraldehyde-3-phosphate dehydrogenase, spermatogenic [Homo sapiens]	2.47E-07	10.15	44472.8	7657116
42	granzyme B precursor [Homo sapiens]	4.17E-06	10.17	27698.4	221625528
43	guanine nucleotide binding protein (G protein), beta polypeptide 2-like 1 [Homo sapiens]	3.14E-06	10.17	35054.6	5174447
44	H2A histone family, member V isoform 1 [Homo sapiens]	5.26E-07	10.22	13500.5	6912616
45	H2A histone family, member V isoform 2 [Homo sapiens]	2.43E-11	20.26	12138.7	20357599
46	H2A histone family, member Y isoform 1 [Homo sapiens]	3.33E-15	50.26	39159.2	20336746
47	H2A histone family, member Y2 [Homo sapiens]	1.83E-12	10.27	40033.4	8923920
48	H3 histone family, member H [Homo sapiens]	1.00E-30	90.32	15394.5	4504291
49	heat shock 70kDa protein 1A [Homo sapiens]	6.58E-12	60.25	70009.2	194248072
50	heat shock 70kDa protein 2 [Homo sapiens]	4.54E-08	50.19	69978.0	13676857
51	heat shock 70kDa protein 8 isoform 1	2.57E-07	70.20	70854.4	5729877

	[Homo sapiens]				
52	heat shock 90kDa protein 1, alpha isoform 1 [Homo sapiens]	2.08E-13	20.28	98099.4	153792590
53	heat shock 90kDa protein 1, beta [Homo sapiens]	1.45E-13	160.27	83212.2	20149594
54	heterogeneous nuclear ribonucleoprotein D isoform d [Homo sapiens]	2.24E-06	10.22	30653.1	51477708
55	heterogeneous nuclear ribonucleoprotein U isoform a [Homo sapiens]	5.77E-11	60.24	90528.0	74136883
56	high mobility group AT-hook 1 isoform b [Homo sapiens]	1.18E-07	20.18	10672.6	22208975
57	high-mobility group box 1 [Homo sapiens]	1.14E-07	10.29	24878.2	4504425
58	histone cluster 1, H1a [Homo sapiens]	2.34E-06	30.20	21828.9	4885373
59	histone cluster 1, H1b [Homo sapiens]	5.98E-12	90.24	22566.5	4885381
60	histone cluster 1, H1c [Homo sapiens]	2.00E-08	50.22	21351.8	4885375
61	histone cluster 1, H1t [Homo sapiens]	1.76E-12	40.28	22005.7	20544168
62	histone cluster 1, H2ad [Homo sapiens]	2.85E-13	80.23	14098.9	10800130
63	histone cluster 1, H2ae [Homo sapiens]	2.84E-10	20.24	14127.0	10645195
64	histone cluster 1, H2bb [Homo sapiens]	6.94E-06	20.22	13941.6	10800140
65	histone cluster 1, H2bi [Homo sapiens]	2.87E-11	100.28	13897.6	4504271
66	histone cluster 1, H4a [Homo sapiens]	2.62E-12	190.28	11360.4	4504301
67	histone cluster 2, H2ab [Homo sapiens]	4.03E-08	30.23	13986.8	28195394
68	histone cluster 2, H3d [Homo sapiens]	1.11E-14	10.35	15378.5	183076548
69	HP1-BP74 [Homo sapiens]	4.21E-04	20.17	61169.3	56676330
70	inter-alpha globulin inhibitor H2 polypeptide [Homo sapiens]	1.31E-05	10.13	101325.8	156119625
71	L-lactate dehydrogenase B [Homo sapiens]	2.45E-05	10.20	36665.4	5031857
72	major histocompatibility complex, class I, A precursor [Homo sapiens]	3.88E-12	50.26	40815.2	24797067
73	major histocompatibility complex, class I, B precursor [Homo sapiens]	7.86E-11	10.21	40435.0	17986001
74	major histocompatibility complex, class I, C precursor [Homo sapiens]	7.25E-09	20.25	40623.0	52630342
75	major histocompatibility complex, class I, F isoform 2 precursor [Homo sapiens]	7.07E-10	20.21	39037.5	149158698
76	major vault protein [Homo sapiens]	2.55E-14	190.29	99266.1	19913412
77	myosin, heavy polypeptide 9, non-muscle [Homo sapiens]	8.51E-08	30.20	226390.6	12667788
78	nucleosome assembly protein 1-like 1 [Homo sapiens]	3.79E-12	40.26	45346.0	4758756
79	Obg-like ATPase 1 isoform 1 [Homo sapiens]	1.76E-08	10.20	44715.4	58761500
80	peptidylprolyl isomerase A [Homo sapiens]	2.20E-09	40.27	18000.9	10863927
81	phosphoglycerate dehydrogenase [Homo sapiens]	7.91E-05	40.18	56614.5	23308577
82	phosphoglycerate kinase 1 [Homo	9.83E-12	40.25	44586.2	4505763

	sapiens]				
83	phosphoglycerate kinase 2 [Homo sapiens]	2.11E-10	20.23	44767.4	31543397
84	poly (ADP-ribose) polymerase family, member 1 [Homo sapiens]	6.97E-08	10.17	113012.4	156523968
85	PREDICTED: similar to complement component 3 [Homo sapiens]	3.34E-08	10.16	44900.9	169214179
86	PREDICTED: similar to complement component C3, partial [Homo sapiens]	3.61E-10	40.17	144718.0	169218213
87	PREDICTED: similar to pyruvate kinase, muscle [Homo sapiens]	5.33E-14	100.25	39567.3	169218111
88	pregnancy-zone protein [Homo sapiens]	3.77E-06	20.20	163759.1	162809334
89	profilin 1 [Homo sapiens]	1.86E-08	20.23	15044.6	4826898
90	pyruvate kinase, muscle isoform M1 [Homo sapiens]	9.47E-05	20.18	58025.1	33286420
91	pyruvate kinase, muscle isoform M2 [Homo sapiens]	2.58E-04	10.12	57900.2	33286418
92	RAP1B, member of RAS oncogene family-like [Homo sapiens]	1.44E-06	10.16	20911.6	148227764
93	ras-related nuclear protein [Homo sapiens]	3.65E-07	10.20	24407.6	5453555
94	RAP1A(B), member of RAS oncogene family [Homo sapiens]	1.44E-06	10.16	20911.6	148227764
95	ribosomal protein L10 [Homo sapiens]	9.91E-04	10.13	54939.0	118498359
96	ribosomal protein L10-like protein [Homo sapiens]	2.22E-08	10.21	24815.5	15431288
97	ribosomal protein L11 [Homo sapiens]	5.13E-06	20.15	24502.7	18152783
98	ribosomal protein L12 [Homo sapiens]	8.93E-08	10.19	20239.7	15431290
99	ribosomal protein L13 [Homo sapiens]	1.08E-04	10.19	17807.5	4506597
100	ribosomal protein L13a [Homo sapiens]	5.90E-10	50.27	24246.5	15431295
101	ribosomal protein L14 [Homo sapiens]	6.73E-08	30.17	23562.4	6912634
102	ribosomal protein L15 [Homo sapiens]	5.30E-09	50.17	23417.0	78000181
103	ribosomal protein L17 [Homo sapiens]	6.45E-09	40.21	24131.1	15431293
104	ribosomal protein L18 [Homo sapiens]	7.92E-08	30.20	21383.3	4506617
105	ribosomal protein L19 [Homo sapiens]	2.56E-08	70.24	21621.1	4506607
106	ribosomal protein L21 [Homo sapiens]	6.66E-15	20.27	23451.3	4506609
107	ribosomal protein L22 proprotein [Homo sapiens]	5.50E-05	30.19	14777.8	4506613
108	ribosomal protein L24 [Homo sapiens]	5.44E-09	60.19	17767.9	4506619
109	ribosomal protein L27a [Homo sapiens]	1.65E-06	30.21	16551.0	4506625
110	ribosomal protein L3 isoform b [Homo sapiens]	3.05E-12	100.26	40126.6	76496472
111	ribosomal protein L30 [Homo sapiens]	5.61E-07	30.22	12775.7	4506631
112	ribosomal protein L32 [Homo sapiens]	5.54E-10	30.26	15849.8	4506635
113	ribosomal protein L4 [Homo sapiens]	1.50E-11	160.36	47667.5	16579885
114	ribosomal protein L5 [Homo sapiens]	1.05E-10	40.22	34340.7	14591909
115	ribosomal protein L6 [Homo sapiens]	5.85E-10	40.20	32707.6	16753227
116	ribosomal protein L7 [Homo sapiens]	6.26E-10	70.20	29207.2	15431301
117	ribosomal protein L7a [Homo sapiens]	4.27E-13	90.33	29977.0	4506661

118	ribosomal protein L8 [Homo sapiens]	6.64E-06	20.17	28007.3	15431306
119	ribosomal protein P1 isoform 1 [Homo sapiens]	6.14E-09	10.20	11506.7	4506669
120	ribosomal protein S11 [Homo sapiens]	9.66E-06	30.16	18419.0	4506681
121	ribosomal protein S16 [Homo sapiens]	1.37E-07	50.17	16435.0	4506691
122	ribosomal protein S2 [Homo sapiens]	7.22E-14	60.22	31304.6	15055539
123	ribosomal protein S24 isoform a [Homo sapiens]	2.50E-09	30.19	15059.2	14916501
124	ribosomal protein S26 [Homo sapiens]	5.65E-09	30.23	13007.1	15011936
125	ribosomal protein S3 [Homo sapiens]	6.41E-07	40.16	26671.4	15718687
126	ribosomal protein S3a [Homo sapiens]	1.09E-10	60.22	29925.8	4506723
127	ribosomal protein S6 [Homo sapiens]	4.97E-13	60.28	28663.0	17158044
128	ribosomal protein S8 [Homo sapiens]	8.30E-12	80.23	24190.2	4506743
129	ribosomal protein SA [Homo sapiens]	4.33E-13	20.18	32833.4	59859885
130	S100 calcium binding protein A11 [Homo sapiens]	5.12E-06	10.17	11732.8	5032057
131	salivary amylase alpha 1C precursor [Homo sapiens]	6.33E-05	10.18	57731.0	56549664
132	serine (or cysteine) proteinase inhibitor, clade F (alpha-2 antiplasmin, pigment epithelium derived factor), member 1 [Homo sapiens]	2.31E-07	10.23	46283.4	39725934
133	small nuclear ribonucleoprotein D1 polypeptide 16kDa [Homo sapiens]	8.72E-10	50.31	13273.4	5902102
134	small nuclear ribonucleoprotein polypeptide D2 [Homo sapiens]	7.26E-05	10.15	13518.2	29294624
135	smooth muscle myosin heavy chain 11 isoform SM2A [Homo sapiens]	5.38E-05	10.15	223438.2	13124875
136	talin 1 [Homo sapiens]	2.50E-04	20.16	269596.3	223029410
137	T-complex protein 1 isoform a [Homo sapiens]	4.40E-05	20.14	60305.7	57863257
138	thrombospondin 1 precursor [Homo sapiens]	4.29E-07	60.22	129299.2	40317626
139	tripeptidyl peptidase II [Homo sapiens]	4.22E-05	10.20	138262.6	186972143
140	Trypsin_porcine	4.44E-14	30.31	24393.8	
141	tubulin alpha 6 [Homo sapiens]	6.67E-12	30.22	49863.5	14389309
142	tubulin, alpha 3e [Homo sapiens]	1.78E-11	50.20	49884.6	46409270
143	tubulin, alpha 4a [Homo sapiens]	3.71E-08	20.20	49892.4	17921989
144	tubulin, beta [Homo sapiens]	1.05E-06	10.16	49639.0	29788785
145	tubulin, beta 2 [Homo sapiens]	3.33E-15	60.31	49875.0	4507729
146	tubulin, beta 6 [Homo sapiens]	4.73E-10	20.19	49825.0	14210536
147	tubulin, beta, 2 [Homo sapiens]	1.24E-05	10.31	49799.0	5174735
148	tyrosine 3/tryptophan 5 -monooxygenase activation protein, epsilon polypeptide [Homo sapiens]	2.73E-04	10.18	29155.4	5803225
149	tyrosine 3/tryptophan 5 -monooxygenase activation protein, theta polypeptide [Homo sapiens]	2.01E-04	10.15	27746.8	5803227
150	vitronectin precursor [Homo sapiens]	3.93E-09	20.18	54271.2	88853069

Lipid metabolites of C81 and CEM exosomes as determined by LAESI-MS.

Metabolite	Chemical Formula	Charge	m/z (Theo)	m/z (CEM)	m/z (C81)	Err mDa	PPM	Err mDa	PPM	Notes
DG(38:7)	$C_{41}H_{66}O_5$	$M+Na^+$	661.4808	661.4766		4.2	6.3			Diacyl-glycerol
DG(40:10)	$C_{43}H_{64}O_5$	$M+H^+$	661.4832	661.4766		6.6	10.0			Diacyl-glycerol
PE(34:3)	$C_{39}H_{72}NO_8P$	$M+H^+$	714.5073	714.5021		5.2	7.3			Phosphatidyl-ethanolamine
PE(32:0)	$C_{37}H_{74}NO_8P$	$M+Na^+$	714.5049	714.5021		2.8	3.9			Phosphatidyl-ethanolamine
PC(36:3)	$C_{44}H_{82}NO_8P$	$M+H^+$	784.5856	784.5876		2.0	2.5			Phosphatidyl-choline
PC(34:0)	$C_{42}H_{84}NO_8P$	$M+Na^+$	784.5831	784.5876		4.5	5.7			Phosphatidyl-choline
PS(36:0)	$C_{42}H_{82}NO_{10}P$	$M+Na^+$	814.5574	814.5502		7.2	8.8			Phosphatidyl-serine
PE(42:3)	$C_{47}H_{88}NO_8P$	$M+H^+$	826.6326	826.6241		8.5				Phosphatidyl-ethanolamine
PE(40:0)	$C_{45}H_{90}NO_8P$	$M+Na^+$	826.6301	826.6241		6.0	7.3			Phosphatidyl-ethanolamine
PS(40:4)	$C_{46}H_{82}NO_{10}P$	$M+H^+$	840.5754	840.5709		4.5				Phosphatidyl-serine
PS(38:1)	$C_{44}H_{84}NO_{10}P$	$M+Na^+$	840.5730	840.5709		2.1				Phosphatidyl-serine
PC(44:9)	$C_{52}H_{86}NO_8P$	$M+H^+$	884.6169	884.6135		3.4	3.8			Phosphatidyl-choline
PC(42:6)	$C_{50}H_{88}NO_8P$	$M+Na^+$	884.6145	884.6135		1.0	1.1			Phosphatidyl-choline
PG(44:8)	$C_{50}H_{83}O_{10}P$	$M+Na^+$	897.5621	897.5704		8.3				Phosphatidyl-glycerol
PC(44:11)	$C_{52}H_{82}NO_8P$	$M+Na^+$	902.5675	902.5746		7.1	7.9			Phosphatidyl-

										choline
PI(36:2)	$C_{45}H_{86}NO_{13}P$	$M+Na^+$	902.5734	902.5746		1.2	1.3			Phosphatidyl-inositol
DG(43:6)	$C_{46}H_{78}O_5$	$M+H^+$	711.5927		711.5977			5.0	7.0	Diacylglycerol
PC(32:2)	$C_{40}H_{76}NO_8P$	$M+H^+$	730.5387		730.5410			2.3	3.1	low s/n, Phosphatidyl-choline
PE(36:2)	$C_{41}H_{78}NO_8P$	$M+H^+$	744.5543		744.5513			-3.0	4.0	Phosphatidyl-ethanolamine
PE(36:1)	$C_{41}H_{80}NO_8P$	$M+H^+$	746.5700		746.5670			-2.9	4.0	Phosphatidyl-ethanolamine
PG(34:0)	$C_{40}H_{79}O_{10}P$	$M+H^+$	751.5489		751.5524			3.5	4.7	Phosphatidyl-glycerol
PG(35:0)	$C_{41}H_{81}O_{10}P$	$M+H^+$	765.5646		765.5682			3.6	4.7	low s/n, Phosphatidyl-glycerol
PC(36:4)	$C_{44}H_{80}NO_9P$	$M+H^+$	798.5649		798.5605			4.4	5.5	Phosphatidyl-choline
PG(42:3)	$C_{48}H_{89}O_{10}P$	$M+H^+$	857.6271		857.6241			3.0	3.5	Phosphatidyl-glycerol
PG(40:0)	$C_{46}H_{91}O_{10}P$	$M+Na^+$	857.6248		857.6241			0.7	0.8	Phosphatidyl-glycerol
PBS buffer	$(NaCl)_{13}$	$M+Na^+$	782.4430	782.4438	782.4438	0.8	1.0	0.8	1.0	lock mass